Sleep increases firing rate modulation during interictal epileptic activities in mesial structures

Stephen Whitmarsh[1*], **Vi-Huong Nguyen-Michel**[2], **Katia Lehongre**[1], **Bertrand Mathon**[1,3], **Claude Adam**[2], **Virginie Lambrecq**[1,2], **Valerio Frazzini**[1,2†], **Vincent Navarro**[1,2†*]

***For correspondence:** stephen.whitmarsh@icm-institute.org&vincent.navarro@aphp.fr

[†]These authors contributed equally to this work

[1]Sorbonne Université, Institut du Cerveau - Paris Brain Institute - ICM, Inserm, CNRS, APHP, Pitié-Salpêtrière Hospital, Paris, France; [2]AP-HP, Pitié-Salpêtrière Hospital, Epilepsy Unit and Reference Center for Rare Epilepsies, F-75013, Paris, France; [3]AP-HP, Department of Neurosurgery, Pitié-Salpêtrière Hospital and Sorbonne Université, Paris, France

Abstract Epileptic seizures and interictal epileptiform discharges (IEDs) are strongly influenced by sleep and circadian rhythms. However, human data on the effect of sleep on neuronal behavior during interictal activity have been lacking. We analyzed EEG data from epileptic patients implanted with macro and micro electrodes targeting mesial temporal structures. Sleep staging was performed on concomitantly recorded polysomnography and video-EEG. Automated IED detection identified thousands of IEDs per patient. Both the rate and amplitude of IEDs were increased with deeper stages of NREM sleep. Single unit activity (SUA) and multi-unit activity (MUA) increased their firing during the IED spike, and strongly decreased during the subsequent slow wave. These time-locked firing rate modulations were shown to increase during deeper stages of NREM sleep. Finally, during resting behaviour, neuronal firing rate, bursting rate and firing regularity were all shown to progressively decrease with deeper stages of NREM sleep.

Introduction

The relationship between sleep and epileptic seizures has been recognized since antiquity (***Temkin, 1994***). Early modern research recognized that epileptic activity occurs in circadian and ultradian cycles (***Gowers, 1881***; ***Langdon-Down and Russell Brain, 1929***; ***Griffiths and Fox, 1938***). Since the advent of electroencephalography (EEG) and polysomnography (PSG), it is now known that many types of epilepsy (focal and idiopathic generalized) have the highest seizure preponderance during light non-REM sleep (NREM), and the lowest during REM sleep (***Janz, 1962***; ***Autret et al., 1997***; ***Bazil and Walczak, 1997***; ***Shouse et al., 2000***; ***Herman et al., 2001***; ***Jobst et al., 2001***; ***Méndez and Radtke, 2001***; ***Minecan et al., 2002***; ***Malow, 2005***; ***Rocamora et al., 2013***). In temporal epilepsy, focal seizures were also found to be more likely to evolve into bilateral tonic-clonic seizures during sleep than during wakefulness (***Jobst et al., 2001***; ***Herman et al., 2001***; ***Bazil and Walczak, 1997***). In addition, sleep deprivation is the most common trigger for spontaneous "breakthrough seizures" (***Frucht et al., 2000***; ***Ferlisi and Shorvon, 2014***; ***Wassenaar et al., 2014***; ***Cobabe et al., 2015***; ***Reddy et al., 2018***) and seizures in the epilepsy clinic (***Foldvary-Schaefer and Grigg-Damberger, 2006***; ***Jain and Kothare, 2015***), regardless of the type of epilepsy or the epilepsy syndrome. Furthermore, sleep disorders such as sleep apneas, that strongly disturb the quality of sleep, likely worsen epilepsy (***Kataria and Vaughn, 2016***; ***Derry and Duncan, 2013***).

Interictal epileptiform discharges (IEDs) are known to be strongly influenced by sleep and circadian rhythms as well. IEDs are brief non-symptomatic events observed in the EEG of patients predisposed to spontaneous seizures (***Staley and Dudek, 2006***). IEDs are fast ($<200\,\mathrm{ms}$) high-amplitude ($>50\,\mathrm{mV}$) EEG transients, defined as interictal spikes (***de Curtis and Avanzini, 2001***), habitually followed by a slow wave lasting several hundreds of milliseconds (***de Curtis and Avanzini, 2001***; ***Staley and Dudek, 2006***). ***Gibbs and Gibbs*** (***1947***) were the first to demonstrate that the rate of IED occurrence increases with sleep, even if the waking EEG was normal. Using invasive EEG, ***Penfield and Jasper*** (***1954***) later reported an increase of IEDs when certain patients became drowsy or fell asleep. Since then, IEDs have been consistently found to occur more often during sleep (***Lieb et al., 1980***; ***Ferrillo et al., 2000***; ***Bagshaw et al., 2009***; ***Goncharova et al., 2009***; ***Karoly et al., 2016***; ***Rossi et al., 1984***; ***Sammaritano et al., 1991***; ***Spencer et al., 2016***; ***Lambert et al., 2018***; ***Fouad et al., 2022***). Indeed, long-term recordings have found robust 24 hour periods, peaking between midnight and 5pm (***Anderson et al., 2015***; ***Spencer et al., 2016***; ***Baud et al., 2018***). Generally, deeper stages of non-REM (NREM) sleep seem to promote interictal activity, while lighter stages promote seizures (***Jobst et al., 2001***; ***Minecan et al., 2002***), especially in temporal lobe epilepsy (***Lieb et al., 1980***; ***Rossi et al., 1984***; ***Sammaritano et al., 1991***). The average IED rate is lower in rapid eye movement (REM) sleep than in wakefulness, and higher in slow wave sleep (SWS) than in REM (***Ng and Pavlova, 2013***). Furthermore, IED rates are positively correlated with power in the delta ($1\,\mathrm{Hz}$ to $4\,\mathrm{Hz}$) frequency range (***Ferrillo et al., 2000***; ***Malow et al., 1998***; ***Fürbass et al., 2021***).

IEDs are understood to be generated by synchronous neuronal discharges, occurring during depolarization of the neuronal membrane (***McNamara, 1994***; ***de Curtis and Avanzini, 2001***; ***Ulbert et al., 2004***), consistent with paroxysmal depolarizing shifts (PDS) studied in animal models of epilepsy, in which a large depolarization phase is followed by a long hyperpolarization (***Matsumoto***

and Marsan, 1964; *Prince, 1968*). In humans, microelectrode recordings have shown that firing rates increase during the interictal spike, and are subsequently reduced (and often completely silenced) during the subsequent slow wave (*Alvarado-Rojas et al., 2013*; *Keller et al., 2010*; *Ulbert et al., 2004*; *Fabó et al., 2008*). The effect of sleep on seizures and IEDs are hypothesized to be due to enhanced brain synchronization during SWS, and decreased synchronization during REM (*Nayak et al., 2018*; *Malow and Aldrich, 2000*). Consistent with sleep-related changes in cortical excitability, neurons in the human hippocampus have been shown to have a higher propensity for bursting during NREM, with the lowest bursting rates during REM (*Staba et al., 2002b*). Although these findings provide a pathophysiological model on the level of single unit and population activity, no studies have yet demonstrated an effect of sleep on neuronal firing behavior during IEDs in human data. However, previous findings have suggested higher baseline firing rates and bursting propensity during NREM sleep, and a reduction during REM (*Timofeev et al., 2001*; *Staba et al., 2002b*; *Vyazovskiy et al., 2009*).

Several studies have shown the clinical potential of basic morphological metrics of IEDs. Aanestad et al. (*Aanestad and Brøgger, 2018*; *Aanestad et al., 2020*) showed a statistically significant reduction in the amplitude of spikes and slow waves with age. In epilepsy, increased IED amplitudes during sleep and after awakening have been anecdotally reported in benign epilepsy with centrotemporal spikes (BECTS) (*Beaumanoir et al., 1974*; *Blom and Heijbel, 1975*; *Dalla Bernardina et al., 1991*; *Clemens and Oláh, 1987*). *Hufnagel et al.* (*2000*) later observed that the highest spike amplitude and shortest spike duration occurred within 2 cm from the site of seizure origin in 24 (75%) and 22 (69%) out of 32 patients, respectively. *Malow et al.* (*1998*) and *Sammaritano et al.* (*1991*) reported that during REM spikes were often of lower voltage than those recorded during wakefulness or NREM sleep. *Malow et al.* (*1998*) reported fluctuations in the sharpness and amplitude of IEDs during NREM, even within the same 30 seconds epoch. However, neither *Sammaritano et al.* (*1991*) nor *Malow et al.* (*1998*) provided quantification or statistical comparisons between sleep stages. *Frost et al.* (*1991*) reported a statistically significant increase in spike amplitudes in NREM versus REM sleep. *Del Felice et al.* (*2015*) reported a statistical increase in the amplitude of cortical and mesial temporal spikes during N2 versus wakefulness, but these findings were based on a very limited number of observations (an average of 39 spikes in N2, 21 spikes during wakefulness, none during SWS or REM). Recently, *Fouad et al.* (*2022*) investigated differences in spike morphology using a feature extraction method (*Liu et al., 2013*), reporting amplitude differences between brain regions and SOZ, but no statistically significant differences between sleep stages. A non-significant trend towards increased amplitudes in deeper stages of sleep could be observed, but only within median brain regions, and only from the SOZ. Together, while previous studies suggest that IED amplitudes are increased during deeper stages of sleep, consistent and statistically robust comparisons of IED amplitudes across all sleep stages have not yet been reported.

The current study investigated the influence of sleep on short and long-term dynamics of interictal activities, i.e. on time-locked neuronal activity during interictal events as well as on baseline activity without interictal events. For this purpose we analysed recordings from intracerebral electrodes containing both macro and micro contacts implanted in the hippocampal-amygdala

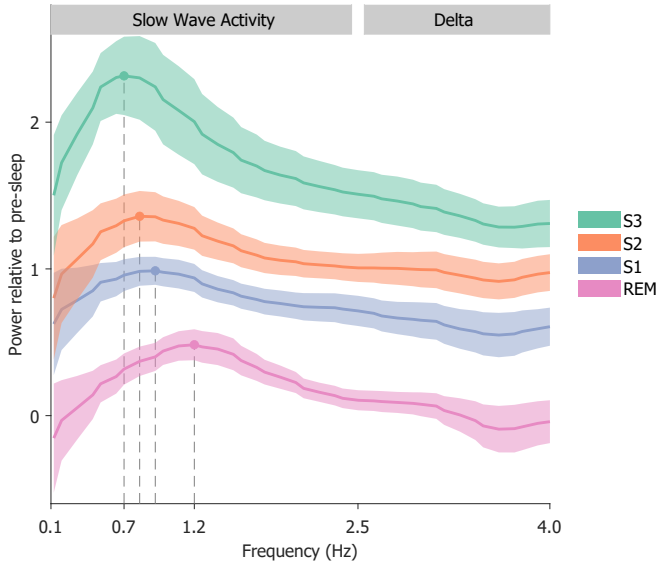

Figure 1. Power in the SWA and delta range, relative to the pre-sleep period, and separated per sleep stage. Lines show average power over patients per sleep stage, with shaded regions showing the standard error of the mean.

complex of patients with focal epilepsy. An automatic template matching procedure was used to objectively identify IEDs in continuous long-term (2-3 weeks) recordings. Implanted micro electrodes allowed for the recording of neuronal action potentials during the full sleep and wake cycle. Polysomnography allowed detailed multilevel analyses during different stages of sleep.

We expected deeper stages of NREM sleep to increase the rate of IEDs, as well as their amplitude, while increasing baseline firing rates and bursting propensity. During the IEDs, we expected to find increased neuronal firing rates during IED spikes, and decreased neuronal firing rates during subsequent slow waves. Importantly, we expected these firing rate modulations during IEDs to increase with deeper stages of NREM sleep compared to REM and wake. Finally, we explored the effect of sleep on the regularity of neuronal firing with CV2 (***Ponce-Alvarez et al., 2009***).

Results

Slow wave peak frequency increases with deeper stages of sleep

For each patient, 72 hours of LFP data were epoched in 10-second non-overlapping intervals, and labeled according to the sleep stage, while excluding those that overlapped with IEDs or artefacts. Power in $0.1\,\mathrm{Hz}$ to $5\,\mathrm{Hz}$ was calculated in steps of $0.1\,\mathrm{Hz}$, then averaged for each sleep stage, as well as over all sleep stages. Power at each frequency was then calculated relative to the pre-sleep period. Relative power showed a peak in the SWA frequency range ($0.1\,\mathrm{Hz}$ to $2.5\,\mathrm{Hz}$) which increased from $0.7\,\mathrm{Hz}$ in S3, to $0.8\,\mathrm{Hz}$ in S2, $0.9\,\mathrm{Hz}$ in S1, and $1.2\,\mathrm{Hz}$ in REM sleep (***Figure 1***).

Mixed effects analyses verified that variance in both SWA and delta power were significantly explained by sleep stage (***Figure 4***C-F, ***Table 9*** & ***Table 10***), with post-hoc comparisons confirming that SWA and delta power increased with depth of sleep ($Pre < REM < S1 < S2 < S3$).

IED detection

Manual annotation of IEDs resulted in an average detection of 5667 IEDs per patient (2106 to 12912) during the first 24 hours (***Table 4***). Automatic detection resulted in a similar average of 5618 IED detections per patient (3054 to 12811) in the same 24 hours, showing an average hit-rate of 98.0%, and an average false-alarm (false positive) rate of 6.5%. The total continuous recording time was on average 314 hours, i.e., just over 13 days, in which the automatic procedure detected an average of 50271 IEDs per patient (9224 to 113832, ***Table 4***). In all patients, the six templates showed morphologies consistent with spike-wave interictal discharges (***Gotman, 1980***; ***Altafullah et al., 1986***; ***de Curtis and Avanzini, 2001***; ***Fabó et al., 2008***), with only modest variations in the amplitude of sharp peaks and slow waves (***Figure 2***).

Circadian distribution of interictal and ictal activity

IED rates showed a significant deviation from a uniform circadian distribution in all patients (***Figure 3***A & ***Table 5***). Seven out of eight patients show a median phase between 01:00 and 03:30 at night, and the remaining patient presented a median phase at 17:25.

Seizure occurrence showed a significant deviation from a uniform circadian distribution in four of eight patients (***Figure 3***B & ***Table 5***). In contrast to IED rates, the median phases of seizures were distributed throughout the day/night cycle. Of those patients who's phase differed significantly from a flat distribution, the medium phase was found at 17:43, 10:31, 18:26 & 01:59.

Increased IED rate with deeper stages of NREM sleep

IED rates increased significantly from wake to sleep (***Figure 4***A,B & ***Table 7***), showing higher IED rates with increasing depth of NREM sleep ($S3 > S2 > S1 > Wake$). REM and wake did not differ significantly in IED rates.

Increased IED rate with increased slow wave activity and delta power

For each patient, LFP data were epoched in 10-second non-overlapping intervals for the whole , and labeled according to the sleep stage, while excluding those that overlapped with IEDs or artefacts. Power in $0.1\,\mathrm{Hz}$ to $5\,\mathrm{Hz}$ was calculated in steps of $0.1\,\mathrm{Hz}$, then averaged for each sleep stage, as well as over all sleep stages. Power at each frequency was then calculated relative to the pre-sleep period. Relative power showed a peak in the SWA frequency range ($0.1\,\mathrm{Hz}$ to $2.5\,\mathrm{Hz}$) which increased from $0.7\,\mathrm{Hz}$ in S3, to $0.8\,\mathrm{Hz}$ in S2, $0.9\,\mathrm{Hz}$ in S1, and $1.2\,\mathrm{Hz}$ in REM sleep (***Figure 1***).

Variations in IED rate were significantly explained by power in slow wave activity ($0.1\,\mathrm{Hz}$ to $2.5\,\mathrm{Hz}$), and delta ($2.5\,\mathrm{Hz}$ to $4\,\mathrm{Hz}$) (***Figure 5*** & ***Table 8***).

Increased IED amplitudes with deeper stages of NREM sleep

Figure 6 shows the LFP of all detected IEDs, averaged per sleep stage, showing that the magnitude of both the peak and the slow wave components increased with decreasing stages of NREM sleep, in all but one patient (patient 7).

To statistically test the amplitude modulation of the spike and slow wave components of the IEDs, the average amplitude during their respective intervals, as determined earlier (***Figure 2***),

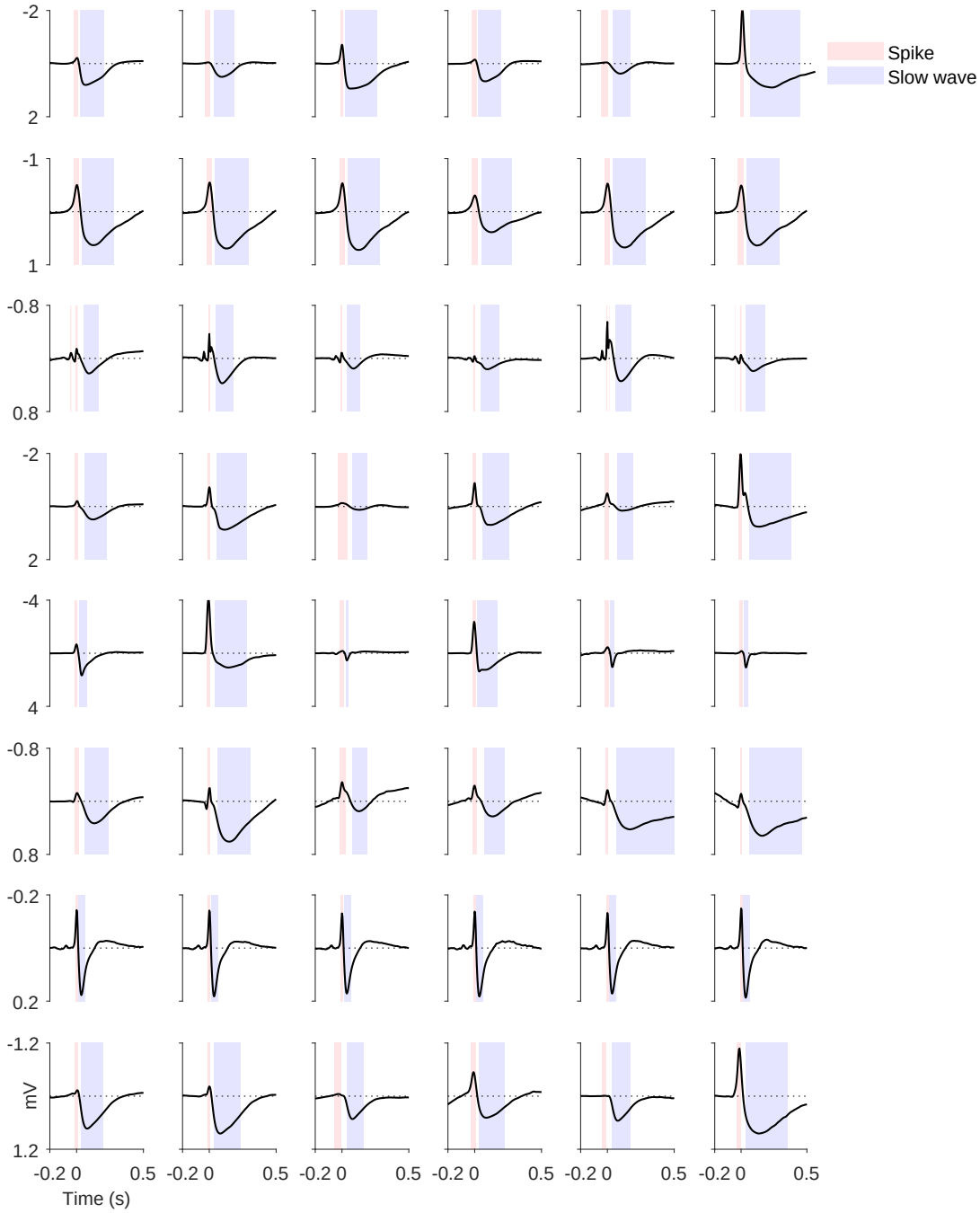

Figure 2. Templates for automatic detection of IEDs and statistical time intervals. Each row represents the six templates of one patient (from top to bottom: Patient 1 to 8). Black lines show the template at the channel with the largest response over templates. Red overlays show the spike period [$< \frac{1}{2}min(V)$], blue overlays the slow wave period [$> \frac{1}{2}max(V)$]. Note the clinical direction of the current (top = negative).

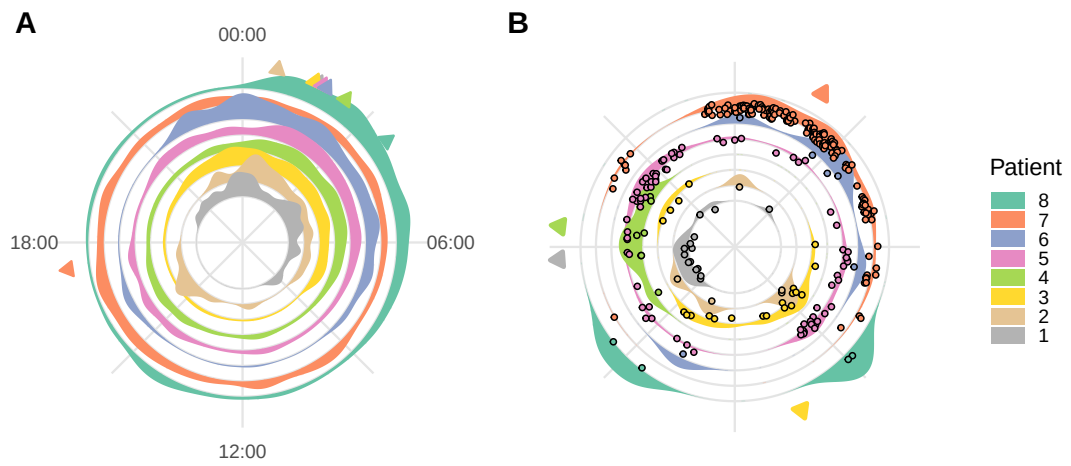

Figure 3. Polar representations of 24 hours circadian distributions of (**A**) interictal activity, (**B**) seizures. Significant mean angles of interictal density and seizure occurrence are shown by arrows. See ***Table 5*** for details

were entered into a mixed-effects analysis with patient and template as a random factor, and pre-sleep as the reference. Post-hoc comparisons allowed the evaluation of differences between sleep stages. The amplitudes of the IED spikes were increased in SWS compared to pre-sleep, WASO and REM, and increased progressively with increased depth within SWS ($S3 > S2 > S1$, ***Figure 7***A,B & ***Table 12***). Slow wave amplitudes decrease further (i.e. increased the deflection) during SWS compared to WASO and REM sleep, but were not significantly different within SWS stages. (***Figure 7***C,D). When comparing the difference in peak and slow wave amplitudes ($V^{peak} - V^{SW}$), a clear gradual increase with decreasing arousal could be seen (***Figure 7***E,F), with post-hoc tests showing a gradual increase of spike-wave deflection with increasing depth of sleep ($S3 > S2 > S1$). Neither the spike, wave or difference, was different between pre-sleep and REM.

Firing rate modulation during IEDs increases deeper stages of NREM sleep

Over all patients and nights, 112 putative single units (SUA), and 131 multiunits (MUA) were extracted (***Table 11***). In all patients, individual peri-stimulus time histograms (PSTHs) showed increases in firingrates time-locked to the IED spike, as well as more gradual and sustained decreases during the subsequent slow wave period (***Figure 23-Figure 32***). Some units only responded with an increase during the spike, while some responded with only a decrease during the slow wave. Many units showed both, however, and the average response showed a strong modulation consistent with the LFP (***Figure 8***). Together, the majority of units were shown to be responsive to IEDs, i.e. showed significant changes in firing rates during IEDs versus baseline (SUA: 75.9%, MUA: 65.6%, ***Table 11***).

To statistically test the effect of sleep stages on firing rate modulation during IEDs, the average firing rates of each unit during the spike or slow wave periods (***Figure 8***) were entered into a mixed model. Firing rates during IED spikes increased significantly during NREM sleep (***Figure 9***A&B, ***Table 13***) compared to the period before and after sleep. Firing rates during IED spikes were also

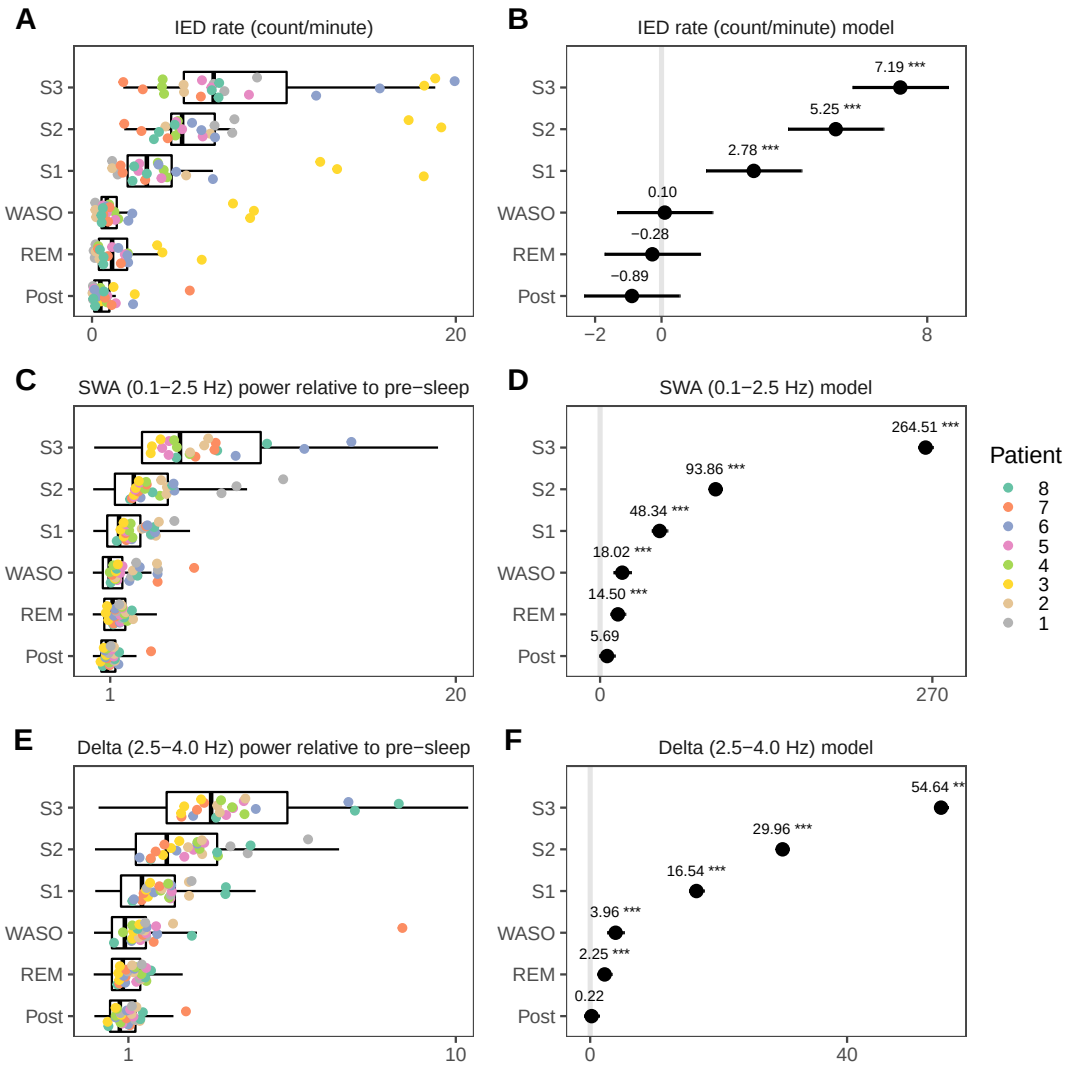

Figure 4. Summary statistics of IED rate, slow wave activity (SWA) and delta power per sleep stage, with box plots overlaid by values representing averages per patient (colored) and night. **A** and **B** show the rate of IEDs relative to the Pre-sleep period, and the fixed effects estimations, respectively. See ***Table 7*** for statistical tests. **C** and **D** show the power in the SWA band ($0.1\,\mathrm{Hz}$ to $2.5\,\mathrm{Hz}$) relative to the pre-sleep period, and the fixed effects estimations, respectively. See ***Table 9*** for statistical tests. **E** and **F** show the power in the delta band ($2.5\,\mathrm{Hz}$ to $4\,\mathrm{Hz}$) relative to the pre-sleep period, and the fixed effects estimations, respectively. See ***Table 10*** for statistical tests.

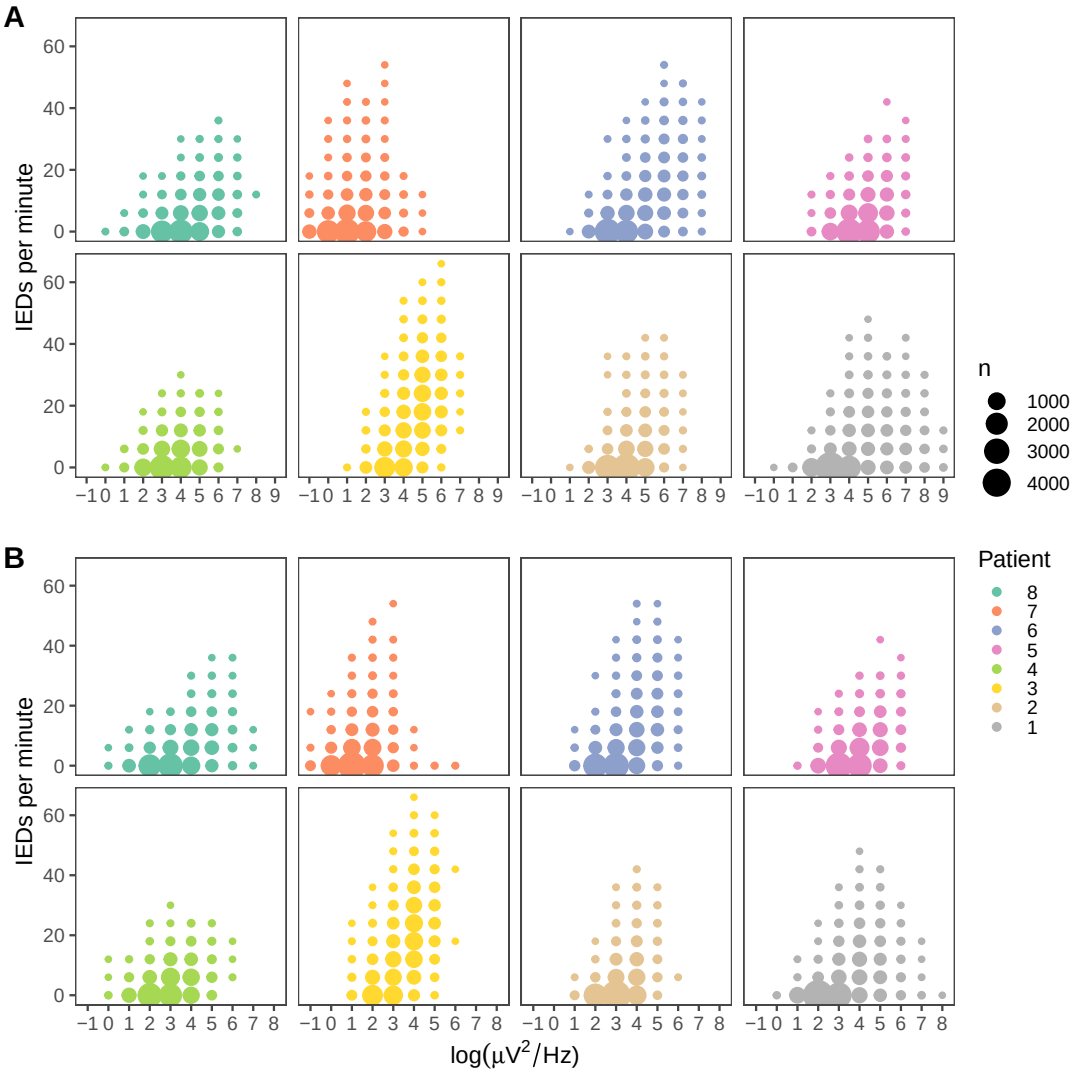

Figure 5. IED rates increase with increasing (**A**) slow wave activity ($0.1\,\mathrm{Hz}$ to $2.5\,\mathrm{Hz}$), and (**B**) delta ($2.5\,\mathrm{Hz}$ to $4\,\mathrm{Hz}$) power. For visualization, power was log-transformed, and both IED rates and power were binned. The size of the dots are proportional to the total number of observations in each bin. See ***Table 8*** for statistical test.

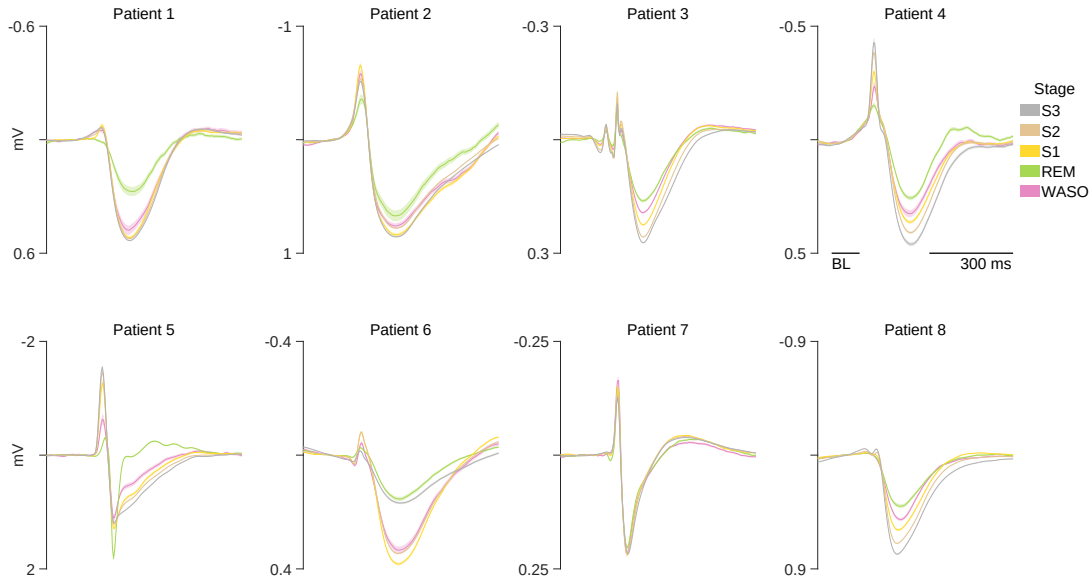

Figure 6. Average IED LFP for each patient (panel) and sleep stage (color).

slightly increased during wake periods sleep onset (WASO). No differences were found between NREM and REM sleep, nor between REM and wake periods. During the subsequent slow wave, NREM (as well as WASO) also significantly decreased firing rates further, compared to waking periods (***Figure 9***C & D). REM was not found to affect firing rates during either the peak or slow wave. Finally, the normalized difference in firing rates between peak and slow waves (***Figure 9***E&F) summarized the effect of NREM sleep on firing rate modulation during IEDs. During NREM sleep, as well as during WASO, the firing rate difference between peak and slow wave were increased. None of comparisons showed differences between S1, S2 and S3, and in all comparisons REM sleep did not differ significantly from waking periods.

Unit resting behavior changes with deeper stages of NREM sleep

Resting baseline activity of units, i.e. during periods in which no IEDs occurred, was investigated by epoching the first 72 hours in 10-second non-overlapping intervals. These epochs were labeled according to the stage of sleep in which they occurred, and excluded if they overlapped with IEDs or artefacts.

Mixed models showed that SUA and MUA firing rates, as well as bursting rates decreased significantly with increasing depth of sleep, with post-hoc tests verifying a progressive increase ($pre > REM > S1 > S2 > S3$, ***Figure 10***A-F & ***Table 14***). CV2 also increased significantly, in an almost linear fashion until a large increase during S3 ($S3 >> S2 > S1 > Wake > REM$), indicating decreasing regularity of action potential firing with decreasing depth of sleep **(*Figure 11*A & B)**. Finally, the amplitudes of the action potential increased significantly during all stages of sleep compared to both the pre and post period (***Figure 11***C & D), in which post-hoc comparisons showed a progressive increase wioth $S3 > S2 > S1$.

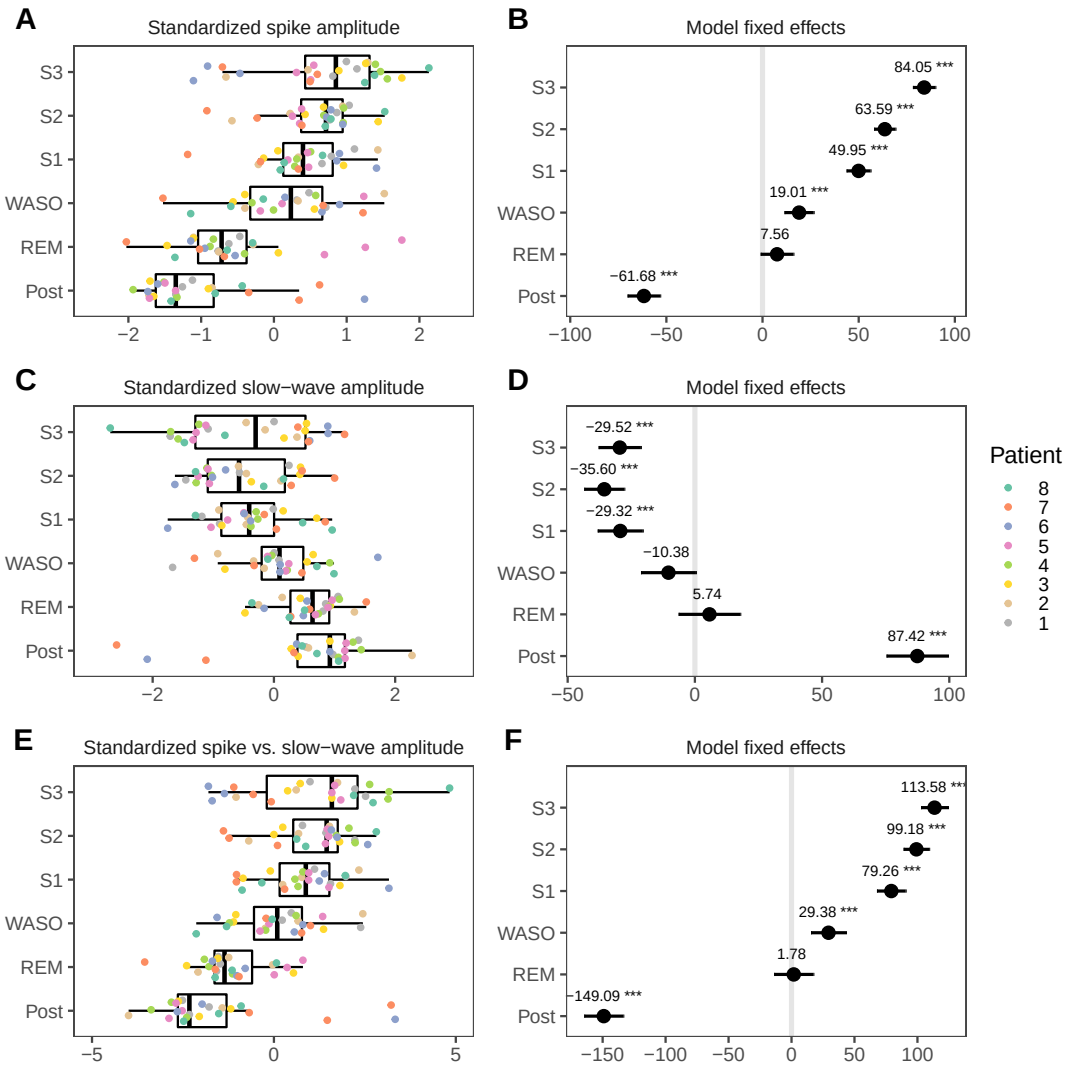

Figure 7. Summary statistics of IED amplitude per sleep stage, with box plots overlaid by values representing averages per night, per patient (colored). **A** & **B** shows the average amplitude during the IED spike relative to those during the pre-sleep period, and the fixed effects estimations of the comparisons, respectively. **C** & **D** shows the average amplitude during the IED slow wave relative to those during the pre-sleep period, and the fixed effects estimations of the comparisons, respectively. **E** & **F** show the total deflection of the spike and wave ($V^{peak} - V^{SW}$) relative to the pre-sleep period, and the fixed effects estimations, respectively. See ***Table 12*** for a summary of statistics.

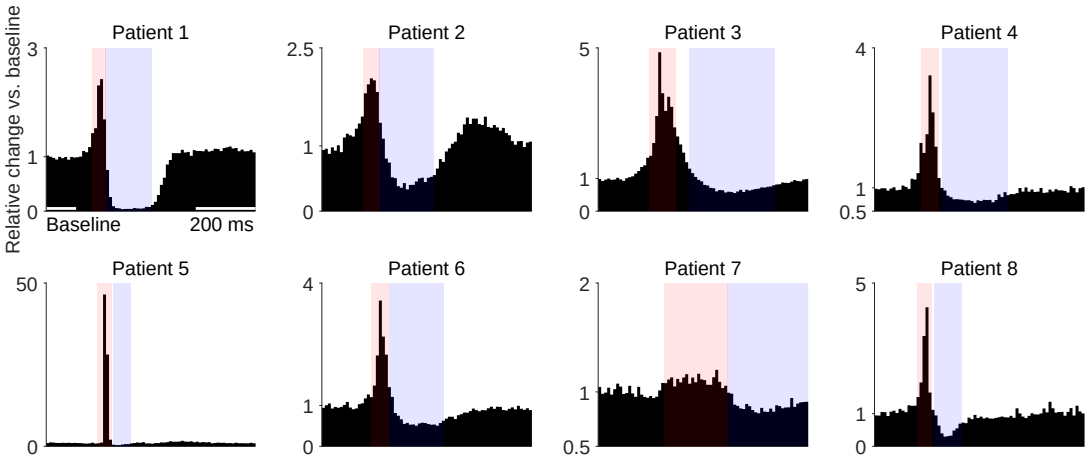

Figure 8. Peri-stimulus time histograms (PSTH) of all responsive units, templates and sleep stages, separately for each patient, including the average LFP showing the consistency between the PSTH and the LFP. For each patient, template and unit, firing rates were standardized by dividing the PSTH by the mean firing rate during baseline (indicated in the first panel). Red and blue overlays indicate intervals for statistical tests of the sharp wave and slow wave, based on the width at half-prominence (***Figure 9*** & ***Table 13***).

Discussion

Rate of interictal activities in mesial structures are under circadian influence

All eight patients showed a circadian distribution of IED rates, with seven peaking between 01:00 and 03:30 at night, consistent with previous reports (11:00-05:00 in ***Anderson et al.*** (***2015***), 02:21-04:12 in ***Spencer et al.*** (***2016***) and one of the clusters at 04:00, 02:00, and 06:00 in ***Baud et al.*** (***2018***)). While our population was heterogeneous with regard to the seizure onset zone (SOZ), including prefrontal, temporal, multifocal, and amydalo-hippocampal regions, all showed IEDs in mesial structures. Only one patient, with a SOZ in the left parietal region, did not show a nightly peak in IED rates from mesial structures. Although the sample size of our study prevent conclusions on the effect of the SOZ, previous studies have shown that the seizure onset zone (SOZ) and anatomical location do not effect circadian influences on interictal activity (***Lieb et al., 1980***; ***Rossi et al., 1984***; ***Sammaritano et al., 1991***; ***Malow, 2005***; ***Foldvary-Schaefer and Grigg-Damberger, 2006***; ***Hofstra and de Weerd, 2009***; ***Derry and Duncan, 2013***; ***Daley and DeWolfe, 2018***; ***Khan et al., 2018***), but see ***Lambert et al.*** (***2018***).

Seizure occurrence is under influence circadian influence

Several patients showed a circadian influence on the occurrence of seizures. However, peaks of seizure occurrence were spread out along the day/night cycle. Patient 1, 3, 4 & 7 showed a circadian peak in the early evening, late morning, early evening, and night, respectively. This did not seem to be associated with a particular SOZ, which were frontal, temporal, temporal and parietal, respectively. Patient 5, and possibly Patient 3, showed a bimodal distribution, with a peak in the morning and evening, and a multifocal and temporal SOZ, respectively. The number of seizures of Patient 2, 6 & 8 were not sufficient to identify any potential circadian pattern. These results are in line with previous literature, showing circadian peaks in seizure occurrence (***Anderson et al., 2015***;

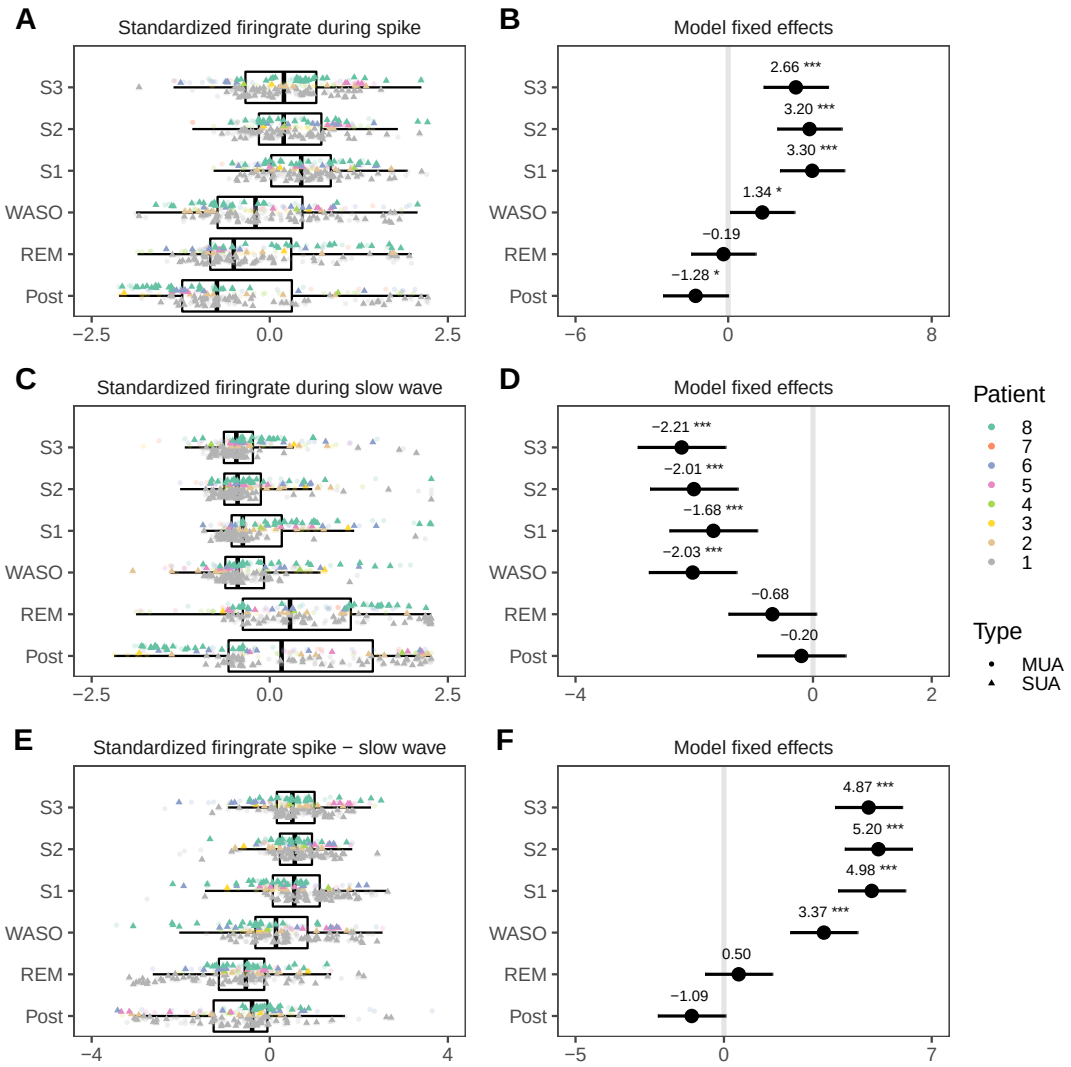

Figure 9. Unit firing rates during the spike and slow wave periods of the interictal discharges. **A**, **C** & **E** show box plots overlaid by values representing averages per patient (colored) and unit. Pyramid shapes and dots represent SUA and MUA, respectively. For display purposes, values were normalized over all sleep stages. **B**, **D** & **F** show model estimates of fixed effects, including annotations for significant differences versus pre-sleep ($p < 0.05^{\cdot}$, $p < 0.01^{*}$, $p < 0.001^{**}$, $p < 0.0001^{***}$). See ***Table 13*** for a summary of the statistics.

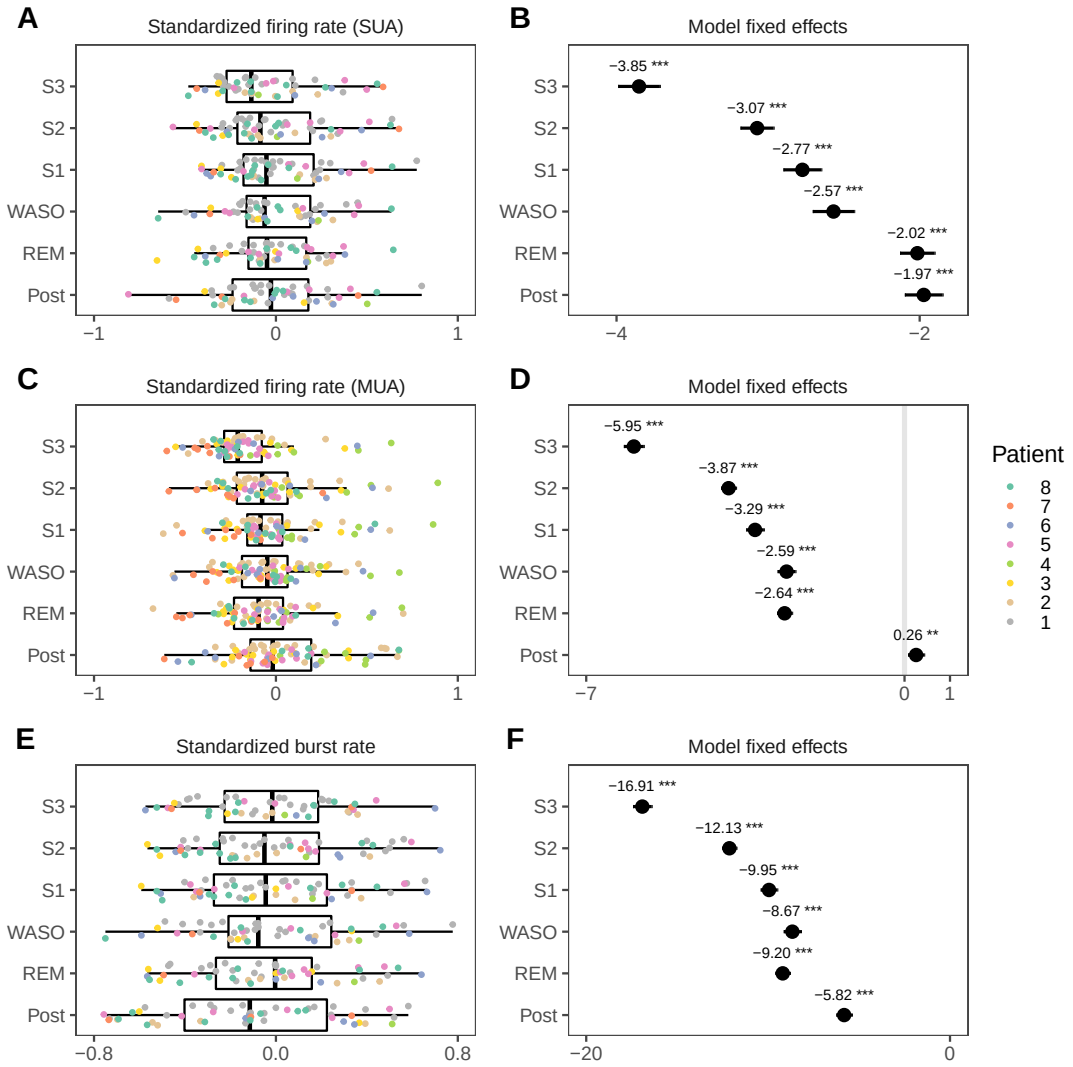

Figure 10. Summary statistics of average unit characteristics during rest, in different sleep stages. **A**, **C** & **E** show box plots overlaid by values representing averages per patient (colored) and unit. For display purposes, values were standardized as relative change versus pre-sleep according to $\frac{x-Pre}{x+Pre}$). **B**, **D** & **F** show model estimates of fixed effects, including annotations for significant differences versus pre-sleep ($p < 0.05^{\cdot}$, $p < 0.01^{*}$, $p < 0.001^{**}$, $p < 0.0001^{***}$). Only SUA were included in the calculation of burst rates. See ***Table 14*** for a summary of statistics.

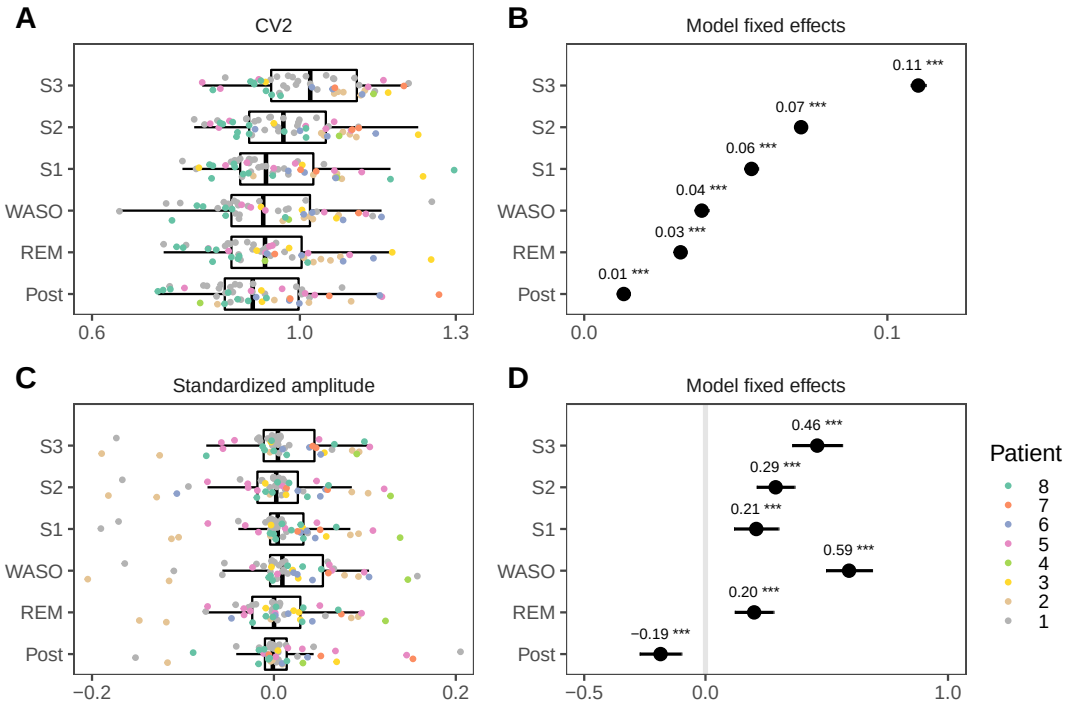

Figure 11. Summary statistics of average unit characteristics during rest, for different sleep stages. **A** & **C** show box plots overlaid by values representing averages per patient (colored) and unit. For display purposes, values were standardized as relative change versus pre-sleep: $\frac{x-Pre}{x+Pre}$). **B** & **D** show model estimates of fixed effects, including annotations for significant differences versus pre-sleep ($p < 0.05^{\cdot}$, $p < 0.01^{*}$, $p < 0.001^{**}$, $p < 0.0001^{***}$). Only SUA were included. See ***Table 14*** for a summary of statistics.

Durazzo et al., 2008; *Karafin et al., 2010*; *Hofstra et al., 2009b*,a; *Pavlova et al., 2009*; *Badawy et al., 2009*) with frontal lobe seizures generally peaking very early in the morning, and mesial temporal lobe seizures showing a more bimodal distribution, with a primary peak in the late afternoon and a secondary peak in the morning (*Quigg, 2000*; *Quigg et al., 2000*; *Durazzo et al., 2008*; *Hofstra et al., 2009a*,b; *Pavlova et al., 2009*; *Nzwalo et al., 2016*; *Spencer et al., 2016*). The exact timing of the peaks are known to vary considerably between studies and patients, likely due to inconsistencies in protocols and analyses, as well as factors such as samples size, sample demographic, geographic location, seizure focus, and individual differences in circadian rhythms *Mirzoev et al.* (*2012*); *Hofstra and de Weerd* (*2009*); *Smyk and van Luijtelaar* (*2020*). Our results are consistent with varied circadian patterns in seizure occurrence, showing that temporal seizures display single and bimodal distributions throughout the day/night cycle, although the fact that our patient population had heterogeneous SOZ location might also have contributed to the variation in circadian distributions.

IED rate and amplitude are modulated by sleep stage

Consistent with previous studies, the IED rate increased progressively during NREM sleep ($S3 > S2 > S1 > Wake$) (*Lieb et al., 1980*; *Rossi et al., 1984*; *Sammaritano et al., 1991*; *Ferrillo et al., 2000*; *Bagshaw et al., 2009*; *Karoly et al., 2016*; *Spencer et al., 2016*; *Lambert et al., 2018*) and no differences in IED rates between REM and wake (*Sammaritano et al., 1991*), although the latter has been occasionally reported (*Ng and Pavlova, 2013*; *Rossi et al., 1984*). Consistent with previous reports (*Malow et al., 1998*; *Ferrillo et al., 2000*; *Fürbass et al., 2021*), we found that IED rates were positively correlated with power in the slow wave ($0.1\,\mathrm{Hz}$ to $2.5\,\mathrm{Hz}$) and delta ($1\,\mathrm{Hz}$ to $4\,\mathrm{Hz}$) frequency range.

The increase in IED rates during SWS and their suppression during REM sleep has been hypothesized to be due to increased brain synchronization during SWS and decreased synchronization during REM sleep (*Nayak et al., 2018*; *Malow and Aldrich, 2000*). In fact, the same networks of cortical neurons involved in synchronizing thalamically generated delta oscillations during SWS may serve as the preferential substrate for epileptiform spike-wave activity (*Steriade and Contreras, 1995*; *Steriade et al., 1998*; *Steriade, 2005*; *Halász, 2013*). Several studies reported an increase in the spatial distribution of IEDs during SWS and a decrease during REM sleep (*Sammaritano et al., 1991*; *Malow and Aldrich, 2000*; *Méndez and Radtke, 2001*; *Busek et al., 2010*; *Rocamora et al., 2013*; *Del Felice et al., 2015*; *Okanari et al., 2015*; *Scarlatelli-Lima et al., 2016*; *Janca et al., 2018*; *Nayak et al., 2018*; *Conrad et al., 2020*; *Kang et al., 2020*). However, differences in IED amplitudes were rarely reported and in none of the aforementioned studies. An increase in IED amplitudes could result in increases in electrical field spread, which could be misinterpreted as an increase in spike propagation. Furthermore, the extent of the reported changes in the spatial distribution has generally been small and not unequivocally found. For example, *Rocamora et al.* (*2013*) found that while interictal activity shifted from anterior to posterior and from mesial to lateral during sleep, the source of interictal activity remained localized within the amygdalo-hippocampal complex. *Asano et al.* (*2007*) found no effects of sleep on the spatial distribution, and *Conrad et al.* (*2020*) found spatial distribution not to be predictive of seizure occurrence. Finally, *Lambert et al.* (*2018*) found

an increase in co-occurrence of different interictal sources during SWS, but only for neocortical spikes, not mesial-temporal spikes. Together, the reported changes in the spatial distribution of IEDs are small and inconsistent, while robust studies of the effect of sleep on the amplitude of IEDs have been missing. The current study analyzed an unprecedented number of IEDs (3500 to 12811 per patient) from continuous data recorded over three day/night cycles and found clear evidence of an increase in IED amplitude during sleep. The LFP deflections of both the spike and slow wave were found to be gradually increased with deeper stages of sleep.

Interictal activity modulates firing rates of the majority of neurons

Early studies found that some neocortical neurons discharged in time with interictal spikes (***Ishijima et al., 1975***). These have been termed "positive" (***Ishijima, 1972***) or "involved" neurons (***Prince and Futamachi, 1970***), and were considered to reflect the intensity of epileptic activity. More recent studies have consistently found that a proportion of units increase their firing rate during the interictal spike, which is then reduced during the subsequent slow wave (***Wyler et al., 1982***; ***Ulbert et al., 2004***; ***Fabó et al., 2008***; ***Keller et al., 2010***; ***Alvarado-Rojas et al., 2013***).

Our results show a consistent pattern across all patients. Units increased their firing rate sharply during, or right before, the upward flank of the sharp LFP spike, then reduced their firing rates to below baseline, highly consistent with the shape of the LFP slow wave. Only one patient (Patient 7) did not show fast and strong firing rate modulation during the IED spike. However, in the rest of the patients, the majority of units showed significant changes in firing rates versus baseline (SUA: 75.9%, MUA: 65.5%). This high proportion of "involved" units is somewhat higher than the 49% found by ***Wyler et al.*** (***1982***), the 48% by ***Keller et al.*** (***2010***), and the 40% by ***Alvarado-Rojas et al.*** (***2013***). However, methods to determine whether a unit modulates its firing rate during IEDs depend on the sensitivity of the design and statistical methods. The early work by ***Wyler et al.*** (***1982***) was visually performed based on a relatively small number of IEDs, the number of which were not reported but indicated to be less than 50 in the representative figures. ***Keller et al.*** (***2010***) removed sleep periods in their analysis and reported a large variability in the number of manually annotated IEDs per patient (31–608). In the current study, IEDs were automatically detected on three days, resulting in 2106 to 12912 IEDs *per patient*. While it stands to reason that the increased number of data points increased the sensitivity, clinical differences could also explain the higher rate of responsive neurons. In ***Wyler et al.*** (***1982***) and ***Alvarado-Rojas et al.*** (***2013***) clinical information was not provided. In ***Keller et al.*** (***2010***), 269 out of 363 units were recorded from dysplasic cortex, of which 26 had a cryptogenic origin, and the remaining 73 units came from patients with various lesions. Furthermore, different recording methods were used to record LFP and spike data from diverse regions and with a large variation in the distance to the SOZ. Although our population also showed heterogeneous SOZs, recordings of LFP and spike data were all restricted to the hippocampal-amygala complex. The hippocampal formation has anatomical and physiological mechanisms that promote neuronal synchronization, making this region very prone to epileptic discharges. It should be noted that using a similarly sensitive statistical approach in a recent study on periventricular nodular heterotopia, all units were shown to respond to interictal events (***Frazzini et al., 2022***). Together, our findings are consistent with the paroxysmal depolarizing shift (PDS)

mechanism in which a large depolarization phase is followed by a long hyperpolarization found in animal (***Matsumoto and Marsan, 1964***; ***Prince, 1968***), and consistent with *in vitro* studies on hippocampal slices from human patients with temporal lobe epilepsy (***Cohen et al., 2002***; ***Wittner et al., 2009***; ***Keller et al., 2010***).

Firing rates modulation increases with deeper stages of NREM sleep

While modulation of firing rates during IEDs has been established and replicated here, it is unknown whether this modulation is under the influence of sleep. Our results show for the first time that the firing rate during the sharp LFP peak is significantly increased during sleep compared to waking periods, while firing rates during the subsequent slow wave are significantly reduced.

The first part of the PDS depolarization phase is believed to be generated by intrinsic membrane conductances (***de Curtis et al., 1999***), and the later from feedback recurrent synaptic excitation mediated by AMPA and NMDA receptor subtypes, and glutamate receptor-coupled calcium conductances (***Traub et al., 1993***). The subsequent hyperpolarization represents GABA-mediated recurrent inhibition, as well as Ca2+-dependent outwards K+ currents. Our results suggest that sleep increases excitability and synchronization of neuronal populations, increasing both the probability of the occurrence of IEDs, as well the degree of de-facilitation by subsequent hyperpolarization.

Neuronal baseline activity is modulated by sleep stages

Neuronal baseline activity, i.e. resting behaviour in the absence of IEDs, was investigated by means of firing rates, burst rates and CV2. These were calculated from a large number of non-overlapping 10-second time windows in 72 hours, allowing robust estimations of conditional means within patients. By using mixed models, we dealt with both between-subject and within-subject variance. Firing rates, burst rates and CV2 were all shown to be lower under increasing depth of sleep, and especially pronounced during SWS. A reduction in the firing rate during SWS is consistent with the periodic suppression of neuronal firing due to SWA during NREM sleep, as shown in animal *in vivo* intracellular recordings (***Timofeev et al., 2001***; ***Vyazovskiy et al., 2009***). Although measures of regularity were not reported in these studies, decreased regularity with decreased depth of sleep could be explained by such “clumping together” (***Timofeev et al., 2001***) of action potentials.

These studies, as well as our own findings, are in partial disagreement with ***Staba et al.*** (***2002b***), who reported a reduced firing rate in REM versus wake and SWS, a higher propensity for bursting during SWS versus wake and NREM, and increased variability (CV2) in SWS versus wake. However, these analyses were performed on only 23 neurons and, as the authors themselves noted, potential influences from interictal discharges were not considered. Another study of the same lab included a larger number of isolated neurons (72), and reported higher burst rates in MTL regions, but only during sleep (SWS and REM), and lacking consistent difference in firing rates between sleep stages or between epileptic versus non-epileptic regions (***Staba et al., 2002a***).

Although early human studies found indications of bursting in epileptic regions (***Calvin et al., 1968***; ***Wyler et al., 1973***), others found no differences in firing patterns such as bursting between neurons in the epileptic focus or surrounding area (***Ishijima et al., 1975***). In fact, while some studies continued to associate bursting behavior with epilepsy in both animal (***Connors, 1984***) and human

in vitro studies (***Prince and Wong, 1981***; ***Hofer et al., 2022***), microelectrode recordings in epileptic patients have so far returned contradictory results, showing both increased (***Staba et al., 2002a***; ***Gast et al., 2016***) and decreased (***Colder et al., 1996***) bursting in the SOZ of MTL patients.

Automatic detection of IEDs

The current study exploited the possibility of analyzing a very large number of IEDs by using automatic detection of IEDs. Many algorithms have been proposed for IED detection over the last decades (***Wilson and Emerson, 2002***; ***Halford, 2009***; ***Halford et al., 2013***; ***da Silva Lourenço et al., 2021***), with recent implementations showing good, or better, performance than human experts (***Brown et al., 2007***; ***Nonclercq et al., 2012***; ***Scheuer et al., 2017***; ***Reus et al., 2022***). Recent examples include the use of adaptive morphological filters (***Krishnan et al., 2014***), signal envelope distribution modeling (***Janca et al., 2015***; ***Peter-Derex et al., 2020***), convolutional neural networks (CNN) and deep learning (***Lourenço et al., 2020***; ***Constantino et al., 2021***; ***Fukumori et al., 2019***; ***Tjepkema-Cloostermans et al., 2018***; ***Fürbass et al., 2020***; ***Antoniades et al., 2017***), long short-term memory (LSTM) neural networks (***Medvedev et al., 2019***) and generative adversarial networks (GANs) (***Geng et al., 2021***; ***Tanaka and Aranha, 2019***). Two-step methods have been proposed to reduce the need to manually optimize parameters per different datasets (***Liu et al., 2013***; ***Bagheri et al., 2019***). Furthermore, machine learning models need to be trained on large standardized datasets of annotated data to deal with the challenge of generalizing models over different patients. Such datasets currently do not exist, but are necessary to objectively compare the performance of the available machine learning approaches (***Wilson and Emerson, 2002***; ***Halford et al., 2013***; ***da Silva Lourenço et al., 2021***). Furthermore, the inherent unbalanced nature of interictal data, i.e. the small ratio of positive events within large periods of background activity, has only recently been addressed (***Wang et al., 2023***).

The use of LFP templates provide a more robust and transparent alternative, and have been shown to outperform any classifier trained on morphological features (***Horak et al., 2015***). Template matching approaches have also been shown to perform very well even with high noise situations such as recordings taken from within an fMRI scanner (***Hao et al., 2018***). Some studies have used templates derived from databases (***Lodder and van Putten, 2014***), used patient-specific annotations (***Quon et al., 2022***), or performed clustering of patient-specific IEDs for rapid visual inspection and validation ***Fürbass et al.*** (***2020***). In the current study, we chose to employ template matching based on patient-specific IED templates, extracted from visual annotations of 24 hours. The approach showed to be highly effective, while remaining relatively straightforward. Importantly, the templates can be visually evaluated, in contrast to “black-box” approaches using machine learning. By expanding the IEDs into six templates per patient, potential variations in the morphology of IEDs were taken into account as well.

Conclusion

The current study evaluated for the first time the influence of sleep stages on neuronal firing during interictal activity, by means of *in vivo* recordings from hippocampal structures in epileptic patients. This was done with an unprecedented large dataset of continuous recordings of several nights, and

thousands of IEDs per patient. The IED rate as well as amplitude were found to be increased with deeper stages of NREM sleep. Neuronal firing rates were found to increase during the IED spike, and decreased during the slow wave. Importantly, these firing rate modulations during IEDs were increased with deeper stages of NREM (SWS) sleep, versus REM and wake. Finally, during resting default behaviour, the neuronal firing rate, bursting rate and firing regularity were all shown to progressively decrease with deeper stages of NREM sleep. Together, this study provides the first evidence from human *in vivo* recordings, showing that sleep increases neuronal synchronization and subsequent de-facilitation during interictal epileptiform activity.

Methods and Materials

Patients

Eight drug-resistant focal epilepsy patients were selected from our database (***Lehongre et al., 2022***), with the following criteria: 1) Implantation of macroelectrodes targeting the mesial temporal structures, 2) microelectrode recordings with visible MUA, and 3) polysomnography recordings during the first three nights. See ***Table 1*** for clinical details.

SEEG recording

Patients were implanted with intracerebral depth electrodes (Ad-Tech®, Oak Creek, Wisconsin, USA), consisting of 4 to 8 platinum macroelectrode contacts, $2.41\,\mathrm{mm}$ long (Ø=$1.1\,\mathrm{mm}$). Each patient was also implanted with one to three Behnke-Fried type macro-micro electrodes (Ø=$1.3\,\mathrm{mm}$) that included eight additional microelectrodes and a reference wire of $\approx 2\,\mathrm{mm}$ long (Ø=$40\,\mu\mathrm{m}$), extending from the tip of the electrode shaft and capable of recording non-overlapping cell populations (***Fried et al., 1999***). Trajectories, anatomical targets, number, type and the number of contacts were all determined according to the clinical practice and the epilepsy features of the patients. Implantation was performed in the Department of Neurosurgery of the Pitié-Salpêtrière Hospital using a Leksell Model G stereotactic system (Elekta, Inc., Norcross, GA) or using a robotic assistant device (ROSA® Brain, Medtech, France). For more details and evaluation of the implantation procedures, see ***Mathon et al.*** (***2015***) and ***Lehongre et al.*** (***2022***).

The locations of the anatomical electrodes after implantation were determined by VF (***Table 2***), based on pre-implantation $3\,\mathrm{T}$ 3D-MRI, post-implantation $1.5\,\mathrm{T}$ 3D-MRI and post-implantation CT scan, combined using the EpiLoc plugin (***Pérez-García et al., 2015***) for 3D-Slicer (***Fedorov et al., 2012***), developed by the STIM engineering facility at the Paris Brain Institute. Spatial locations of the electrodes were automatically computed in native space using the EpiLoc plugin, and visualized (***Figure 12***) using BrainNet Viewer (***Xia et al., 2013***), after transformation from to MNI-space (***Table 3***) using the Freesurfer image analysis suite integrated in Epiloc.

All patients gave their written informed consent (project C11-16 conducted by INSERM and approved by the local ethics committee, CPP Paris VI).

Polysomnography

During long-term video-EEG monitoring, video-EEG and polysomnography (PSG) were simultaneously recorded for the first three nights post-implantation. When the first night was too disturbed,

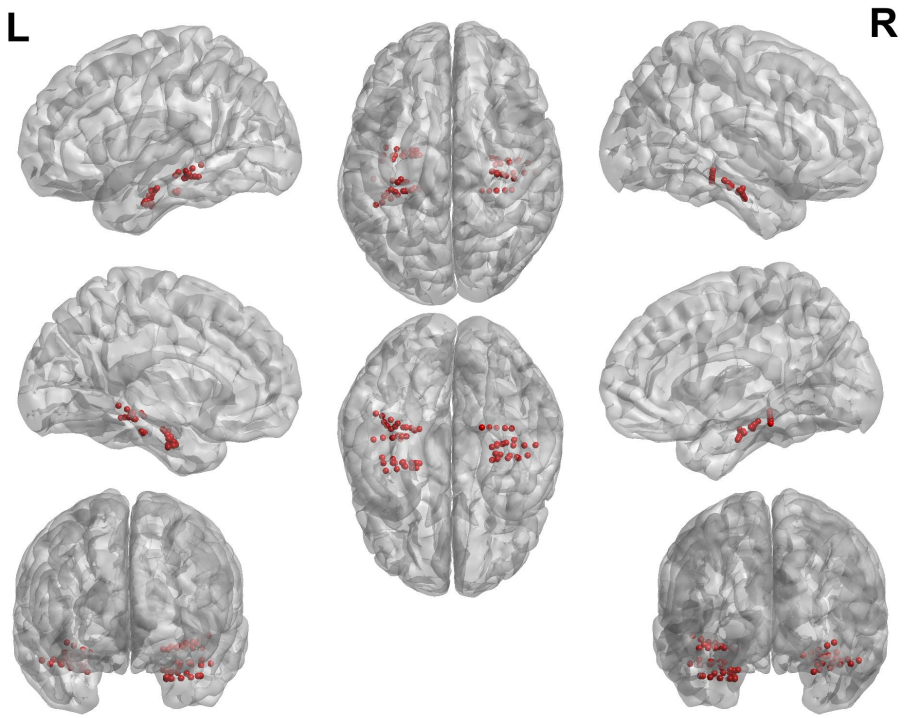

Figure 12. Locations of each analysed electrode contact, transformed to MNI space. See ***Table 3*** for MNI coordinates

an extra night was scored and the first night was not analyzed. PSG included three EEG channels (Fp2, C4 & O2, or Fp1, C3 & O1, referenced to linked mastoids M1 or M2, respectively), right and left electro-oculography (EOG) channels, chin electromyography (EMG) and electrocardiography (ECG). Sleep scoring using PSG recording was performed by VH-NM, according to the American Academy of Sleep Medicine (AASM) 2017 criteria (***Berry et al., 2017***). Before sleep onset, and after the final awakening, a continuous period of two hours was labelled *pre-sleep* (or *pre*) and *post-sleep* (or *post*), respectively.

Sleep quality was varied among patients and nights (***Table 6***). However, all patients had a sufficient amount of sleep per night (average = 8 hrs., range = 6.5-11.9 hrs.). Light sleep (S1) somewhat increased above normal (15% vs. <5%), while deep sleep (average S3 = 20%) and REM (average = 19%) were normal (***Dauvilliers and Billiard, 2005***). Hypnograms show a frequent sleep fragmentation (***Figure 14***), which might be explained by multiple factors, including the post-surgery and hospitalized condition.

Analysis

Analyses were performed with a combination of FieldTrip functions (***Oostenveld et al., 2011***), custom MATLAB scripts (Version 2020b, The Mathworks Inc., Natick, Massachusetts). All analysis scripts are available here.

Artefact detection

In the first three days (72 hours) of continuous recording, periods with movement artefacts or instrumentation noise in macro- or microelectrode recordings were manually annotated using software developed in-house (MUSE) for synchronous visualization of macro- and microelectrode signals (***Lehongre et al., 2022***). Data from one night (second) of a patient (patient 3) was replaced by a fourth night, due to excessive artefacts, and the polysomnography was then performed on that night as well.

IED detection

For each patient, IEDs were manually annotated for the first 24 hours, according to standard guidelines (***Hirsch et al., 2013***, ***2021***) using in-house developed software (MUSE) (***Lehongre et al., 2022***). IEDs were subsequently automatically detected for the full duration of the recording during (2-3 weeks) based on the following procedure (***Figure 13***):

1. The time-courses (trials) of the five deepest contacts were extracted ($-500\,\mathrm{ms}$ to $1000\,\mathrm{ms}$) at the original sample rate of $4\,\mathrm{kHz}$ according to manual annotations.
2. Trials were temporally aligned (c.f. ***Frazzini et al.*** (***2022***)) based on the cross-correlation between each trial and the average of all trials. This procedure was performed iteratively by calculating a new average after all trials were shifted to their peak cross-correlation lag, until either the cross-correlation did not improve or a maximum of 10 iterations was reached. To calculate the cross-correlation lag over channels simultaneously, signals from the five electrode contacts were concatenated over time.
3. Once aligned, the trials were clustered in six k-mediods clusters using the MATLAB *kmedoids* function (The Mathworks Inc., Natick, Massachusetts).
4. If a cluster contained less than 2.5% of the total number of trials in that patient, these trials were automatically removed from the clustering procedure and the k-mediods clustering was repeated.
5. Each cluster was aligned to the LFP average of the cluster, similar to (2), then re-averaged, resulting in a patient-specific Channel $\times$ Time IED template.
6. Normalized cross-correlation was calculated between each template and the original data using the MATLAB *normxcorr2* function (The Mathworks Inc., Natick, Massachusetts).
7. Patient-specific correlation thresholds were visually determined based on the distribution of correlation values over time. IEDs were then detected when the peaks in the correlation values exceeded the threshold, using the MATLAB *findpeaks* function (The Mathworks Inc., Natick, Massachusetts)
8. IED detections that overlapped within a $\pm 50\,\mathrm{ms}$ period were assigned to the template with the highest normalized cross-correlation value.

The above automatic IED detection procedure effectively dealt with the within-subject variability of IED morphologies by using six clusters rather than a single template, as well as their spatial distribution by using normalized correlation over five contacts. Only a single patient-specific parameter (z-threshold) was needed. Importantly, this parameter was unbiased with regard to sleep stages.

The procedure was straightforward and allowed the visual inspection of templates. To test the performance of the automatic detection procedure, the hit and false alarm rates were determined using a tolerance of $\pm 50\,\mathrm{ms}$ to allow for small differences in timing between manual and automatic detection.

Spike sorting

After selecting electrodes that visually showed multi-unit activity (MUA) activity, clusters of action-potentials were automatically detected and clustered using Spyking Circus (***Yger et al., 2018***). Data was first high-pass filtered as $300\,\mathrm{Hz}$ using a 3rd order Butterworth filter, then temporally whitened. Action potentials were detected at a user-defined 6 to 9 median absolute deviation, depending on the signal-to-noise level of the recording. Action potentials that occurred during artefacted periods were ignored. A combination of density-based clustering and template matching algorithms was used to cluster the detected action potentials (***Yger et al., 2018***). Clusters that did not show a clear morphology of action potentials or that were not stable across the recording were discarded manually. Finally, the clusters were labeled as putative single-unit activity (SUA) when they reflected well-isolated activity, based on the inter-spike interval (ISI), the percentage of violations of the refractory period ($RPV = ISI < 1\,\mathrm{ms}$), and action potential morphology. Otherwise, the clusters were labeled multiunit activity (MUA).

Time-locked analyses

For each IED, the average LFP amplitudes of the sharp spike and slow wave were extracted at latencies based on the patient average, i.e. independently from any analysis of sleep stages. LFPs were first baseline-corrected at $-0.15\,\mathrm{s}$ to $-0.05\,\mathrm{s}$. For the sharp (positive) peaks, the latency was defined as periods between $-0.15\,\mathrm{s}$ to $0.15\,\mathrm{s}$ at which the average LFP exceeded half of the maximum amplitude. For slow (negative) waves, the latency was defined as periods between $-0.15\,\mathrm{s}$ to $0.05\,\mathrm{s}$ at which the average LFP was less than half of the minimum amplitude.

Spike times were epoched and time-locked to time periods identical to the LFP. For each IED, peri-stimulus time histogram (PSTH) spike rates were calculated with a bin size of $10\,\mathrm{ms}$. To control for multiple comparisons and non-normal distributions of firing-rates, non-parametric cluster-based permutation tests (***Maris and Oostenveld, 2007***) were used to determine time-periods where firing-rates changed significantly from baseline ($-0.3\,\mathrm{s}$ to $0.1\,\mathrm{s}$). A threshold of $p < 0.01$ (first-level t-test) was used to determine contiguous temporal clusters, after which a threshold of $p < 0.05$ (one-sided correction) determined whether the clusters could be explained by permutation (sum of t values, $n = 10.000$). Those clusters that significantly increased or decreased their firing rate time-locked to the IEDs were considered responsive. Clusters that showed spurious statistically significant results due to lack of data were manually changed to non-responsive. To increase the robustness of the PSTH spike rates during IEDs, templates were combined. Latencies for comparing the PSTH spike rates between sleep stages of the peak and slow wave were determined on the basis of the width at half-prominence of the average PSTH, i.e. independently from sleep stage. Pearson's correlations between LFP and PSTH of each unit were calculated after downsampling LFP to the PSTH time axis ($\frac{1}{10\,\mathrm{ms}} = 100\,\mathrm{Hz}$).

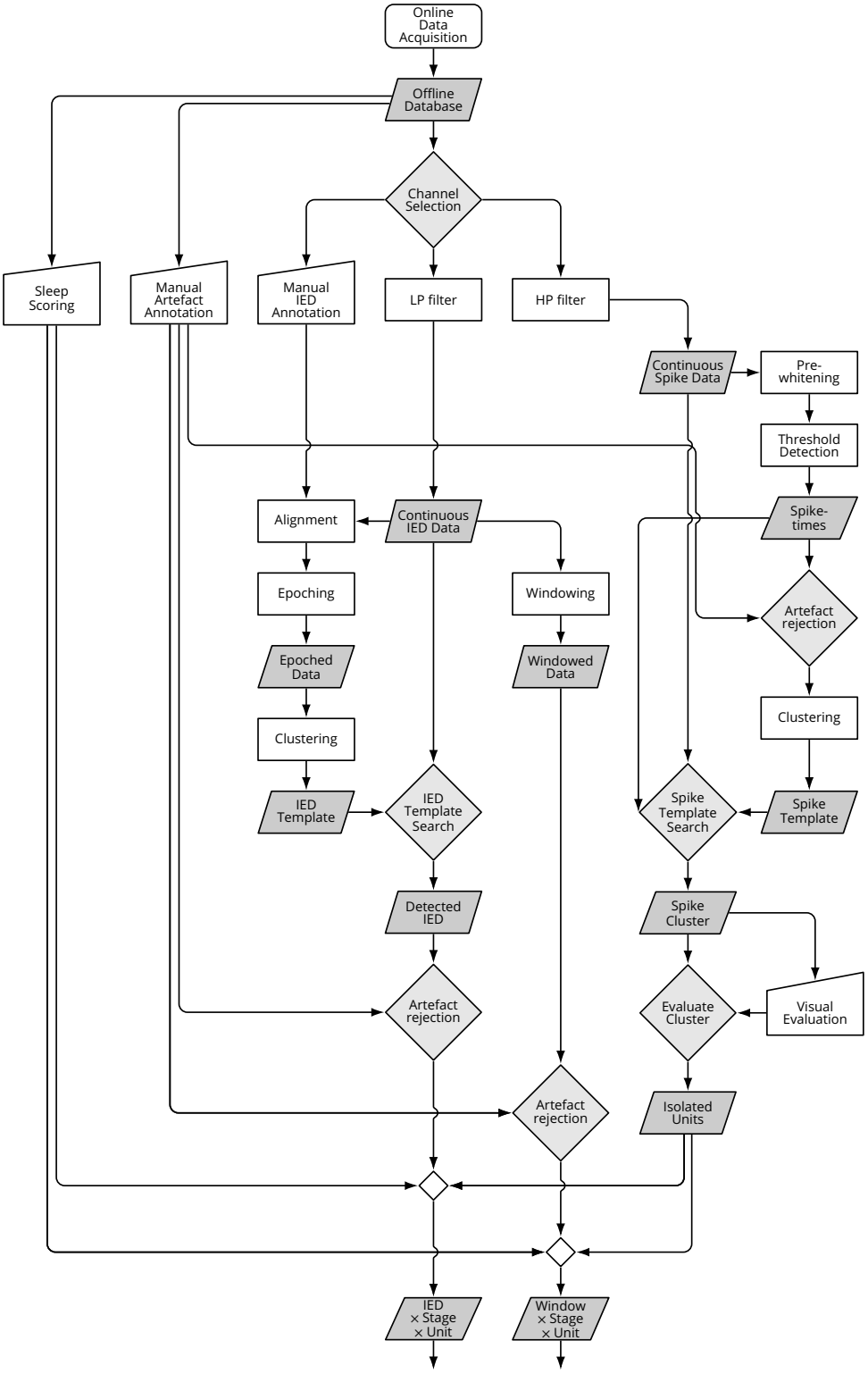

Figure 13. Visual depiction of the LFP and spike analysis workflow. See the Methods section for details.

Sliding window analyses

Analyses of continuous data were based on segmentation of the data into non-overlapping windows of 10 seconds for both LFP and spike data. The number of IEDs that occurred during these time periods was determined. If a window overlapped $> 50\%$ with a sleep stage, it was labeled with the corresponding sleep stage. Windows that overlapped with an artefacted period were removed from further analyses. Oscillatory power was calculated for every window using a Hanning tapered fast Fourier transform (FFT). The $10\,\mathrm{s}$ windows provided a frequency resolution of $\frac{1}{T} = 0.1\,\mathrm{Hz}$. Slow wave activity (SWA) (***Steriade et al., 1993***; ***Massimini et al., 2003***) was defined as the mean power in the range of $0.1\,\mathrm{Hz}$ to $2.5\,\mathrm{Hz}$, including the $0.5\,\mathrm{Hz}$ to $2\,\mathrm{Hz}$ range as suggested by the guidelines of the American Academy of Sleep (***Iber and Medicine, 2007***). Delta activity was defined as the average power in the $2.5\,\mathrm{Hz}$ to $4\,\mathrm{Hz}$ range. For each window, the firing behavior of the unit was explored. Besides firing rate analyses, inter-spike variability was determined by means of CV2 (***Holt et al., 1996***; ***Ponce-Alvarez et al., 2010***) and bursts were detected according to ***Colder et al.*** (***1996***); ***Staba et al.*** (***2002b***), using a cut-off inter-spike intervals $<5\,\mathrm{ms}$. Interspike intervals and firing rates were corrected for bursts by removing bursting action potentials beyond the first action potential in a burst.

Statistics

Statistical test were conducted with R (***R Core Team, 2013***, ***2015***), version 4.1.2. Circular statistics were performed with the circular R package (***Agostinelli and Lund, 2017***). Statistical plots were created with the ggplot R package (***Wickham, 2016***). Models of the relationships between physiological measures were tested using mixed-effects linear models (***Bates et al., 2014***), using the lmer R package (***Kuznetsova et al., 2017***), with patient, template and night (LFP analyzes) or unit (spike analyzes) as random effects. Tukey's post hoc tests were performed using the emmeans R package (***Lenth, 2016***). The R scripts for all statistical analyzes and graphs can be found together with the analysis scripts here.

Data availability

All scripts are made available here. Anonymous electrophysiology data can be made available on reasonable request for research purposes, but cannot be publicly shared due to legal constraints.

Article and author information

According to CRediT standard:

Stephen Whitmarsh

Sorbonne Université, Institut du Cerveau - Paris Brain Institute - ICM, Inserm, CNRS, APHP, Pitié-Salpêtrière Hospital, Paris, France

Contributions: Conceptualization, Methodology, Software, Validation, Formal Analysis, Investigation, Original Draft Preparation, Review & Editing, Visualization

Competing interests: No competing interests declared

Correspondance: stephen.whitmarsh@icm-institute.org

Vi-Huong Nguyen-Michel
AP-HP, Pitié-Salpêtrière Hospital, Epilepsy Unit and Reference Center for Rare Epilepsies, F-75013, Paris, France
Contributions: Methodology, Validation, Investigation, Review & Editing
Competing interests: No competing interests declared

Katia Lehongre
Sorbonne Université, Institut du Cerveau - Paris Brain Institute - ICM, Inserm, CNRS, APHP, Pitié-Salpêtrière Hospital, Paris, France
Contributions: Data-Curation, Software, Methodology, Review & Editing
Competing interests: No competing interests declared

Bertrand Mathon
Sorbonne Université, Institut du Cerveau - Paris Brain Institute - ICM, Inserm, CNRS, APHP, Pitié-Salpêtrière Hospital, Paris, France
AP-HP, Department of Neurosurgery, Pitié-Salpêtrière Hospital and Sorbonne Université, Paris, France
Contributions: Validation, Methodology, Review & Editing
Competing interests: No competing interests declared

Claude Adam
AP-HP, Pitié-Salpêtrière Hospital, Epilepsy Unit and Reference Center for Rare Epilepsies, F-75013, Paris, France
Contributions: Validation, Investigation, Project Administration, Review & Editing
Competing interests: No competing interests declared

Virginie Lambrecq
Sorbonne Université, Institut du Cerveau - Paris Brain Institute - ICM, Inserm, CNRS, APHP, Pitié-Salpêtrière Hospital, Paris, France
AP-HP, Pitié-Salpêtrière Hospital, Epilepsy Unit and Reference Center for Rare Epilepsies, F-75013, Paris, France
Contributions: Validation, Investigation, Review & Editing
Competing interests: No competing interests declared

Valerio Frazzini
Sorbonne Université, Institut du Cerveau - Paris Brain Institute - ICM, Inserm, CNRS, APHP, Pitié-Salpêtrière Hospital, Paris, France
AP-HP, Pitié-Salpêtrière Hospital, Epilepsy Unit and Reference Center for Rare Epilepsies, F-75013, Paris, France
Contributions: Validation, Formal Analysis, Investigation, Supervision, Review & Editing
Competing interests: No competing interests declared

Vincent Navarro

Sorbonne Université, Institut du Cerveau - Paris Brain Institute - ICM, Inserm, CNRS, APHP, Pitié-Salpêtrière Hospital, Paris, France

AP-HP, Pitié-Salpêtrière Hospital, Epilepsy Unit and Reference Center for Rare Epilepsies, F-75013, Paris, France

Contributions: Conceptualization, Validation, Investigation, Resources, Review & Editing, Supervision, Project Administration, Funding Acquisition

Competing interests: No competing interests declared

Correspondance: vincent.navarro@aphp.fr

Funding

Agence nationale de la recherche "Investissements d'avenir" (ANR-10-IAIHU-06)

- Vincent Navarro

Fondation de l'APHP pour la Recherche - Marie-Laure PLV Merchandising

- Vincent Navarro

The funders had no role in study design, data collection and interpretation, or the decision to submit the work for publication.

Acknowledgements

Part of this work was carried out on the CENIR-STIM and the Data Analysis (DAC) core facilities of the Paris Brain Institute (ICM). We would like to thank the Reddit communities r/LaTeX and r/stat for their help on plotting and statistics.

Tables

Table 1. Clinical summary

Patient	Sex	Age	Onset	Type	MRI	PET	SPECT	Medication	Implantation	SOZ	Surgery
1	F	18	10	FSLA, FTBS	Normal	Mesial prefrontal cortex (R)	No localization	LTG, OXC	Fronto-Temporal (R)	Mesial prefrontal cortex (R)	Yes
2	M	25	14	FSLA	Normal	Temporo-polar and temporo-mesial (L)	Amygdala, anterior insula, and frontal opercular cortex (L)	ESL, TPM, PER	Temporo-Fronto-Insular (L)	Amygdalo-hippocampal region (L)	Amygdalo-hippocampectomy (L)
3	F	34	25	FSWLA, FSLA, FTBS	Right SH (already resected at implantation)	Not available	Not available	VPA, CBZ, LTG	Bi-temporal	Bitemporal. Previously SH. Independent SOC in hippocampus (L)	No
4	F	47	24	FSWLA, FSLA, FTBS	Normal	Temporal pole (L)	Temporo basal and Lateral T1 (L)	ESL, LTG	Bi-temporal	Temporal (L)	No
5	F	30	14	FSLA, FTBS	Temporo posterior PNH (R), temporal SNH and PMG	No localization	Temporo-polar cortex (R), PNH and PMG	LTG, ZNG, LCS	Temporo-Insular (R)	Multifocal	No
6	F	27	11	FSWLA, FSLA, FTBS	Occipital porencephalic region (L)	Anterior hippocampus (L)	Temporal (L) and occipital	LCS, LTG	Temporo-Occipital (L)	Unknown	No
7	F	21	14	FSWLA, FSLA	Parietal gliotic lesion (L)	Parietal, temporal pole and temporo-lateral (L)	Temporal pole (L)	LCS, LTG	Parieto-Temporal (L)	Parietal (L)	No
8	F	38	35	FSLA	Normal	Temporomesial (R)	Lateral temporal cortex (L)	LTC, VPA, CBZ	Temporal (R)	Amigdalo-hippocampal (R)	Amygdalo-hippocampectomy (R)

PET findings indicate regions of hypometabolism. SOZ are based on sEEG evaluation, but not yet validated post-surgery. AED: Antiepileptic drugs, CBZ: Carbamazepine, ESL: Eslicarabazepine, FBTCS: Focal to Bilateral Tonic-Clonic Seizures, FIAS: Focal Impaired Awareness Seizure, FSWLA: Focal seizures without loss of awareness, IEDs: Interictal Epileptiform discharges, LCS: Lacosamide, LTG: Lamotrigine, MRI: Indications from Magnetic Resonance Imaging, OXC: Oxicarbazepine, PER: Perampanel, PMG: Polymicrogyria, PNH: Periventricular Nodular Heterotopia, SNH: Subcortical Nodular Heterotopia, SOZ: Seizure Onset Zone, TPM: Topiramate VPA: Valproic Acid, ZNG: Zonisamide.

Table 2. Anatomical locations of macro and micro electrodes

Patient	Side	Region	Subregion	SOZ
Macro contacts				
1	R	Hippocampal formation	Head of the Hippocampus	No
2	L	Hippocampal formation	Head of the Hippocampus	Yes
	L	Hippocampal formation	Hippocampus/CA1	Yes
3	L	Hippocampal formation	Head of the Hippocampus	Yes
	L	Hippocampal formation	Entorhinal cortex	No
4	L	Hippocampal formation	Hippocampus	No
	L	Hippocampal formation	Hippocampus/CA3	No
5	R	Hippocampal formation	Subiculum	Yes
	R	Nodule	Nodule	Yes
6	L	Hippocampal formation	Entorhinal cortex	No
	L	Hippocampal formation	Parahippocampus	No
7	R	Hippocampal formation	Entorhinal cortex	Yes
	R	Hippocampal formation	Hippocampus/CA1	Yes
8	R	Hippocampal formation	Hippocampus/CA1	Yes
Micro electrodes				
1	R	Hippocampal formation	Entorhinal cortex	Yes
2	L	Hippocampal formation	Entorhinal cortex	Yes
3	R	Temporo-basal cortex	Parahippocampus	No
	L	Temporo-basal cortex	Parahippocampus	Yes
4	L	Temporo-anterior lobe	Amygdala	No
	L	Mesial temporal cortex	CA3-CA4	No
5	R	Periventricular nodule	Nodule	Yes
	R	Periventricular nodule	Nodule	Yes
	R	Hippocampal formation	Subiculum	No
6	L	Hippocampal formation	Parahippocampal gyrus	No
7	R	Temporo-anterior lobe	Amygdala	Yes
8	R	Hippocampal formation	CA1/WM	Yes
	R	Hippocampal formation	CA1	Yes

Table 3. Anatomical locations of micro electrodes

Patient	Electrode	Contact	X	Y	Z
1	HaT2	1	27.0	-12.2	-27.1
		2	30.3	-12.9	-25.9
		3	36.9	-13.4	-24.7
		4	42.6	-14.1	-22.6

		5	49.3	-15.1	-22.3
2	HmT2	1	-18.8	-31.7	-13.5
		2	-23.8	-32.3	-11.9
		3	-28.8	-32.8	-11.5
		4	-33.9	-33.2	-11.0
		5	-39.1	-33.8	-10.6
	HaT1	1	-20.6	-7.2	-30.3
		2	-23.4	-7.2	-27.7
		3	-28.2	-8.7	-24.6
		4	-34.0	-10.4	-21.4
3	Hm2g	1	-21.7	-30.9	-13.7
		2	-27.0	-32.8	-12.6
		3	-32.4	-35.2	-12.6
		4	-36.7	-37.5	-12.6
		5	-42.1	-39.9	-12.8
4	HmT2	1	-30.3	-25.4	-12.0
		2	-32.3	-27.2	-9.9
		3	-36.6	-31.8	-9.2
		4	-40.9	-36.1	-7.5
		5	-46.0	-41.4	-5.3
	HaT2	1	-20.3	-9.0	-26.3
		2	-23.5	-10.2	-25.6
		3	-28.9	-10.9	-23.5
		4	-35.3	-12.8	-21.0
		5	-42.0	-13.8	-20.0
5	HmT3	1	30.0	-22.2	-17.5
		2	33.4	-22.3	-18.0
		3	40.3	-21.4	-19.1
		4	47.3	-21.4	-19.6
		5	54.3	-21.6	-20.2
	HpNI	1	20.6	-32.7	-17.1
		2	25.3	-32.7	-15.5
		3	29.7	-32.5	-13.8
		4	35.1	-32.3	-11.3
		5	39.3	-32.0	-9.4
6	HaT2	1	-20.6	-10.5	-31.3
		2	-23.6	-10.5	-31.2
		3	-29.5	-10.6	-30.9
		4	-35.4	-10.5	-30.3
		5	-41.3	-10.3	-29.5

	HmT2	1	-26.9	-27.1	-21.5
		2	-29.8	-27.1	-21.3
		3	-35.6	-26.2	-22.4
		4	-41.6	-26.2	-22.9
		5	-47.5	-25.1	-22.2
7	HaTB	1	-18.7	-10.2	-25.9
		2	-20.9	-9.4	-26.2
		3	-27.5	-8.2	-27.6
		4	-32.9	-6.5	-28.0
		5	-39.8	-5.5	-29.6
8	HmT2	1	26.9	-20.4	-19.2
		2	29.9	-21.3	-18.5
		3	35.8	-23.1	-17.3
		4	40.8	-24.9	-15.6
	HaT2	1	29.1	-16.2	-23.0
		2	32.1	-15.7	-21.9
		3	38.0	-14.8	-21.9
		4	43.6	-13.4	-20.6

Table 4. Automatic IED detection performance

	Visual	Automatic detection				
Patient	24 hrs.	24 hrs.	Hit (%)	FA (%)	Total	Total hrs.
1	2106	3500	99.8	5.4	63345	453.5
2	3330	4618	99.3	6.9	9224	358.3
3	12912	12811	98.8	1.2	113832	305.6
4	3669	3664	97.9	11.0	43757	308.8
5	7086	4630	96.5	8.6	32782	237.2
6	3077	3054	98.9	3.8	29810	233.6
7	10439	3985	98.4	0.8	55465	305.6
8	2714	1965	94.1	14.3	53951	307.7
Mean	5667	4778	98.0	6.5	50271	313.8
Std.	4050	3359	1.9	4.7	30945	69.7

Table 5. Circular statistics of circadian epileptic activity

	Interictal activity			Seizures		
Patient	Time	Rayleigh	*p*	Time	Rayleigh	*p*
1	01:56	0.61	<.0001***	17:43	0.76	<.0001***
2	00:46	0.29	<.0001***	08:56	0.36	0.55
3	01:37	0.50	<.0001***	10:31	0.48	<.01*
4	02:23	0.26	<.0001***	18:26	0.94	<.001**
5	01:48	0.28	<.0001***	20:21	0.13	0.3
6	01:42	0.56	<.0001***	03:33	0.57	0.14
7	17:25	0.08	<.0001***	01:59	0.81	<.0001***
8	03:38	0.41	<.0001***	11:44	0.70	0.14

. = $p < 0.05$, $* = p < 0.01$, $** = p < 0.001$, $*** = p < 0.0001$

Table 6. Time spend in sleep stages.

			% TST				
Patient	Night	TST	S3	S2	S1	REM	WASO
1	1	11.9	13	44	21	22	1.6
	2	8.7	14	42	18	25	0.9
	3	7.5	22	42	17	19	3
2	1	8.5	26	52	7	15	2.3
	2	7.6	33	39	8	19	0.4
	3	8.1	24	52	8	16	0.4
3	1	9.2	13	45	26	16	1.7
	2	7.2	27	33	24	16	1.7
	3	7.2	28	33	27	12	1.5
4	1	7.5	23	38	26	13	1.7
	2	6.7	16	41	26	17	1.3
	3	6.5	22	27	19	31	0.9
5	1	9.6	9	67	9	15	1.3
	2	7.2	26	42	10	22	0.4
	3	7.2	15	46	9	30	0.2
6	1	7.5	15	43	25	17	1.2
	2	8.2	21	35	15	29	0.9
	3	8.9	18	38	18	26	1.3
7	1	6.9	31	41	14	14	0.4
	2	9.6	28	46	7	19	0.5
	3	10.3	35	37	8	20	0.9
8	1	7	16	54	10	19	0.4
	2	7.1	10	52	16	22	0.6
	3	6.8	15	50	20	15	3.7
Mean		8.0	20.8	43.3	16.2	19.5	1.2

TST = Total sleep time (hrs.), WASO = Wake after sleep onset (hrs.)

Table 7. Effect of sleep stage on IEDs rate

Predictor	Coef β	SE(β)	df	z	p
Sleep stages					
Intercept	0.26	0.23	7.03	1.12	0.3
S3	1.13	0.01	93176.95	79.21	<.0001***
S2	0.90	0.01	93176.88	70.85	<.0001***
S1	0.54	0.02	93176.31	35.04	<.0001***
WASO	0.10	0.02	93176.64	6.08	<.0001***
REM	0.00	0.01	93176.50	-0.31	0.76
Post	0.01	0.02	93176.92	0.43	0.67
Post-hoc comparisons					
Pre - S3	-1.13	0.01		-79.21	<.0001***
Pre - S2	-0.90	0.01		-70.85	<.0001***
Pre - S1	-0.54	0.02		-35.04	<.0001***
Pre - WASO	-0.10	0.02		-6.08	<.0001***
Pre - REM	0.00	0.01		0.31	1
Pre - Post	-0.01	0.02		-0.43	1
S3 - S2	0.23	0.01		21.19	<.0001***
S3 - S1	0.59	0.01		41.55	<.0001***
S3 - WASO	1.03	0.02		63.83	<.0001***
S3 - REM	1.14	0.01		85.89	<.0001***
S3 - Post	1.12	0.01		80.70	<.0001***
S2 - S1	0.36	0.01		28.35	<.0001***
S2 - WASO	0.79	0.01		54.16	<.0001***
S2 - REM	0.90	0.01		78.83	<.0001***
S2 - Post	0.89	0.01		72.45	<.0001***
S1 - WASO	0.43	0.02		25.56	<.0001***
S1 - REM	0.54	0.01		37.38	<.0001***
S1 - Post	0.53	0.02		35.00	<.0001***
WASO - REM	0.11	0.02		6.65	<.0001***
WASO - Post	0.10	0.02		5.78	<.0001***
REM - Post	-0.01	0.01		-0.77	0.99

. = $p < 0.05$, $*$= $p < 0.01$, $**$= $p < 0.001$, $***$= $p < 0.0001$

Table 8. Effect of Slow Wave activity (0.1-2.5Hz) and Delta power (2.5-4Hz) on rate of IEDs

	Coef β	SE(β)	df	z	p
Intercept	0.412	0.217	7	1.90	0.1
Slow Wave	0.000	0.000	93182	14.02	<.0001***
Delta	0.010	0.000	93184	101.95	<.0001***

. = $p < 0.05$, $*$= $p < 0.01$, $**$= $p < 0.001$, $***$= $p < 0.0001$

Table 9. Effect of sleep stage on Slow Wave (0.1-2.5Hz) power

Predictor	Coef β	SE(β)	df	z	p
Coefficients					
Intercept	29.03	25.16	7.11	1.15	0.29
S3	264.51	3.00	93179.16	88.30	<.0001***
S2	93.86	2.65	93178.96	35.37	<.0001***
S1	48.34	3.22	93177.11	15.00	<.0001***
WASO	18.02	3.59	93178.22	5.02	<.0001***
REM	14.50	3.05	93177.76	4.76	<.0001***
Post	5.69	3.20	93179.09	1.78	0.08
Post-hoc comparisons					
Pre - S3	-264.51	3.00		-88.30	<.0001***
Pre - S2	-93.86	2.65		-35.37	<.0001***
Pre - S1	-48.34	3.22		-15.00	<.0001***
Pre - WASO	-18.02	3.59		-5.02	<.0001***
Pre - REM	-14.50	3.05		-4.76	<.0001***
Pre - Post	-5.69	3.20		-1.78	0.56
S3 - S2	170.65	2.33		73.38	<.0001***
S3 - S1	216.17	2.99		72.20	<.0001***
S3 - WASO	246.49	3.38		73.03	<.0001***
S3 - REM	250.02	2.77		90.14	<.0001***
S3 - Post	258.82	2.92		88.53	<.0001***
S2 - S1	45.52	2.65		17.17	<.0001***
S2 - WASO	75.84	3.07		24.72	<.0001***
S2 - REM	79.36	2.40		33.11	<.0001***
S2 - Post	88.17	2.58		34.22	<.0001***
S1 - WASO	30.32	3.56		8.51	<.0001***
S1 - REM	33.85	3.04		11.12	<.0001***
S1 - Post	42.65	3.19		13.39	<.0001***
WASO - REM	3.52	3.42		1.03	0.95
WASO - Post	12.33	3.54		3.48	<.01*
REM - Post	8.81	2.99		2.95	<.05

. = $p < 0.05$, $*= p < 0.01$, $**= p < 0.001$, $***= p < 0.0001$

Table 10. Effect of sleep stage on Delta (2.5-4 Hz) power

Predictor	Coef β	SE(β)	df	z	p
Coefficients					
Intercept	15.24	6.58	7.05	2.31	0.05
S3	54.64	0.55	93177.66	99.54	<.0001***
S2	29.96	0.49	93177.55	61.61	<.0001***
S1	16.54	0.59	93176.55	28.02	<.0001***
WASO	3.96	0.66	93177.13	6.02	<.0001***
REM	2.25	0.56	93176.89	4.03	<.0001***
Post	0.22	0.59	93177.62	0.38	0.71
Post-hoc comparisons					
Pre - S3	-54.64	0.55		-99.54	<.0001***
Pre - S2	-29.96	0.49		-61.61	<.0001***
Pre - S1	-16.54	0.59		-28.02	<.0001***
Pre - WASO	-3.96	0.66		-6.02	<.0001***
Pre - REM	-2.25	0.56		-4.03	<.01*
Pre - Post	-0.22	0.59		-0.38	1
S3 - S2	24.68	0.43		57.92	<.0001***
S3 - S1	38.09	0.55		69.44	<.0001***
S3 - WASO	50.68	0.62		81.95	<.0001***
S3 - REM	52.39	0.51		103.08	<.0001***
S3 - Post	54.42	0.54		101.58	<.0001***
S2 - S1	13.42	0.49		27.63	<.0001***
S2 - WASO	26.00	0.56		46.25	<.0001***
S2 - REM	27.71	0.44		63.09	<.0001***
S2 - Post	29.74	0.47		63.00	<.0001***
S1 - WASO	12.59	0.65		19.28	<.0001***
S1 - REM	14.30	0.56		25.62	<.0001***
S1 - Post	16.32	0.58		27.96	<.0001***
WASO - REM	1.71	0.63		2.73	0.09
WASO - Post	3.74	0.65		5.76	<.0001***
REM - Post	2.03	0.55		3.70	<.01*

. = $p < 0.05$, $*$= $p < 0.01$, $**$= $p < 0.001$, $***$= $p < 0.0001$

Table 11. Number of responsive or unresponsive putatively isolated single units (SUA) and multiunits (MUA)

	SUA		MUA	
Patient	Responsive	Unresponsive	Responsive	Unresponsive
1	47	4	36	3
2	8	0	2	0
3	1	5	5	19
4	2	0	15	0
5	4	10	6	13
6	5	1	10	0
7	0	6	3	6
8	18	1	9	4
Sum	85	27	86	45
Responsive (%)	75.9	24.1	65.6	34.4

Table 12. Effect of sleep stage on ERP peak amplitude

	Spike amplitude					Slow wave amplitude					Difference amplitude				
	Coef β	SE(β)	df	z	p	Coef β	SE(β)	df	z	p	Coef β	SE(β)	df	z	p
Sleep stages															
Intercept	425.78	108.40	7	3.93	<.01*	-260.53	97.66	7	-2.67	<.05$^{.}$	-260.53	97.66	7	-2.67	<.05$^{.}$
S3	84.05	2.98	78969	28.19	<.0001***	-29.52	4.24	78968	-6.96	<.0001***	-29.52	4.24	78968	-6.96	<.0001***
S2	63.59	2.83	78967	22.46	<.0001***	-35.60	4.03	78967	-8.85	<.0001***	-35.60	4.03	78967	-8.85	<.0001***
S1	49.95	3.18	78966	15.70	<.0001***	-29.32	4.53	78966	-6.48	<.0001***	-29.32	4.53	78966	-6.48	<.0001***
WASO	19.01	3.88	78965	4.91	<.0001***	-10.38	5.51	78966	-1.88	0.06	-10.38	5.51	78966	-1.88	0.06
Post	7.56	4.35	78970	1.74	0.08	5.74	6.18	78969	0.93	0.35	5.74	6.18	78969	0.93	0.35
REM	-61.68	4.33	78977	-14.24	<.0001***	87.42	6.16	78973	14.19	<.0001***	87.42	6.16	78973	14.19	<.0001***
Post-hoc comparisons															
Pre - S3	-84.05	2.98		-28.19	<.0001***	29.52	4.24		6.96	<.0001***	-113.58	5.45		-20.82	<.0001***
Pre - S2	-63.59	2.83		-22.46	<.0001***	35.60	4.03		8.85	<.0001***	-99.18	5.18		-19.15	<.0001***
Pre - S1	-49.95	3.18		-15.70	<.0001***	29.32	4.53		6.48	<.0001***	-79.26	5.82		-13.61	<.0001***
Pre - WASO	-19.01	3.88		-4.91	<.0001***	10.38	5.51		1.88	0.49	-29.38	7.09		-4.14	<.001**
Pre - REM	-7.56	4.35		-1.74	0.59	-5.74	6.18		-0.93	0.97	-1.78	7.95		-0.22	1
Pre - Post	61.68	4.33		14.24	<.0001***	-87.42	6.16		-14.19	<.0001***	149.09	7.92		18.81	<.0001***
S3 - S2	20.46	1.76		11.63	<.0001***	6.08	2.50		2.43	0.19	14.40	3.22		4.47	<.001**
S3 - S1	34.10	2.38		14.32	<.0001***	-0.21	3.39		-0.06	1	34.32	4.36		7.88	<.0001***
S3 - WASO	65.04	3.26		19.95	<.0001***	-19.14	4.63		-4.13	<.001**	84.19	5.96		14.12	<.0001***
S3 - REM	76.49	3.76		20.32	<.0001***	-35.26	5.35		-6.59	<.0001***	111.80	6.89		16.23	<.0001***
S3 - Post	145.73	3.80		38.33	<.0001***	-116.94	5.41		-21.63	<.0001***	262.67	6.95		37.77	<.0001***
S2 - S1	13.64	2.17		6.30	<.0001***	-6.29	3.08		-2.04	0.39	19.92	3.96		5.03	<.0001***
S2 - WASO	44.58	3.12		14.29	<.0001***	-25.22	4.44		-5.68	<.0001***	69.80	5.71		12.23	<.0001***
S2 - REM	56.03	3.66		15.32	<.0001***	-41.34	5.20		-7.95	<.0001***	97.40	6.69		14.55	<.0001***
S2 - Post	125.27	3.69		33.91	<.0001***	-123.02	5.25		-23.42	<.0001***	248.27	6.76		36.73	<.0001***
S1 - WASO	30.94	3.44		9.00	<.0001***	-18.93	4.89		-3.87	<.01*	49.87	6.29		7.93	<.0001***
S1 - REM	42.39	3.95		10.72	<.0001***	-35.05	5.62		-6.23	<.0001***	77.48	7.23		10.71	<.0001***
S1 - Post	111.63	4.01		27.85	<.0001***	-116.73	5.70		-20.48	<.0001***	228.35	7.33		31.15	<.0001***
WASO - REM	11.45	4.55		2.52	0.15	-16.12	6.46		-2.49	0.16	27.61	8.32		3.32	<.05$^{.}$
WASO - Post	80.69	4.59		17.56	<.0001***	-97.80	6.53		-14.97	<.0001***	178.48	8.41		21.23	<.0001***
REM - Post	69.23	4.95		13.98	<.0001***	-81.68	7.04		-11.59	<.0001***	150.87	9.06		16.65	<.0001***

. = $p < 0.05$, ∗= $p < 0.01$, ∗∗= $p < 0.001$, ∗∗∗= $p < 0.0001$

Table 13. Effect of sleep stage on firing rates during IED

	Spike					Wave					Ratio				
	Coef β	SE(β)	df	z	p	Coef β	SE(β)	df	z	p	Coef β	SE(β)	df	z	p
Sleep stages															
Intercept	6.20	1.49	6	4.17	<.01*	11.05	3.08	7	3.59	<.01*	4.83	2.20	7	2.19	0.07
S3	-2.21	0.38	1237	-5.88	<.0001***	2.66	0.65	1237	4.12	<.0001***	4.87	0.58	1237	8.45	<.0001***
S2	-2.01	0.38	1237	-5.33	<.0001***	3.20	0.65	1237	4.95	<.0001***	5.20	0.58	1237	9.02	<.0001***
S1	-1.68	0.38	1237	-4.45	<.0001***	3.30	0.65	1237	5.11	<.0001***	4.98	0.58	1237	8.63	<.0001***
WASO	-2.03	0.38	1237	-5.38	<.0001***	1.34	0.65	1237	2.08	<.05$^{.}$	3.37	0.58	1237	5.84	<.0001***
Post	-0.68	0.38	1237	-1.82	0.07	-0.19	0.65	1237	-0.29	0.77	0.50	0.58	1237	0.86	0.39
REM	-0.20	0.38	1237	-0.51	0.61	-1.28	0.65	1237	-1.97	<.05$^{.}$	-1.09	0.58	1237	-1.87	0.06
Post-hoc comparisons															
Pre - S3	2.21	0.38		5.88	<.0001***	-2.66	0.65		-4.12	<.001**	-4.87	0.58		-8.45	<.0001***
Pre - S2	2.01	0.38		5.33	<.0001***	-3.20	0.65		-4.95	<.0001***	-5.20	0.58		-9.02	<.0001***
Pre - S1	1.68	0.38		4.45	<.001**	-3.30	0.65		-5.11	<.0001***	-4.98	0.58		-8.63	<.0001***
Pre - WASO	2.03	0.38		5.38	<.0001***	-1.34	0.65		-2.08	0.37	-3.37	0.58		-5.84	<.0001***
Pre - REM	0.68	0.38		1.82	0.54	0.19	0.65		0.29	1	-0.50	0.58		-0.86	0.98
Pre - Post	0.20	0.38		0.51	1	1.28	0.65		1.97	0.44	1.09	0.58		1.87	0.5
S3 - S2	-0.21	0.38		-0.55	1	-0.54	0.65		-0.83	0.98	-0.33	0.58		-0.57	1
S3 - S1	-0.54	0.38		-1.42	0.79	-0.64	0.65		-0.99	0.96	-0.11	0.58		-0.18	1
S3 - WASO	-0.19	0.38		-0.50	1	1.32	0.65		2.05	0.39	1.51	0.58		2.61	0.12
S3 - REM	-1.53	0.38		-4.06	<.01*	2.85	0.65		4.41	<.001**	4.38	0.58		7.59	<.0001***
S3 - Post	-2.02	0.38		-5.32	<.0001***	3.94	0.65		6.06	<.0001***	5.96	0.58		10.26	<.0001***
S2 - S1	-0.33	0.38		-0.87	0.98	-0.10	0.65		-0.16	1	0.22	0.58		0.39	1
S2 - WASO	0.02	0.38		0.05	1	1.86	0.65		2.88	0.06	1.84	0.58		3.18	<.05$^{.}$
S2 - REM	-1.32	0.38		-3.51	<.01*	3.38	0.65		5.24	<.0001***	4.70	0.58		8.16	<.0001***
S2 - Post	-1.81	0.38		-4.77	<.0001***	4.48	0.65		6.89	<.0001***	6.29	0.58		10.83	<.0001***
S1 - WASO	0.35	0.38		0.93	0.97	1.96	0.65		3.04	<.05$^{.}$	1.61	0.58		2.80	0.08
S1 - REM	-0.99	0.38		-2.64	0.12	3.49	0.65		5.40	<.0001***	4.48	0.58		7.77	<.0001***
S1 - Post	-1.48	0.38		-3.91	<.01*	4.58	0.65		7.05	<.0001***	6.07	0.58		10.44	<.0001***
WASO - REM	-1.34	0.38		-3.56	<.01*	1.53	0.65		2.36	0.21	2.87	0.58		4.97	<.0001***
WASO - Post	-1.83	0.38		-4.83	<.0001***	2.62	0.65		4.03	<.01*	4.45	0.58		7.67	<.0001***
REM - Post	-0.49	0.38		-1.29	0.86	1.09	0.65		1.68	0.63	1.58	0.58		2.73	0.09

. $= p < 0.05$, $* = p < 0.01$, $** = p < 0.001$, $*** = p < 0.0001$

Table 14. Effect of sleep stage on spontanious neuronal behaviour

	Firing Rate (SUA)					Firing Rate (MUA)					Bursts					Amplitude					CV2				
	Coef β	SE(β)	df	z	p	Coef β	SE(β)	df	z	p	Coef β	SE(β)	df	z	p	Coef β	SE(β)	df	z	p	Coef β	SE(β)	df	z	p
Sleep stages																									
Intercept	7.12	0.33	123	21.62	<.0001***	10.80	1.11	6	9.70	<.0001***	23.18	4.19	6	5.53	<.01*	67.65	11.55	8	5.86	<.001**	0.92	0.01	2	77.06	<.001**
S3	-3.85	0.07	28868	-54.95	<.0001***	-5.95	0.11	78794	-53.18	<.0001***	-16.91	0.26	107669	-64.55	<.0001***	0.46	0.05	107584	8.78	<.0001***	0.11	0.00	107596	87.57	<.0001***
S2	-3.07	0.06	28877	-55.06	<.0001***	-3.87	0.08	78811	-46.14	<.0001***	-12.13	0.20	107692	-61.12	<.0001***	0.29	0.04	107584	7.28	<.0001***	0.07	0.00	107611	75.09	<.0001***
S1	-2.77	0.06	28866	-43.48	<.0001***	-3.29	0.10	78799	-33.20	<.0001***	-9.95	0.23	107668	-42.69	<.0001***	0.21	0.05	107584	4.49	<.0001***	0.06	0.00	107595	49.32	<.0001***
WASO	-2.57	0.07	28880	-36.80	<.0001***	-2.59	0.10	78827	-25.89	<.0001***	-8.67	0.24	107704	-35.86	<.0001***	0.59	0.05	107585	12.23	<.0001***	0.04	0.00	107588	33.40	<.0001***
REM	-2.02	0.06	28873	-34.64	<.0001***	-2.64	0.08	78801	-31.05	<.0001***	-9.20	0.20	107680	-45.27	<.0001***	0.20	0.04	107584	4.93	<.0001***	0.03	0.00	107604	32.59	<.0001***
Post	-1.97	0.06	28875	-30.98	<.0001***	0.26	0.09	78824	2.82	<.01*	-5.82	0.22	107699	-26.61	<.0001***	-0.19	0.04	107584	-4.23	<.0001***	0.01	0.00	107618	12.42	<.0001***
Post-hoc comparisons																									
Pre - S3	3.85	0.07		54.95	<.0001***	5.95	0.11		53.18	<.0001***	16.91	0.26		64.55	<.0001***	-0.46	0.05		-8.78	<.0001***	-0.11	0.00		-87.57	<.0001***
Pre - S2	3.07	0.06		55.06	<.0001***	3.87	0.08		46.14	<.0001***	12.13	0.20		61.12	<.0001***	-0.29	0.04		-7.28	<.0001***	-0.07	0.00		-75.09	<.0001***
Pre - S1	2.77	0.06		43.48	<.0001***	3.29	0.10		33.20	<.0001***	9.95	0.23		42.69	<.0001***	-0.21	0.05		-4.49	<.001**	-0.06	0.00		-49.32	<.0001***
Pre - WASO	2.57	0.07		36.80	<.0001***	2.59	0.10		25.89	<.0001***	8.67	0.24		35.86	<.0001***	-0.59	0.05		-12.23	<.0001***	-0.04	0.00		-33.40	<.0001***
Pre - REM	2.02	0.06		34.64	<.0001***	2.64	0.08		31.05	<.0001***	9.20	0.20		45.27	<.0001***	-0.20	0.04		-4.93	<.0001***	-0.03	0.00		-32.59	<.0001***
Pre - Post	1.97	0.06		30.98	<.0001***	-0.26	0.09		-2.82	0.07	5.82	0.22		26.61	<.0001***	0.19	0.04		4.23	<.001**	-0.01	0.00		-12.42	<.0001***
S3 - S2	-0.78	0.06		-13.80	<.0001***	-2.08	0.11		-19.36	<.0001***	-4.79	0.24		-19.73	<.0001***	0.17	0.05		3.53	<.01*	0.04	0.00		33.17	<.0001***
S3 - S1	-1.08	0.07		-16.48	<.0001***	-2.67	0.12		-21.84	<.0001***	-6.97	0.28		-25.15	<.0001***	0.25	0.06		4.53	<.001**	0.06	0.00		41.36	<.0001***
S3 - WASO	-1.28	0.07		-17.61	<.0001***	-3.36	0.12		-26.90	<.0001***	-8.25	0.29		-28.50	<.0001***	-0.13	0.06		-2.27	0.26	0.07	0.00		51.39	<.0001***
S3 - REM	-1.84	0.06		-30.89	<.0001***	-3.32	0.11		-30.05	<.0001***	-7.72	0.25		-30.77	<.0001***	0.26	0.05		5.18	<.0001***	0.08	0.00		65.09	<.0001***
S3 - Post	-1.88	0.07		-28.68	<.0001***	-6.21	0.12		-53.95	<.0001***	-11.10	0.27		-41.83	<.0001***	0.65	0.05		12.16	<.0001***	0.10	0.00		76.26	<.0001***
S2 - S1	-0.30	0.05		-5.93	<.0001***	-0.58	0.10		-5.97	<.0001***	-2.18	0.22		-9.96	<.0001***	0.08	0.04		1.82	0.53	0.02	0.00		15.58	<.0001***
S2 - WASO	-0.50	0.06		-8.45	<.0001***	-1.27	0.10		-12.68	<.0001***	-3.46	0.23		-14.81	<.0001***	-0.30	0.05		-6.47	<.0001***	0.03	0.00		29.21	<.0001***
S2 - REM	-1.06	0.04		-24.74	<.0001***	-1.23	0.08		-14.95	<.0001***	-2.93	0.19		-15.84	<.0001***	0.09	0.04		2.39	0.2	0.04	0.00		44.74	<.0001***
S2 - Post	-1.10	0.05		-22.00	<.0001***	-4.12	0.09		-46.57	<.0001***	-6.31	0.20		-31.02	<.0001***	0.47	0.04		11.65	<.0001***	0.06	0.00		59.91	<.0001***
S1 - WASO	-0.21	0.07		-3.06	<.05$^{.}$	-0.69	0.11		-6.13	<.0001***	-1.28	0.26		-4.88	<.0001***	-0.38	0.05		-7.26	<.0001***	0.02	0.00		13.00	<.0001***
S1 - REM	-0.76	0.05		-14.34	<.0001***	-0.65	0.10		-6.58	<.0001***	-0.75	0.22		-3.36	<.05	0.01	0.04		0.19	1	0.02	0.00		21.73	<.0001***
S1 - Post	-0.80	0.06		-13.80	<.0001***	-3.54	0.10		-34.21	<.0001***	-4.13	0.24		-17.38	<.0001***	0.39	0.05		8.29	<.0001***	0.04	0.00		36.93	<.0001***
WASO - REM	-0.55	0.06		-8.90	<.0001***	0.04	0.10		0.42	1	0.53	0.24		2.22	0.28	0.39	0.05		8.18	<.0001***	0.01	0.00		6.08	<.0001***
WASO - Post	-0.60	0.07		-9.00	<.0001***	-2.85	0.11		-26.88	<.0001***	-2.85	0.25		-11.37	<.0001***	0.78	0.05		15.50	<.0001***	0.03	0.00		21.39	<.0001***
REM - Post	-0.04	0.05		-0.80	0.99	-2.89	0.09		-32.10	<.0001***	-3.38	0.21		-16.13	<.0001***	0.39	0.04		9.20	<.0001***	0.02	0.00		18.64	<.0001***

. $= p < 0.05$, $* = p < 0.01$, $** = p < 0.001$, $*** = p < 0.0001$

Supplementary Materials

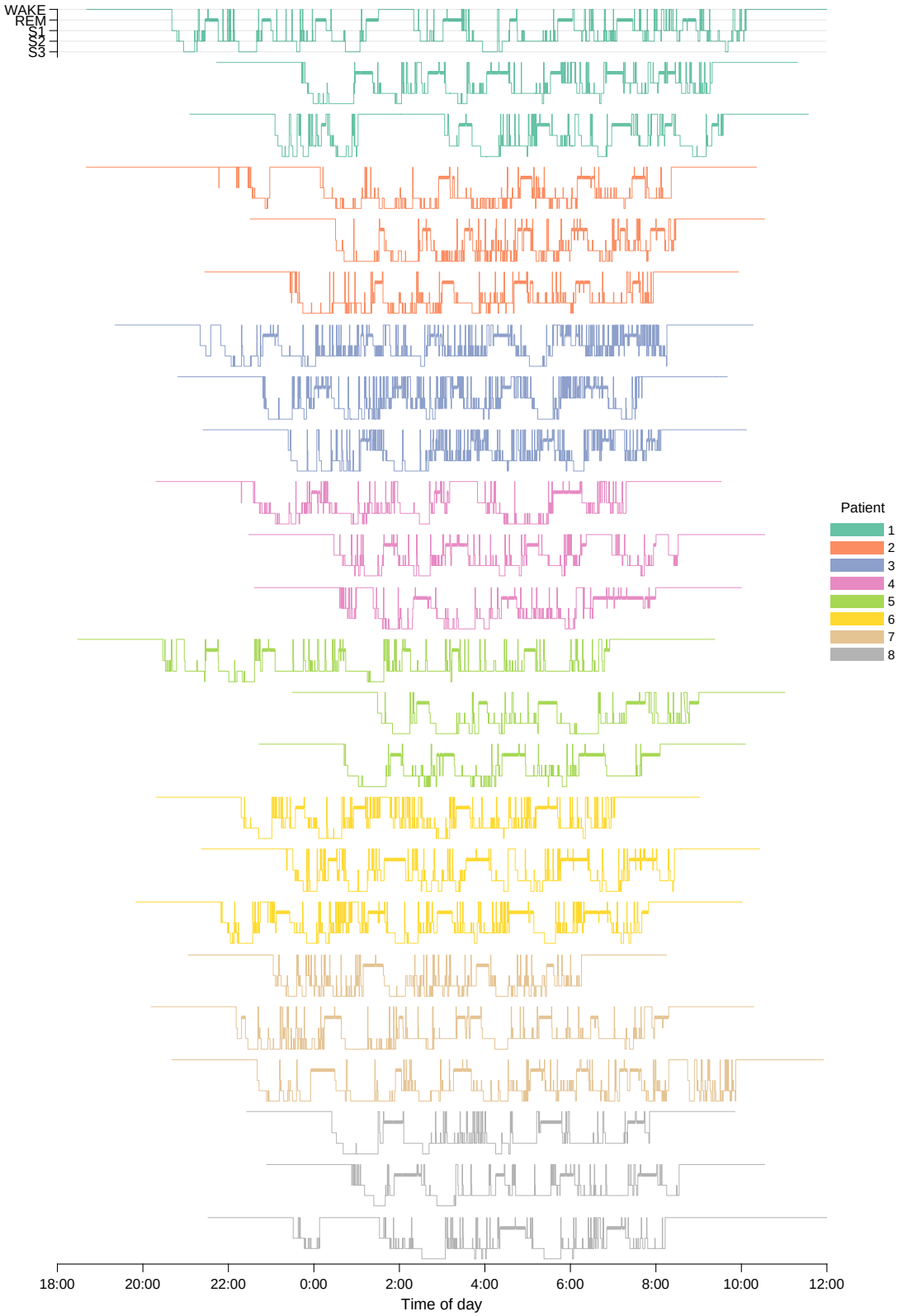

Figure 14. All hypnograms, including 2 hours pre-sleep and post-sleep.

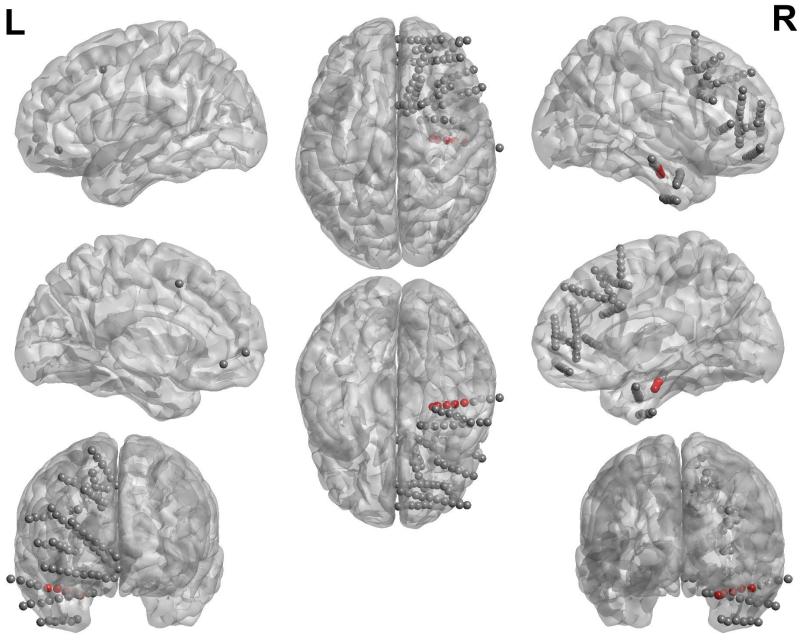

Figure 15. Electrode locations Patient 1. Analysed contacts in red.

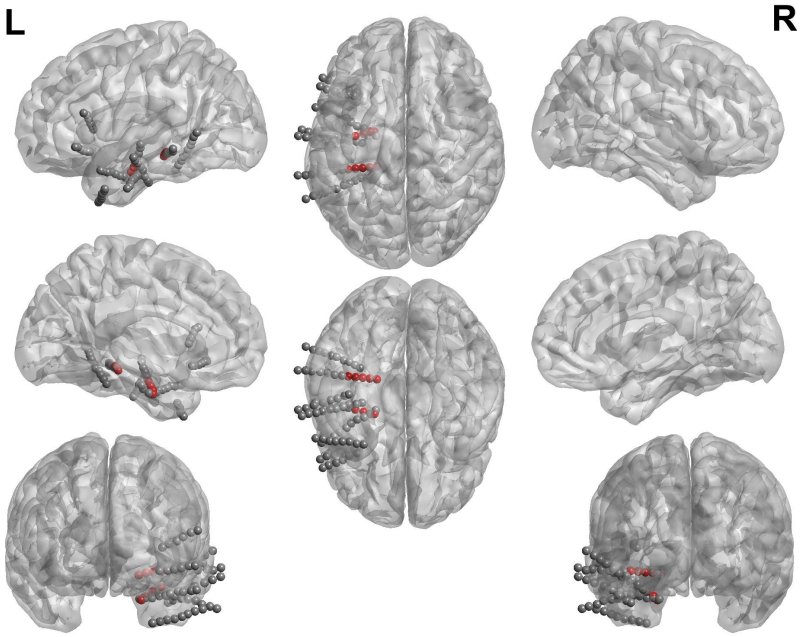

Figure 16. Electrode locations Patient 2. Analysed contacts in red.

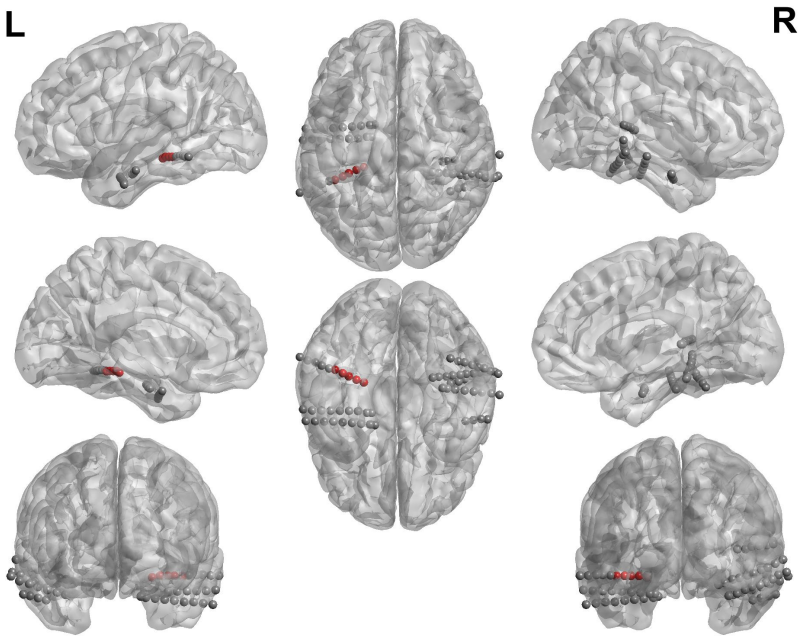

Figure 17. Electrode locations Patient 3. Analysed contacts in red.

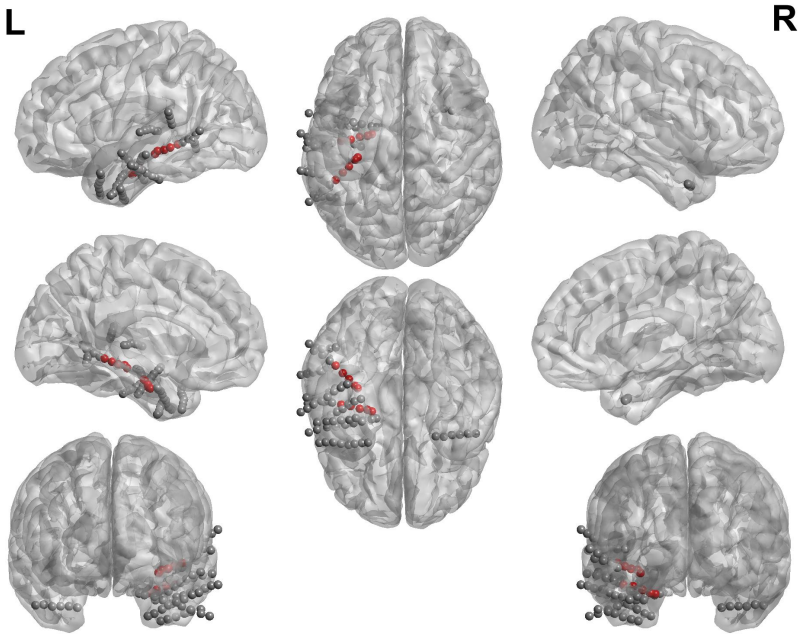

Figure 18. Electrode locations Patient 4. Analysed contacts in red.

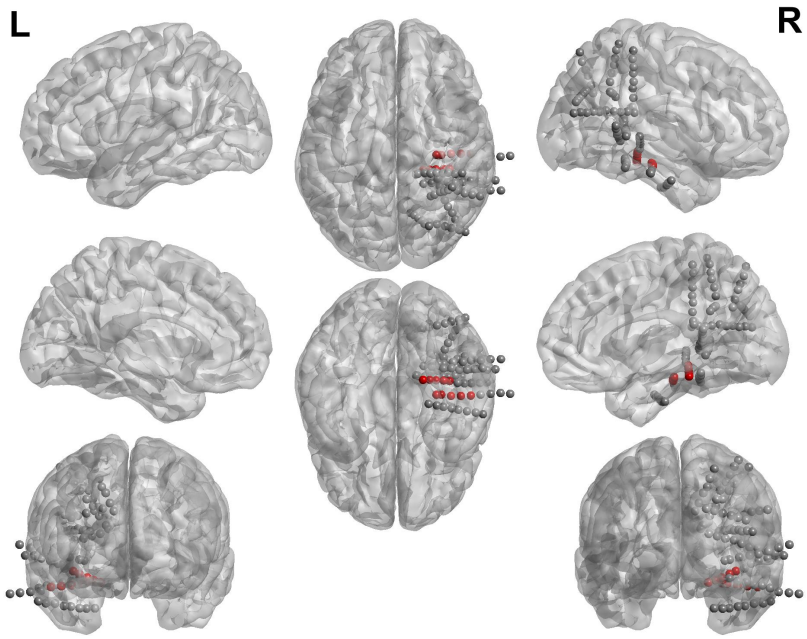

Figure 19. Electrode locations Patient 5. Analysed contacts in red.

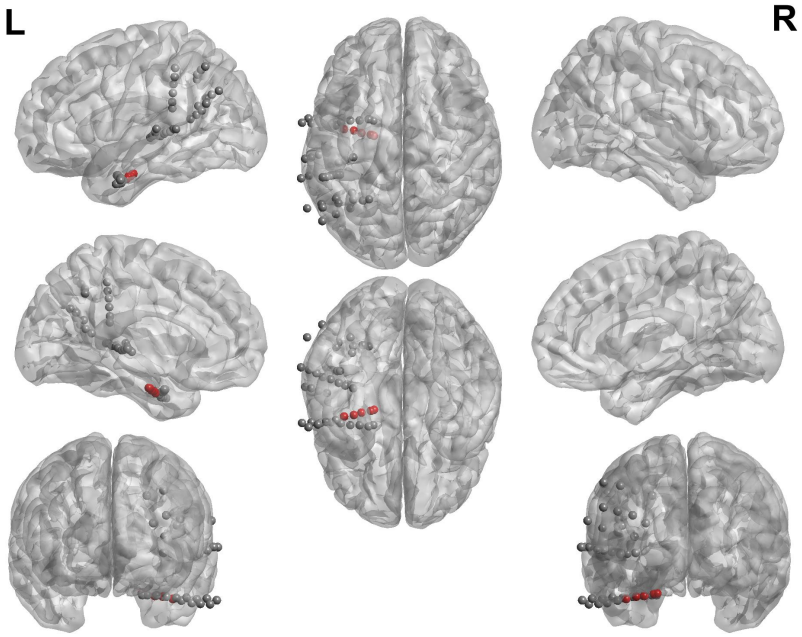

Figure 20. Electrode locations Patient 6. Analysed contacts in red.

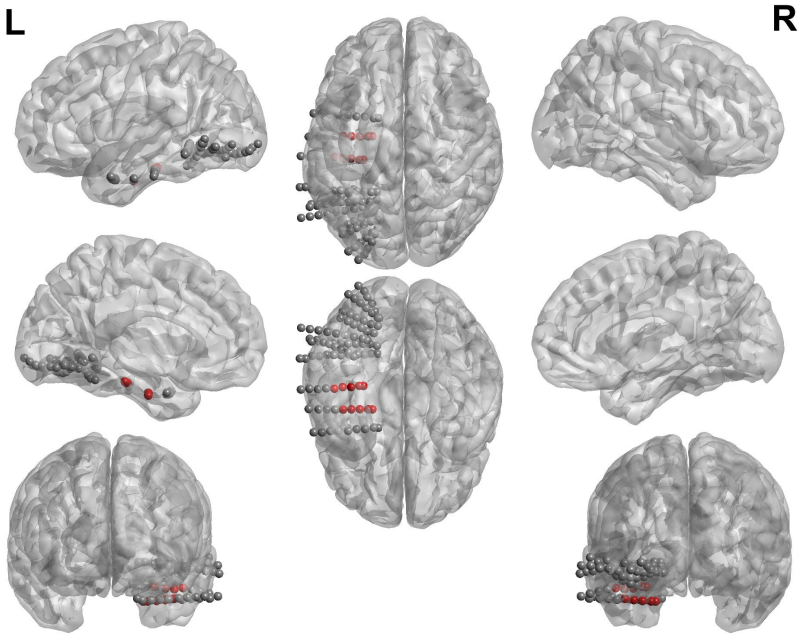

Figure 21. Electrode locations Patient 7. Analysed contacts in red.

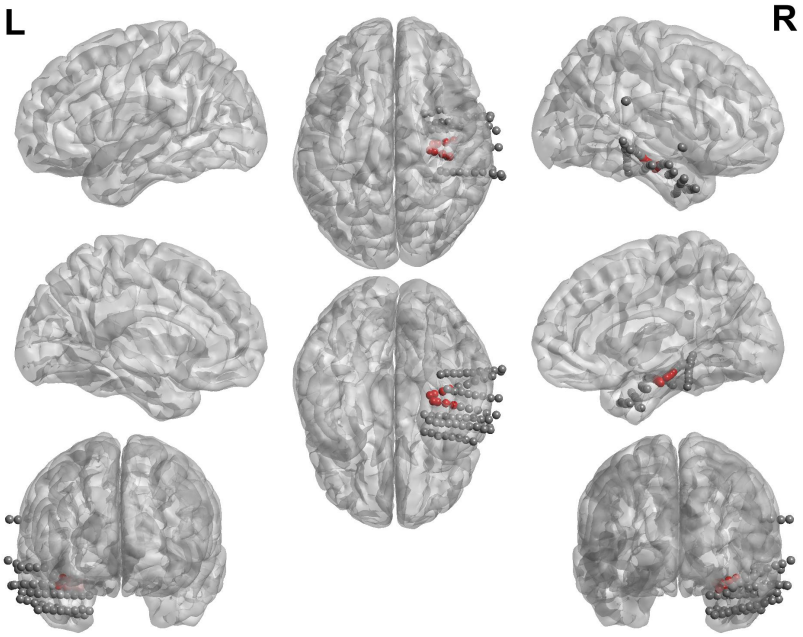

Figure 22. Electrode locations Patient 8. Analysed contacts in red.

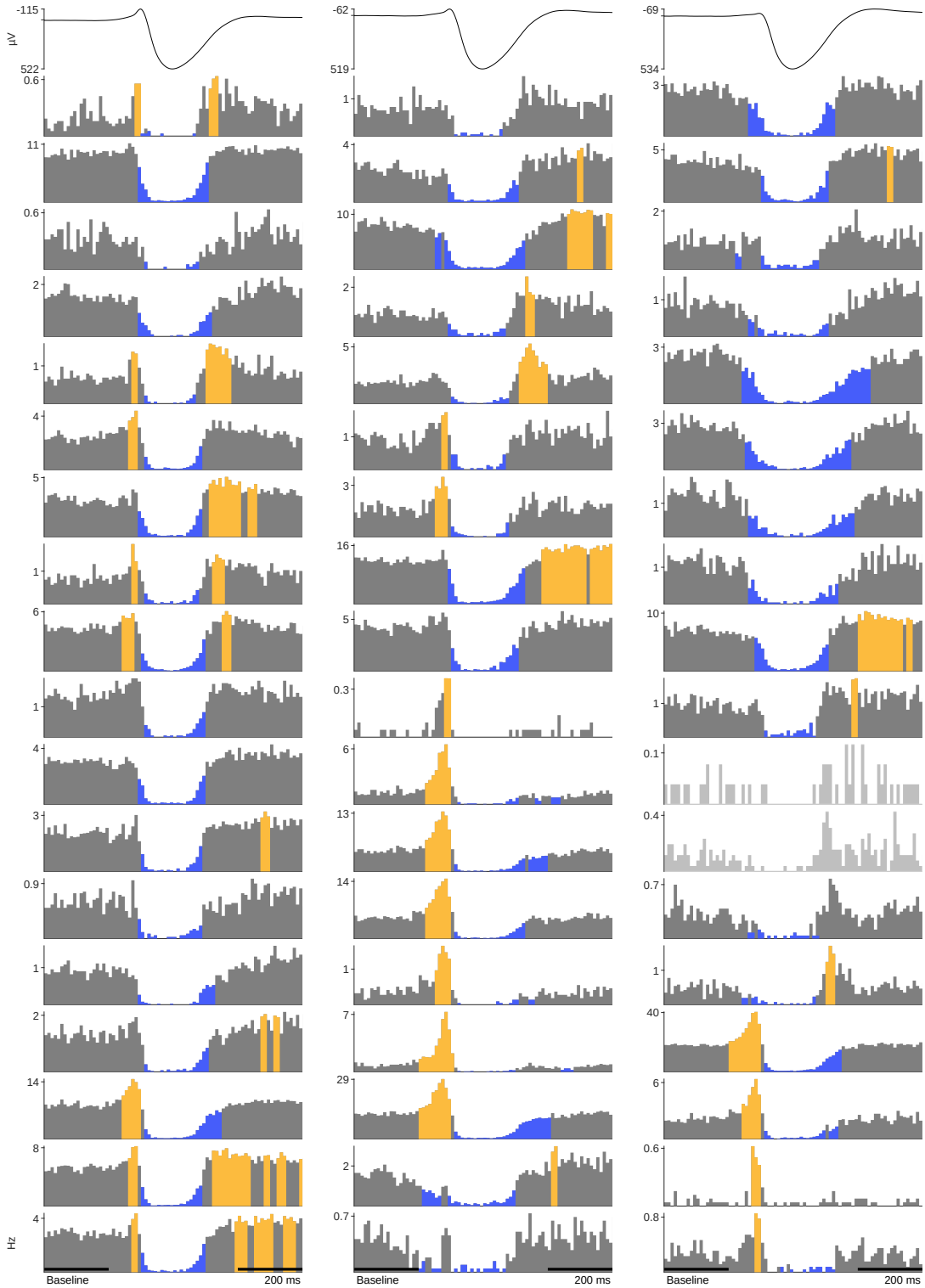

Figure 23. Patient 1 (1/3): PSTH of each unit. Top row shows time-locked LFP. Units are organized over nights (columns). The yellow color indicates significant increases and the blue color decreases compared with the average firing rate during baseline, indicated in the x-axis of bottom left plot.

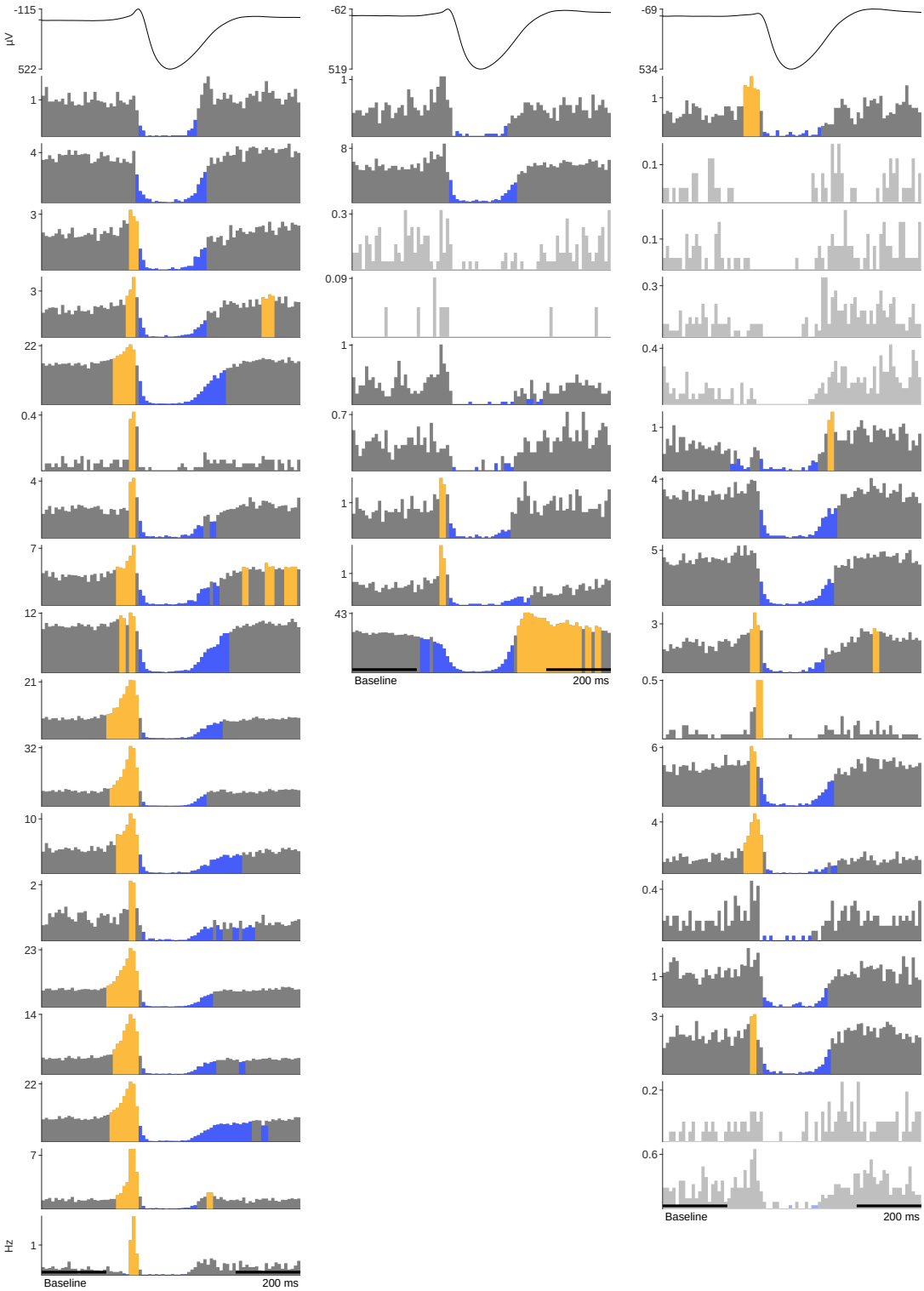

Figure 24. Patient 1 (2/3): PSTH of each unit. Top row shows time-locked LFP. Units are organized over nights (columns). The yellow color indicates significant increases and the blue color decreases compared with the average firing rate during baseline, indicated in the x-axis of bottom left plot.

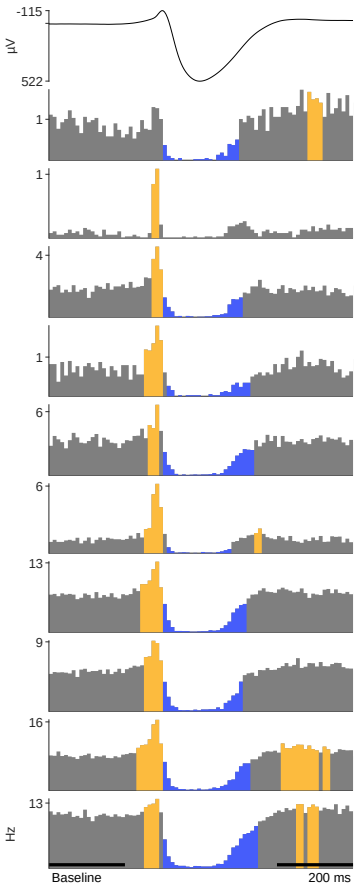

Figure 25. Patient 1 (3/3): PSTH of each unit. Top row shows time-locked LFP. Units are organized over nights (columns). The yellow color indicates significant increases and the blue color decreases compared with the average firing rate during baseline, indicated in the x-axis of bottom left plot.

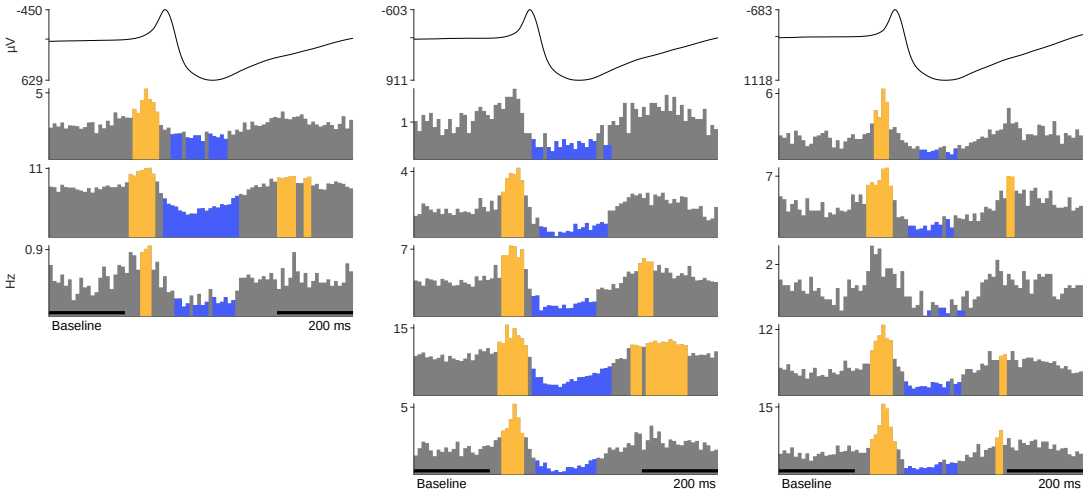

Figure 26. Patient 2: PSTH of each unit. Top row shows time-locked LFP. Units are organized over nights (columns). The yellow color indicates significant increases and the blue color decreases compared with the average firing rate during baseline, indicated in the x-axis of bottom left plot.

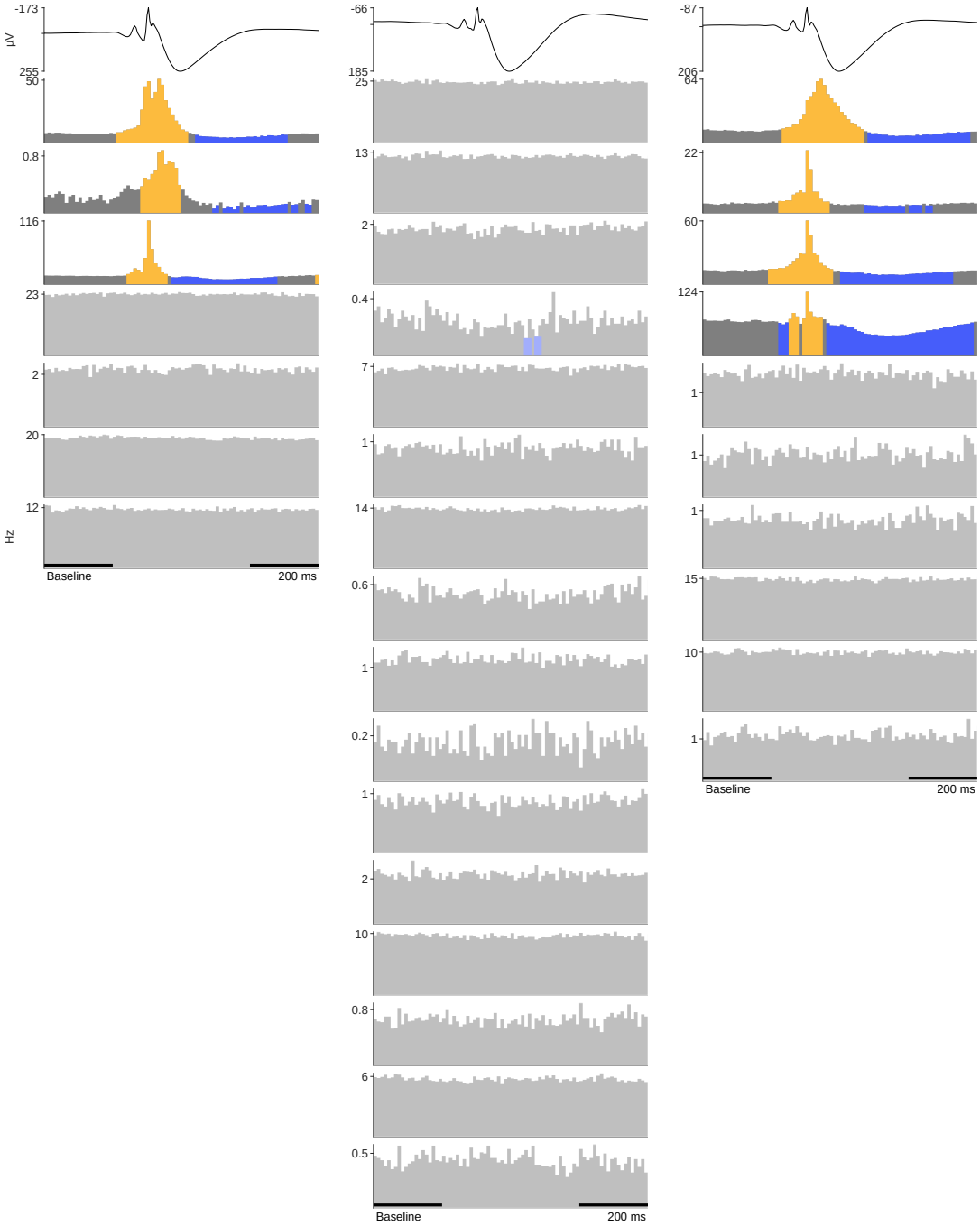

Figure 27. Patient 3: PSTH of each unit. Top row shows time-locked LFP. Units are organized over nights (columns). The yellow color indicates significant increases and the blue color decreases compared with the average firing rate during baseline, indicated in the x-axis of bottom left plot.

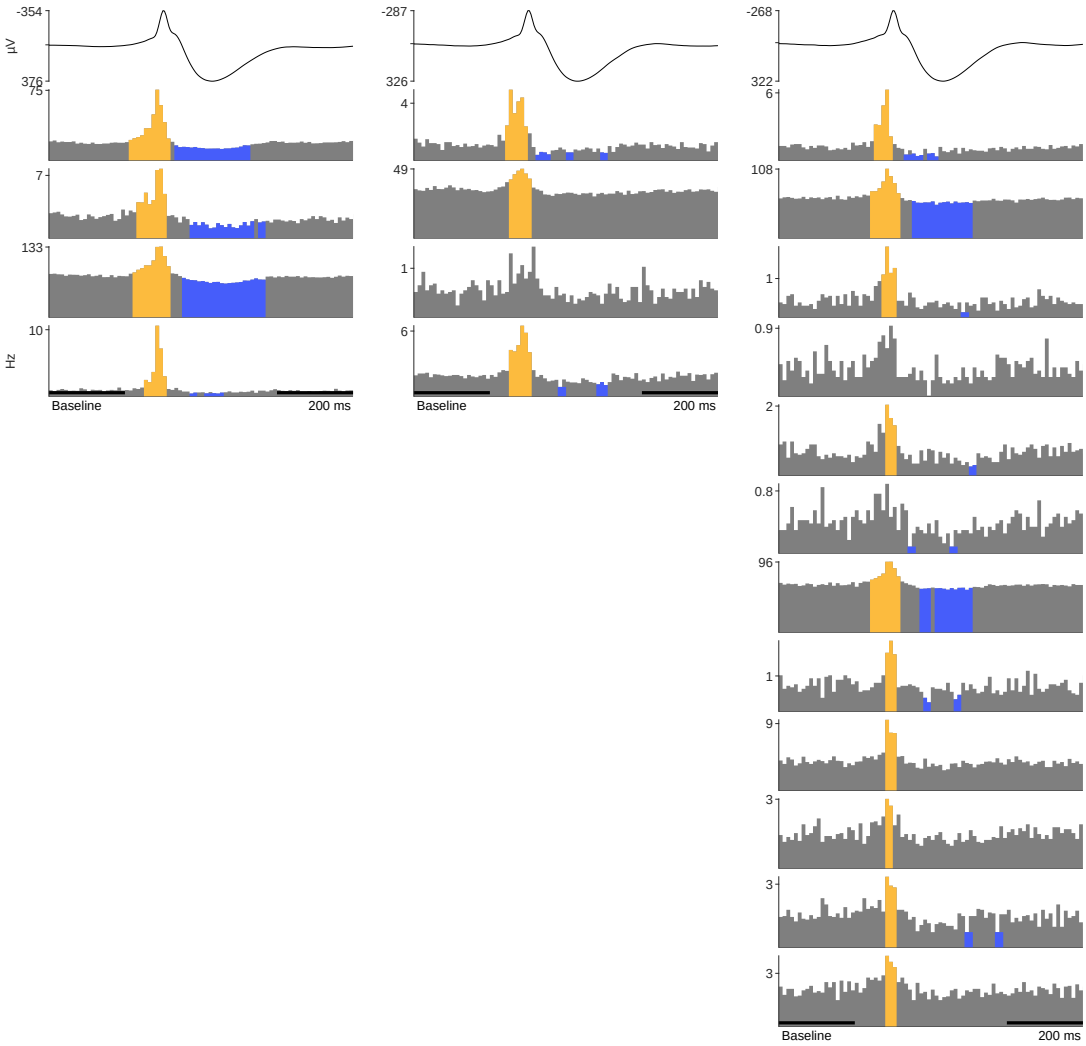

Figure 28. Patient 4: PSTH of each unit. Top row shows time-locked LFP. Units are organized over nights (columns). The yellow color indicates significant increases and the blue color decreases compared with the average firing rate during baseline, indicated in the x-axis of bottom left plot.

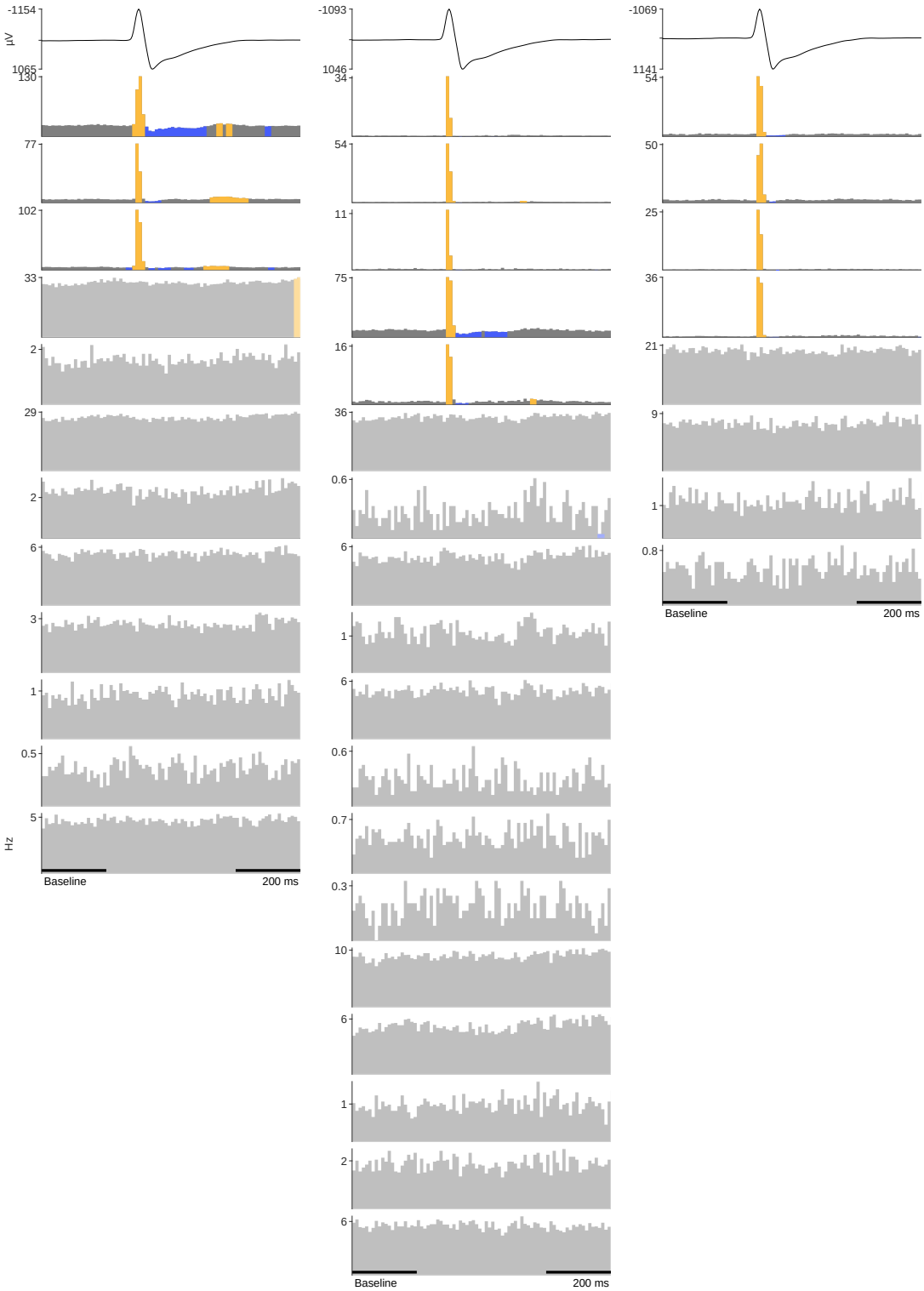

Figure 29. Patient 5: PSTH of each unit. Top row shows time-locked LFP. Units are organized over nights (columns). The yellow color indicates significant increases and the blue color decreases compared with the average firing rate during baseline, indicated in the x-axis of bottom left plot.

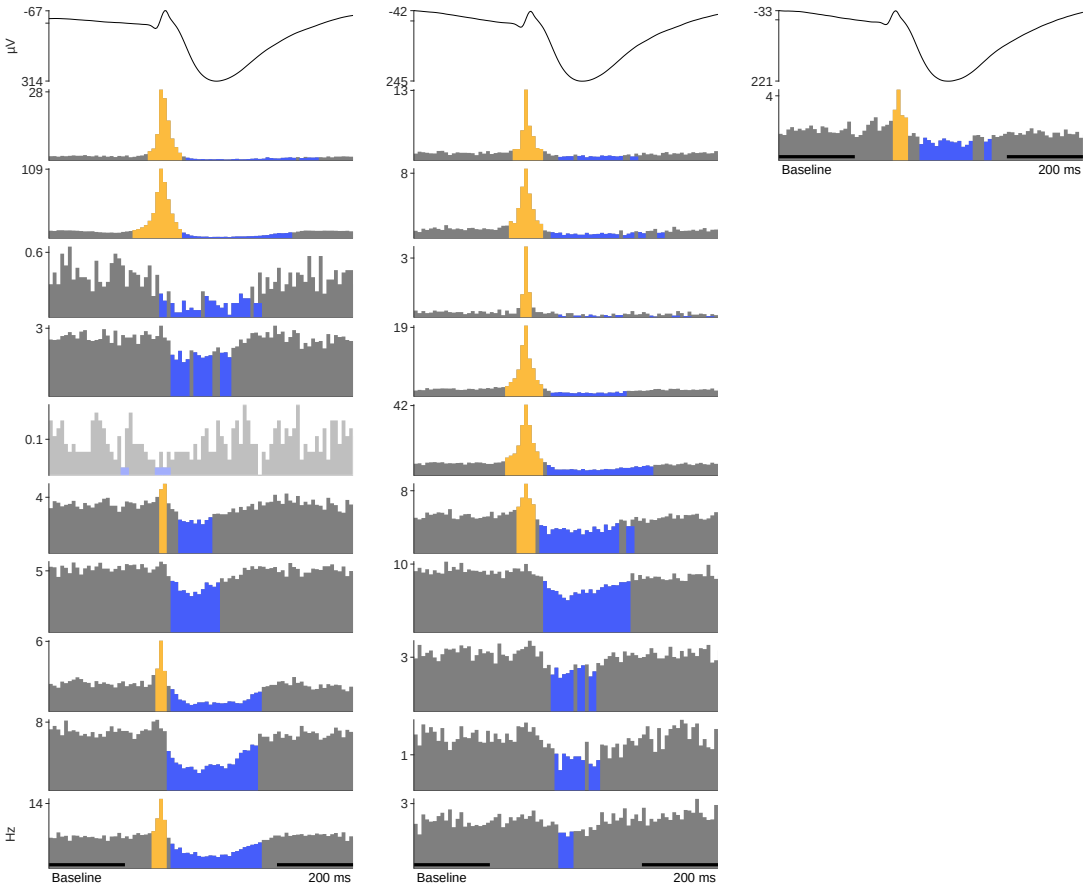

Figure 30. Patient 6: PSTH of each unit. Top row shows time-locked LFP. Units are organized over nights (columns). The yellow color indicates significant increases and the blue color decreases compared with the average firing rate during baseline, indicated in the x-axis of bottom left plot.

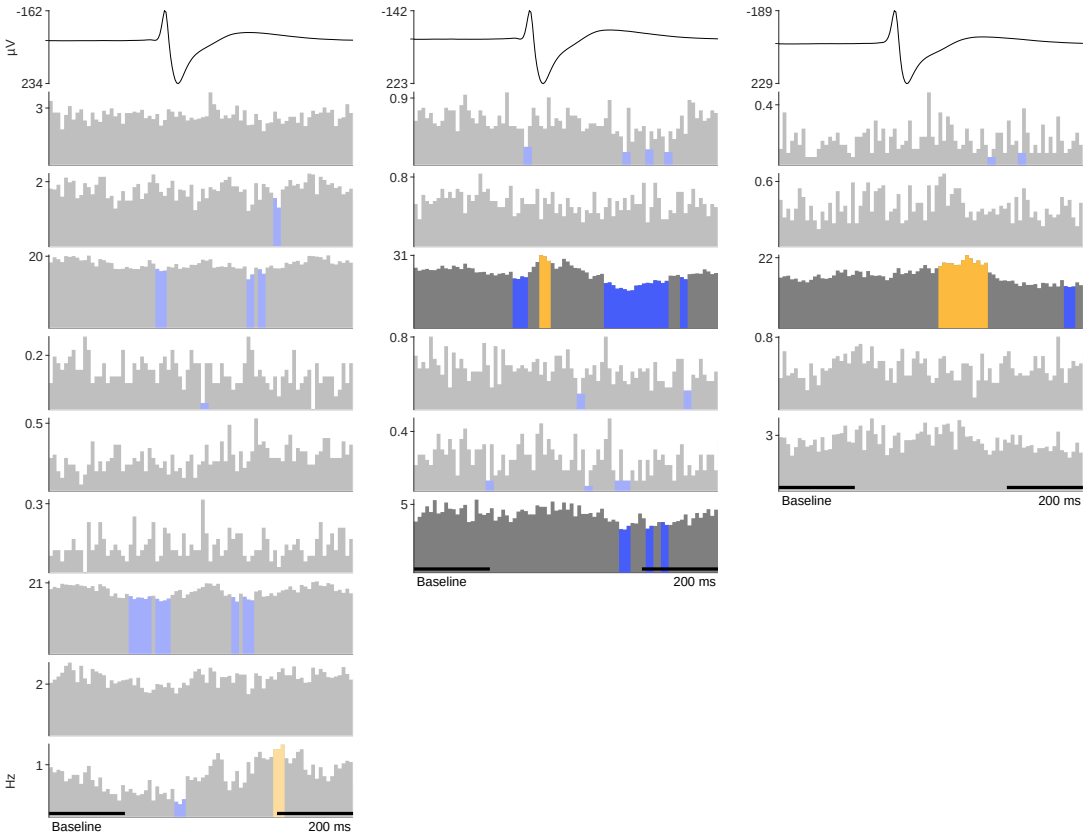

Figure 31. Patient 7: PSTH of each unit. Top row shows time-locked LFP. Units are organized over nights (columns). The yellow color indicates significant increases and the blue color decreases compared with the average firing rate during baseline, indicated in the x-axis of bottom left plot.

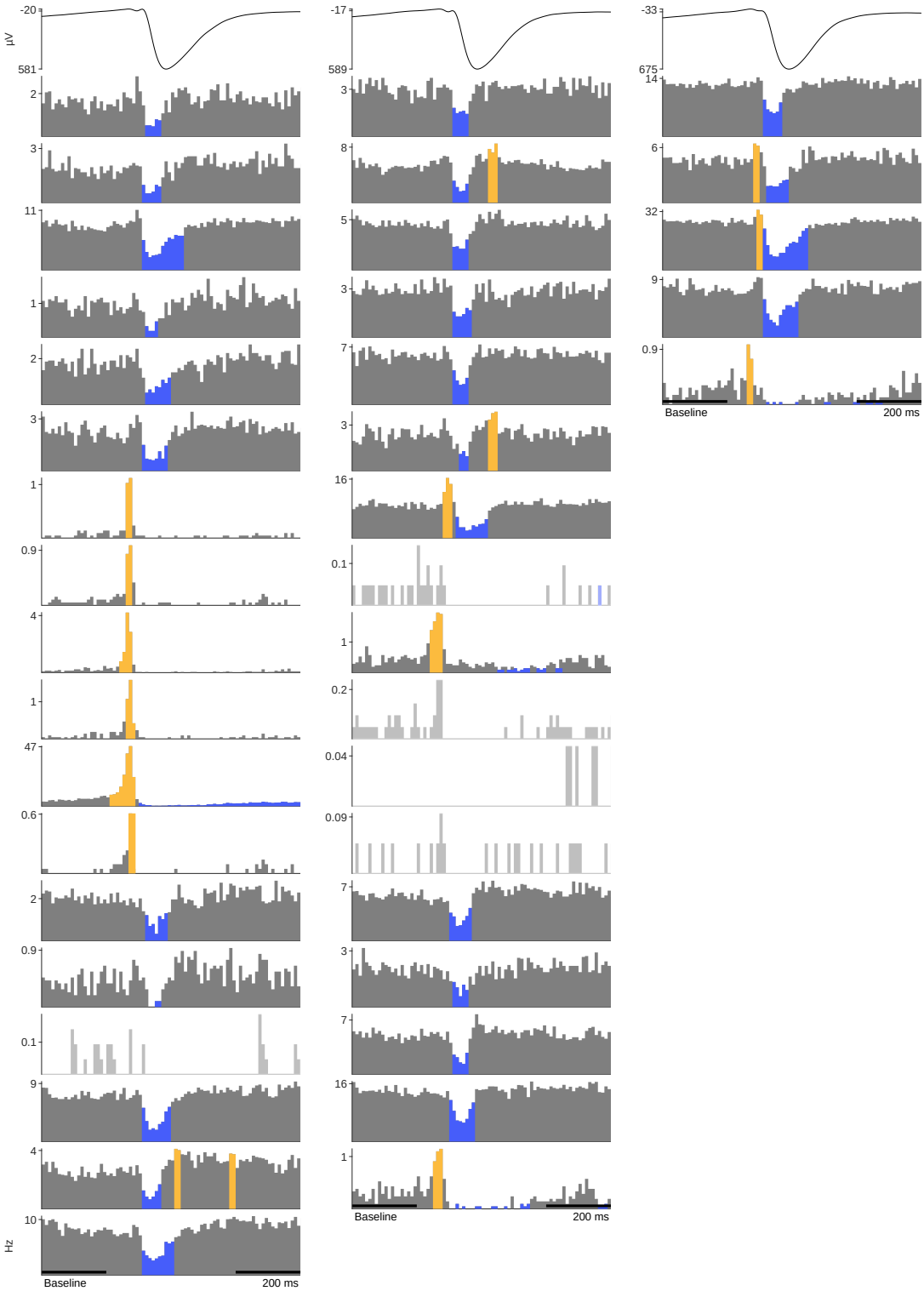

Figure 32. Patient 8: PSTH of each unit. Top row shows time-locked LFP. Units are organized over nights (columns). The yellow color indicates significant increases and the blue color decreases compared with the average firing rate during baseline, indicated in the x-axis of bottom left plot.

References

Aanestad E, Brøgger JC. S84. Variability of Epileptiform Discharges by Age Using SCORE. Clinical Neurophysiology. 2018 May; 129:e173. doi: 10.1016/j.clinph.2018.04.444.

Aanestad E, Gilhus NE, Brogger J. Interictal Epileptiform Discharges Vary across Age Groups. Clinical Neurophysiology. 2020 Jan; 131(1):25–33. doi: 10.1016/j.clinph.2019.09.017.

Agostinelli C, Lund U. R Package <tt>: Circular Statistics (Version 0.4-93)</Tt>. CA: Department of Environmental Sciences, Informatics and Statistics, Ca' Foscari University, Venice, Italy. UL: Department of Statistics, California Polytechnic State University, San Luis Obispo, California, USA; 2017.

Altafullah I, Halgren E, Stapleton JM, Crandall PH. Interictal Spike-Wave Complexes in the Human Medial Temporal Lobe: Typical Topography and Comparisons with Cognitive Potentials. Electroencephalography and Clinical Neurophysiology. 1986 Jun; 63(6):503–516. doi: 10.1016/0013-4694(86)90138-0.

Alvarado-Rojas C, Lehongre K, Bagdasaryan J, Bragin A, Staba R, Engel J, Navarro V, Le Van Quyen M. Single-Unit Activities during Epileptic Discharges in the Human Hippocampal Formation. Frontiers in Computational Neuroscience. 2013; 7:140. doi: 10.3389/fncom.2013.00140.

Anderson CT, Tcheng TK, Sun FT, Morrell MJ. Day–Night Patterns of Epileptiform Activity in 65 Patients With Long-Term Ambulatory Electrocorticography:. Journal of Clinical Neurophysiology. 2015 Oct; 32(5):406–412. doi: 10.1097/WNP.0000000000000183.

Antoniades A, Spyrou L, Martin-Lopez D, Valentin A, Alarcon G, Sanei S, Cheong Took C. Detection of Interictal Discharges With Convolutional Neural Networks Using Discrete Ordered Multichannel Intracranial EEG. IEEE Transactions on Neural Systems and Rehabilitation Engineering. 2017 Dec; 25(12):2285–2294. doi: 10.1109/TNSRE.2017.2755770.

Asano E, Mihaylova T, Juhász C, Sood S, Chugani HT. Effect of Sleep on Interictal Spikes and Distribution of Sleep Spindles on Electrocorticography in Children with Focal Epilepsy. Clinical neurophysiology : official journal of the International Federation of Clinical Neurophysiology. 2007 Jun; 118(6):1360–1368. doi: 10.1016/j.clinph.2007.02.021.

Autret A, Lucas B, Hommet C, Corcia P, Toffol B. Sleep and the Epilepsies. Journal of Neurology. 1997 Apr; 244(S1):S10–S17. doi: 10.1007/BF03160566.

Badawy R, Macdonell R, Jackson G, Berkovic S. The Peri-Ictal State: Cortical Excitability Changes within 24 h of a Seizure. Brain. 2009 Apr; 132(4):1013–1021. doi: 10.1093/brain/awp017.

Bagheri E, Jin J, Dauwels J, Cash S, Westover MB. A Fast Machine Learning Approach to Facilitate the Detection of Interictal Epileptiform Discharges in the Scalp Electroencephalogram. Journal of Neuroscience Methods. 2019 Oct; 326:108362. doi: 10.1016/j.jneumeth.2019.108362.

Bagshaw AP, Jacobs J, LeVan P, Dubeau F, Gotman J. Effect of Sleep Stage on Interictal High-Frequency Oscillations Recorded from Depth Macroelectrodes in Patients with Focal Epilepsy. Epilepsia. 2009 Apr; 50(4):617–628. doi: 10.1111/j.1528-1167.2008.01784.x.

Bates D, Mächler M, Bolker B, Walker S. Fitting Linear Mixed-Effects Models Using Lme4. arXiv:14065823 [stat]. 2014 Jun; .

Baud MO, Kleen JK, Mirro EA, Andrechak JC, King-Stephens D, Chang EF, Rao VR. Multi-Day Rhythms Modulate Seizure Risk in Epilepsy. Nature Communications. 2018 Dec; 9(1). doi: 10.1038/s41467-017-02577-y.

Bazil CW, Walczak TS. Effects of Sleep and Sleep Stage on Epileptic and Nonepileptic Seizures. Epilepsia. 1997 Jan; 38(1):56–62. doi: 10.1111/j.1528-1157.1997.tb01077.x.

Beaumanoir A, Ballis T, Varfis G, Ansari K. Benign Epilepsy of Childhood With Rolandic Spikes. Epilepsia. 1974; 15(3):301–315. doi: 10.1111/j.1528-1157.1974.tb04010.x.

Berry RB, Brooks R, Gamaldo C, Harding SM, Lloyd RM, Quan SF, Troester MT, Vaughn BV. AASM Scoring Manual Updates for 2017 (Version 2.4). Journal of clinical sleep medicine: JCSM: official publication of the American Academy of Sleep Medicine. 2017 May; 13(5):665–666. doi: 10.5664/jcsm.6576.

Blom S, Heijbel J. Benign Epilepsy of Children with Centro-Temporal EEG Foci. Discharge Rate during Sleep. Epilepsia. 1975 Mar; 16(1):133–140. doi: 10.1111/j.1528-1157.1975.tb04730.x.

Brown MW, Porter BE, Dlugos DJ, Keating J, Gardner AB, Storm PB, Marsh ED. Comparison of Novel Computer Detectors and Human Performance for Spike Detection in Intracranial EEG. Clinical Neurophysiology. 2007 Aug; 118(8):1744–1752. doi: 10.1016/j.clinph.2007.04.017.

Busek P, Buskova J, Nevsimalova S. Interictal Epileptiform Discharges and Phasic Phenomena of REM Sleep. Epileptic Disorders: International Epilepsy Journal with Videotape. 2010 Sep; 12(3):217–221. doi: 10.1684/epd.2010.0319.

Calvin WH, Sypert GW, Ward AA. Structured Timing Patterns within Bursts from Epileptic Neurons in Undrugged Monkey Cortex. Experimental Neurology. 1968 Aug; 21(4):535–549. doi: 10.1016/0014-4886(68)90071-X.

Clemens B, Oláh R. Sleep Studies in Benign Epilepsy of Childhood with Rolandic Spikes. I. Sleep Pathology. Epilepsia. 1987; 28(1):20–23. doi: 10.1111/j.1528-1157.1987.tb03616.x.

Cobabe MM, Sessler DI, Nowacki AS, O'Rourke C, Andrews N, Foldvary-Schaefer N. Impact of Sleep Duration on Seizure Frequency in Adults with Epilepsy: A Sleep Diary Study. Epilepsy & Behavior. 2015 Feb; 43:143–148. doi: 10.1016/j.yebeh.2014.12.012.

Cohen I, Navarro V, Clemenceau S, Baulac M, Miles R. On the Origin of Interictal Activity in Human Temporal Lobe Epilepsy in Vitro. Science, New Series. 2002; 298(5597):1418–1421.

Colder BW, Frysinger RC, Wilson CL, Harper RM, Engel J. Decreased Neuronal Burst Discharge Near Site of Seizure Onset in Epileptic Human Temporal Lobes. Epilepsia. 1996 Feb; 37(2):113–121. doi: 10.1111/j.1528-1157.1996.tb00001.x.

Connors BW. Initiation of Synchronized Neuronal Bursting in Neocortex. Nature. 1984 Aug; 310(5979):685–687. doi: 10.1038/310685a0.

Conrad EC, Tomlinson SB, Wong JN, Oechsel KF, Shinohara RT, Litt B, Davis KA, Marsh ED. Spatial Distribution of Interictal Spikes Fluctuates over Time and Localizes Seizure Onset. Brain. 2020 Feb; 143(2):554–569. doi: 10.1093/brain/awz386.

Constantino AC, Sisterson ND, Zaher N, Urban A, Richardson RM, Kokkinos V. Expert-Level Intracranial Electroencephalogram Ictal Pattern Detection by a Deep Learning Neural Network. Frontiers in Neurology. 2021 May; 12:603868. doi: 10.3389/fneur.2021.603868.

da Silva Lourenço C, Tjepkema-Cloostermans MC, van Putten MJAM. Machine Learning for Detection of Interictal Epileptiform Discharges. Clinical Neurophysiology. 2021 Jul; 132(7):1433–1443. doi: 10.1016/j.clinph.2021.02.403.

Daley JT, DeWolfe JL. Sleep, Circadian Rhythms, and Epilepsy. Current Treatment Options in Neurology. 2018 Nov; 20(11):47. doi: 10.1007/s11940-018-0534-1.

Dalla Bernardina B, Sgrò V, Caraballo R, Fontana E, Colamaria V, Zullini E, Simone M, Zanetti R. Sleep and Benign Partial Epilepsies of Childhood: EEG and Evoked Potentials Study. Epilepsy Research Supplement. 1991; 2:83–96.

Dauvilliers Y, Billiard M. Aspects Du Sommeil Normal. In: *Les Troubles de Sommeil* Paris: Masson; 2005.p. 5–17.

de Curtis M, Radici C, Forti M. Cellular Mechanisms Underlying Spontaneous Interictal Spikes in an Acute Model of Focal Cortical Epileptogenesis. Neuroscience. 1999 Jan; 88(1):107–117. doi: 10.1016/s0306-4522(98)00201-2.

de Curtis M, Avanzini G. Interictal Spikes in Focal Epileptogenesis. Progress in Neurobiology. 2001 Apr; 63(5):541–567. doi: 10.1016/S0301-0082(00)00026-5.

Del Felice A, Storti SF, Manganotti P. Sleep Affects Cortical Source Modularity in Temporal Lobe Epilepsy: A High-Density EEG Study. Clinical Neurophysiology. 2015 Sep; 126(9):1677–1683. doi: 10.1016/j.clinph.2014.12.003.

Derry CP, Duncan S. Sleep and Epilepsy. Epilepsy & Behavior. 2013 Mar; 26(3):394–404. doi: 10.1016/j.yebeh.2012.10.033.

Durazzo TS, Spencer SS, Duckrow RB, Novotny EJ, Spencer DD, Zaveri HP. Temporal Distributions of Seizure Occurrence from Various Epileptogenic Regions. Neurology. 2008 Apr; 70(15):1265–1271. doi: 10.1212/01.wnl.0000308938.84918.3f.

Fabó D, Maglóczky Z, Wittner L, Pék Á, Erőss L, Czirják S, Vajda J, Sólyom A, Rásonyi G, Szűcs A, Kelemen A, Juhos V, Grand L, Dombovári B, Halász P, Freund TF, Halgren E, Karmos G, Ulbert I. Properties of in Vivo Interictal Spike Generation in the Human Subiculum. Brain. 2008 Feb; 131(2):485–499. doi: 10.1093/brain/awm297.

Fedorov A, Beichel R, Kalpathy-Cramer J, Finet J, Fillion-Robin JC, Pujol S, Bauer C, Jennings D, Fennessy F, Sonka M, Buatti J, Aylward S, Miller JV, Pieper S, Kikinis R. 3D Slicer as an Image Computing Platform for the Quantitative Imaging Network. Magnetic Resonance Imaging. 2012 Nov; 30(9):1323–1341. doi: 10.1016/j.mri.2012.05.001.

Ferlisi M, Shorvon S. Seizure Precipitants (Triggering Factors) in Patients with Epilepsy. Epilepsy & Behavior. 2014 Apr; 33:101–105. doi: 10.1016/j.yebeh.2014.02.019.

Ferrillo F, Beelke M, De Carli F, Cossu M, Munari C, Rosadini G, Nobili L. Sleep-EEG Modulation of Interictal Epileptiform Discharges in Adult Partial Epilepsy: A Spectral Analysis Study. Clinical Neurophysiology. 2000 May; 111(5):916–923. doi: 10.1016/S1388-2457(00)00246-7.

Foldvary-Schaefer N, Grigg-Damberger M. Sleep and Epilepsy: What We Know, Don't Know, and Need to Know. Journal of Clinical Neurophysiology. 2006 Feb; 23(1):4–20. doi: 10.1097/01.wnp.0000206877.90232.cb.

Fouad A, Azizollahi H, Le Douget JE, Lejeune FX, Valderrama M, Mayor L, Navarro V, Le Van Quyen M. Interictal Epileptiform Discharges Show Distinct Spatiotemporal and Morphological Patterns across Wake and Sleep. Brain Communications. 2022 Jul; 4(5):fcac183. doi: 10.1093/braincomms/fcac183.

Frazzini V, Whitmarsh S, Lehongre K, Yger P, Lemarechal JD, Matching B, Adam C, Hasboun D, Lambrecq V, Navarro V. Human Periventricular Nodular Heterotopia Shows Several Interictal Epileptic Patterns, Associated with Hyperexcitability of Neuronal Firing. bioRxiv. 2022 May; p. 816173. doi: 10.1101/816173.

Fried I, Wilson CL, Maidment NT, Engel J, Behnke E, Fields TA, MacDonald KA, Morrow JW, Ackerson L. Cerebral Microdialysis Combined with Single-Neuron and Electroencephalographic Recording in Neurosurgical Patients. Technical Note. Journal of Neurosurgery. 1999 Oct; 91(4):697–705. doi: 10.3171/jns.1999.91.4.0697.

Frost JD, Hrachovy RA, Glaze DG, McCully MI. Sleep Modulation of Interictal Spike Configuration in Untreated Children with Partial Seizures. Epilepsia. 1991 Jun; 32(3):341–346. doi: 10.1111/j.1528-1157.1991.tb04661.x.

Frucht MM, Quigg M, Schwaner C, Fountain NB. Distribution of Seizure Precipitants Among Epilepsy Syndromes. Epilepsia. 2000; 41(12):6.

Fukumori K, Thu Nguyen HT, Yoshida N, Tanaka T. Fully Data-driven Convolutional Filters with Deep Learning Models for Epileptic Spike Detection. In: *ICASSP 2019 - 2019 IEEE International Conference on Acoustics, Speech and Signal Processing (ICASSP)*; 2019. p. 2772–2776. doi: 10.1109/ICASSP.2019.8682196.

Fürbass F, Koren J, Hartmann M, Brandmayr G, Hafner S, Baumgartner C. Activation Patterns of Interictal Epileptiform Discharges in Relation to Sleep and Seizures: An Artificial Intelligence Driven Data Analysis. Clinical Neurophysiology. 2021 Jul; 132(7):1584–1592. doi: 10.1016/j.clinph.2021.03.052.

Fürbass F, Kural MA, Gritsch G, Hartmann M, Kluge T, Beniczky S. An Artificial Intelligence-Based EEG Algorithm for Detection of Epileptiform EEG Discharges: Validation against the Diagnostic Gold Standard. Clinical Neurophysiology. 2020 Jun; 131(6):1174–1179. doi: 10.1016/j.clinph.2020.02.032.

Gast H, Niediek J, Schindler K, Boström J, Coenen VA, Beck H, Elger CE, Mormann F. Burst Firing of Single Neurons in the Human Medial Temporal Lobe Changes before Epileptic Seizures. Clinical Neurophysiology. 2016 Oct; 127(10):3329–3334. doi: 10.1016/j.clinph.2016.08.010.

Geng D, Alkhachroum A, Bicchi MAM, Jagid JR, Cajigas I, Chen ZS. Deep Learning for Robust Detection of Interictal Epileptiform Discharges. Journal of Neural Engineering. 2021 Apr; 18(5):056015. doi: 10.1088/1741-2552/abf28e.

Gibbs EL, Gibbs FA. Diagnostic and Localizing Value of Electroencephalographic Studies in Sleep. Res Publ Assoc Res Nerv Ment Dis. 1947; 26:366–376.

Goncharova II, Zaveri HP, Duckrow RB, Novotny EJ, Spencer SS. Spatial Distribution of Intracranially Recorded Spikes in Medial and Lateral Temporal Epilepsies. Epilepsia. 2009 Dec; 50(12):2575–2585. doi: 10.1111/j.1528-1167.2009.02258.x.

Gotman J. Quantitative Measurements of Epileptic Spike Morphology in the Human EEG. Electroencephalography and Clinical Neurophysiology. 1980 May; 48(5):551–557. doi: 10.1016/0013-4694(80)90290-4.

Gowers W. Course of Epilepsy. In: *Epilepsy and Other Chronic Convulsive Diseases: Their Causes, Symptoms and Treatment* New York, NY, USA: William Wood; 1881.p. 157–164.

Griffiths G, Fox JT. Rhythm in Epilepsy. The Lancet. 1938 Aug; 232(5999):409–416. doi: 10.1016/S0140-6736(00)41614-4.

Halász P. How Sleep Activates Epileptic Networks? Epilepsy Research and Treatment. 2013; 2013. doi: 10.1155/2013/425697.

Halford JJ. Computerized Epileptiform Transient Detection in the Scalp Electroencephalogram: Obstacles to Progress and the Example of Computerized ECG Interpretation. Clinical Neurophysiology. 2009 Nov; 120(11):1909–1915. doi: 10.1016/j.clinph.2009.08.007.

Halford JJ, Schalkoff RJ, Zhou J, Benbadis SR, Tatum WO, Turner RP, Sinha SR, Fountain NB, Arain A, Pritchard PB, Kutluay E, Martz G, Edwards JC, Waters C, Dean BC. Standardized Database Development for EEG Epileptiform Transient Detection: EEGnet Scoring System and Machine Learning Analysis. Journal of Neuroscience Methods. 2013 Jan; 212(2):308–316. doi: 10.1016/j.jneumeth.2012.11.005.

Hao Y, Khoo HM, von Ellenrieder N, Zazubovits N, Gotman J. DeepIED: An Epileptic Discharge Detector for EEG-fMRI Based on Deep Learning. NeuroImage: Clinical. 2018; 17:962–975. doi: 10.1016/j.nicl.2017.12.005.

Herman ST, Walczak TS, Bazil CW. Distribution of Partial Seizures during the Sleep-Wake Cycle: Differences by Seizure Onset Site. Neurology. 2001 Jun; 56(11):1453–1459. doi: 10.1212/WNL.56.11.1453.

Hirsch LJ, LaRoche SM, Gaspard N, Gerard E, Svoronos A, Herman ST, Mani R, Arif H, Jette N, Minazad Y, Kerrigan JF, Vespa P, Hantus S, Claassen J, Young GB, So E, Kaplan PW, Nuwer MR, Fountain NB, Drislane FW. American Clinical Neurophysiology Society's Standardized Critical Care EEG Terminology: 2012 Version. Journal of Clinical Neurophysiology. 2013; 30(1):27.

Hirsch LJ, Fong MWK, Leitinger M, LaRoche SM, Beniczky S, Abend NS, Lee JW, Wusthoff CJ, Hahn CD, Westover MB, Gerard EE, Herman ST, Haider HA, Osman G, Rodriguez-Ruiz A, Maciel CB, Gilmore EJ, Fernandez A, Rosenthal ES, Claassen J, et al. American Clinical Neurophysiology Society's Standardized Critical Care EEG Terminology: 2021 Version. Journal of Clinical Neurophysiology. 2021 Jan; 38(1):1–29. doi: 10.1097/WNP.0000000000000806.

Hofer KT, Kandrács Á, Tóth K, Hajnal B, Bokodi V, Tóth EZ, Erőss L, Entz L, Bagó AG, Fabó D, Ulbert I, Wittner L. Bursting of Excitatory Cells Is Linked to Interictal Epileptic Discharge Generation in Humans. Scientific Reports. 2022 Apr; 12(1):6280. doi: 10.1038/s41598-022-10319-4.

Hofstra WA, Grootemarsink BE, Dieker R, Palen JVD, Weerd AWD. Temporal Distribution of Clinical Seizures over the 24-h Day: A Retrospective Observational Study in a Tertiary Epilepsy Clinic. Epilepsia. 2009; 50(9):2019–2026. doi: 10.1111/j.1528-1167.2009.02044.x.

Hofstra WA, Spetgens WPJ, Leijten FSS, van Rijen PC, Gosselaar P, van der Palen J, de Weerd AW. Diurnal Rhythms in Seizures Detected by Intracranial Electrocorticographic Monitoring: An Observational Study. Epilepsy & Behavior. 2009 Apr; 14(4):617–621. doi: 10.1016/j.yebeh.2009.01.020.

Hofstra WA, de Weerd AW. The Circadian Rhythm and Its Interaction with Human Epilepsy: A Review of Literature. Sleep Medicine Reviews. 2009 Dec; 13(6):413–420. doi: 10.1016/j.smrv.2009.01.002.

Holt GR, Softky WR, Koch C, Douglas RJ. Comparison of Discharge Variability in Vitro and in Vivo in Cat Visual Cortex Neurons. Journal of Neurophysiology. 1996 May; 75(5):1806–1814. doi: 10.1152/jn.1996.75.5.1806.

Horak PC, Meisenhelter S, Testorf ME, Connolly AC, Davis KA, Jobst BC. Implementation and Evaluation of an Interictal Spike Detector. In: Bones PJ, Fiddy MA, Millane RP, editors. *SPIE Optical Engineering + Applications* San Diego, California, United States; 2015. p. 96000N. doi: 10.1117/12.2189248.

Hufnagel A, Dumpelmann M, Zentner J, Schijns O, Elger CE. Clinical Relevance of Quantified Intracranial Interictal Spike Activity in Presurgical Evaluation of Epilepsy. Epilepsia. 2000 Apr; 41(4):467–478. doi: 10.1111/j.1528-1157.2000.tb00191.x.

Iber C, Medicine AAoS. The AASM Manual for the Scoring of Sleep and Associated Events: Rules, Terminology and Technical Specifications. American Academy of Sleep Medicine; 2007.

Ishijima B. Unitary Analysis of Epileptic Activity in Acute and Chronic Foci and Related Cortex of Cat and Monkey. Epilepsia. 1972 Aug; 13(4):561–581. doi: 10.1111/j.1528-1157.1972.tb04393.x.

Ishijima B, Hori T, Yoshimasa N, Fukushima T, Hirakawa K, Sekino H. Neuronal Activities in Human Epileptic Foci and Surrounding Areas. Electroencephalography and Clinical Neurophysiology. 1975 Dec; 39(6):643–650. doi: 10.1016/0013-4694(75)90077-2.

Jain SV, Kothare SV. Sleep and Epilepsy. Seminars in Pediatric Neurology. 2015 Jun; 22(2):86–92. doi: 10.1016/j.spen.2015.03.005.

Janca R, Jezdik P, Cmejla R, Tomasek M, Worrell GA, Stead M, Wagenaar J, Jefferys JGR, Krsek P, Komarek V, Jiruska P, Marusic P. Detection of Interictal Epileptiform Discharges Using Signal Envelope Distribution Modelling: Application to Epileptic and Non-Epileptic Intracranial Recordings. Brain Topography. 2015 Jan; 28(1):172–183. doi: 10.1007/s10548-014-0379-1.

Janca R, Krsek P, Jezdik P, Cmejla R, Tomasek M, Komarek V, Marusic P, Jiruska P. The Sub-Regional Functional Organization of Neocortical Irritative Epileptic Networks in Pediatric Epilepsy. Frontiers in Neurology. 2018 Mar; 9:184. doi: 10.3389/fneur.2018.00184.

Janz D. The Grand Mal Epilepsies and the Sleeping-Waking Cycle. Epilepsia. 1962 Mar; 3:69–109. doi: 10.1111/j.1528-1157.1962.tb05235.x.

Jobst BC, Williamson PD, Neuschwander TB, Darcey TM, Thadani VM, Roberts DW. Secondarily Generalized Seizures in Mesial Temporal Epilepsy: Clinical Characteristics, Lateralizing Signs, and Association With Sleep–Wake Cycle. Epilepsia. 2001 Oct; 42(10):1279–1287. doi: 10.1046/j.1528-1157.2001.09701.x.

Kang X, Boly M, Findlay G, Jones B, Gjini K, Maganti R, Struck AF. Quantitative Spatio-Temporal Characterization of Epileptic Spikes Using High Density EEG: Differences between NREM Sleep and REM Sleep. Scientific Reports. 2020 Dec; 10(1):1673. doi: 10.1038/s41598-020-58612-4.

Karafin M, St Louis EK, Zimmerman MB, Sparks JD, Granner MA. Bimodal Ultradian Seizure Periodicity in Human Mesial Temporal Lobe Epilepsy. Seizure. 2010 Jul; 19(6):347–351. doi: 10.1016/j.seizure.2010.05.005.

Karoly PJ, Freestone DR, Boston R, Grayden DB, Himes D, Leyde K, Seneviratne U, Berkovic S, O'Brien T, Cook MJ. Interictal Spikes and Epileptic Seizures: Their Relationship and Underlying Rhythmicity. Brain. 2016 Apr; 139(4):1066–1078. doi: 10.1093/brain/aww019.

Kataria L, Vaughn BV. Sleep and Epilepsy. Sleep Medicine Clinics. 2016 Mar; 11(1):25–38. doi: 10.1016/j.jsmc.2015.10.008.

Keller CJ, Truccolo W, Gale JT, Eskandar E, Thesen T, Carlson C, Devinsky O, Kuzniecky R, Doyle WK, Madsen JR, Schomer DL, Mehta AD, Brown EN, Hochberg LR, Ulbert I, Halgren E, Cash SS. Heterogeneous Neuronal Firing Patterns during Interictal Epileptiform Discharges in the Human Cortex. Brain. 2010 Jun; 133(6):1668–1681. doi: 10.1093/brain/awq112.

Khan S, Nobili L, Khatami R, Loddenkemper T, Cajochen C, Dijk PDJ, Eriksson SH. Circadian Rhythm and Epilepsy. The Lancet Neurology. 2018 Oct; doi: 10.1016/S1474-4422(18)30335-1.

Krishnan B, Vlachos I, Faith A, Mullane S, Williams K, Alexopoulos A, Iasemidis L. A Novel Spatiotemporal Analysis of Peri-Ictal Spiking to Probe the Relation of Spikes and Seizures in Epilepsy. Annals of biomedical engineering. 2014 Aug; 42(8):1606. doi: 10.1007/s10439-014-1004-x.

Kuznetsova A, Brockhoff PB, Christensen RHB. lmerTest Package: Tests in Linear Mixed Effects Models. Journal of Statistical Software. 2017 Dec; 82:1–26. doi: 10.18637/jss.v082.i13.

Lambert I, Roehri N, Giusiano B, Carron R, Wendling F, Benar C, Bartolomei F. Brain Regions and Epileptogenicity Influence Epileptic Interictal Spike Production and Propagation during NREM Sleep in Comparison with Wakefulness. Epilepsia. 2018 Jan; 59(1):235–243. doi: 10.1111/epi.13958.

Langdon-Down M, Russell Brain W. Time of Day in Relation to Convulsions in Epilepsy. The Lancet. 1929 May; 213(5516):1029–1032. doi: 10.1016/S0140-6736(00)79288-9.

Lehongre K, Lambrecq V, Whitmarsh S, Frazzini V, Cousyn L, Soleil D, Fernandez-Vidal S, Mathon B, Houot M, Lemarechal JD, Clemenceau S, Hasboun D, Adam C, Navarro V. Long-Term Deep Intracerebral Microelectrode Recordings in Patients with Drug-Resistant Epilepsy: Proposed Guidelines Based on 10-Year Experience. NeuroImage. 2022 Mar; p. 119116. doi: 10.1016/j.neuroimage.2022.119116.

Lenth RV. Least-Squares Means: The *R* Package **Lsmeans**. Journal of Statistical Software. 2016; 69(1). doi: 10.18637/jss.v069.i01.

Lieb JP, Joseph JP, Engel J, Walker J, Crandall PH. Sleep State and Seizure Foci Related to Depth Spike Activity in Patients with Temporal Lobe Epilepsy. Electroencephalography and Clinical Neurophysiology. 1980 Sep; 49(5-6):538–557. doi: 10.1016/0013-4694(80)90396-x.

Liu YC, Lin CCK, Tsai JJ, Sun YN. Model-Based Spike Detection of Epileptic EEG Data. Sensors (Basel, Switzerland). 2013 Sep; 13(9):12536–12547. doi: 10.3390/s130912536.

Lodder SS, van Putten MJAM. A Self-Adapting System for the Automated Detection of Inter-Ictal Epileptiform Discharges. PLOS ONE. 2014 Jan; 9(1):e85180. doi: 10.1371/journal.pone.0085180.

Lourenço C, Tjepkema-Cloostermans MC, Teixeira LF, van Putten MJAM. Deep Learning for Interictal Epileptiform Discharge Detection from Scalp EEG Recordings. In: Henriques J, Neves N, de Carvalho P, editors. *XV Mediterranean Conference on Medical and Biological Engineering and Computing – MEDICON 2019* IFMBE Proceedings, Cham: Springer International Publishing; 2020. p. 1984–1997. doi: 10.1007/978-3-030-31635-8_237.

Malow BA. Sleep and Epilepsy. Neurologic Clinics. 2005 Nov; 23(4):1127–1147. doi: 10.1016/j.ncl.2005.07.002.

Malow BA, Aldrich MS. Localizing Value of Rapid Eye Movement Sleep in Temporal Lobe Epilepsy. Sleep Medicine. 2000 Feb; 1(1):57–60. doi: 10.1016/S1389-9457(99)00008-8.

Malow BA, Lin X, Kushwaha R, Aldrich MS. Interictal Spiking Increases with Sleep Depth in Temporal Lobe Epilepsy. Epilepsia. 1998 Dec; 39(12):1309–1316. doi: 10.1111/j.1528-1157.1998.tb01329.x.

Maris E, Oostenveld R. Nonparametric Statistical Testing of EEG- and MEG-data. Journal of Neuroscience Methods. 2007 Aug; 164(1):177–190. doi: 10.1016/j.jneumeth.2007.03.024.

Massimini M, Rosanova M, Mariotti M. EEG Slow (~1 Hz) Waves Are Associated With Nonstationarity of Thalamo-Cortical Sensory Processing in the Sleeping Human. Journal of Neurophysiology. 2003 Mar; 89(3):1205–1213. doi: 10.1152/jn.00373.2002.

Mathon B, Clemenceau S, Hasboun D, Habert MO, Belaid H, Nguyen-Michel VH, Lambrecq V, Navarro V, Dupont S, Baulac M, Cornu P, Adam C. Safety Profile of Intracranial Electrode Implantation for Video-EEG Recordings in Drug-Resistant Focal Epilepsy. Journal of Neurology. 2015 Dec; 262(12):2699–2712. doi: 10.1007/s00415-015-7901-6.

Matsumoto H, Marsan CA. Cortical Cellular Phenomena in Experimental Epilepsy: Interictal Manifestations. Experimental Neurology. 1964 Apr; 9(4):286–304. doi: 10.1016/0014-4886(64)90025-1.

McNamara JO. Cellular and Molecular Basis of Epilepsy. Journal of Neuroscience. 1994 Jun; 14(6):3413–3425. doi: 10.1523/JNEUROSCI.14-06-03413.1994.

Medvedev AV, Agoureeva GI, Murro AM. A Long Short-Term Memory Neural Network for the Detection of Epileptiform Spikes and High Frequency Oscillations. Scientific Reports. 2019 Dec; 9(1):19374. doi: 10.1038/s41598-019-55861-w.

Méndez M, Radtke RA. Interactions Between Sleep and Epilepsy:. Journal of Clinical Neurophysiology. 2001 Mar; 18(2):106–127. doi: 10.1097/00004691-200103000-00003.

Minecan D, Natarajan A, Marzec M, Malow B. Relationship of Epileptic Seizures to Sleep Stage and Sleep Depth. Sleep. 2002 Dec; 25(8):56–61. doi: 10.1093/sleep/25.8.56.

Mirzoev A, Bercovici E, Stewart LS, Cortez MA, Snead OC, Desrocher M. Circadian Profiles of Focal Epileptic Seizures: A Need for Reappraisal. Seizure. 2012 Jul; 21(6):412–416. doi: 10.1016/j.seizure.2012.03.014.

Nayak CS, Mariyappa N, Majumdar KK, Ravi GS, Prasad PD, Nagappa M, Kandavel T, Taly AB, Sinha S. NREM Sleep and Antiepileptic Medications Modulate Epileptiform Activity by Altering Cortical Synchrony. Clinical EEG and Neuroscience. 2018 Nov; 49(6):417–424. doi: 10.1177/1550059417747436.

Ng M, Pavlova M. Why Are Seizures Rare in Rapid Eye Movement Sleep? Review of the Frequency of Seizures in Different Sleep Stages. Epilepsy Research and Treatment. 2013; 2013:1–10. doi: 10.1155/2013/932790.

Nonclercq A, Foulon M, Verheulpen D, De Cock C, Buzatu M, Mathys P, Van Bogaert P. Cluster-Based Spike Detection Algorithm Adapts to Interpatient and Intrapatient Variation in Spike Morphology. Journal of Neuroscience Methods. 2012 Sep; 210(2):259–265. doi: 10.1016/j.jneumeth.2012.07.015.

Nzwalo H, Menezes Cordeiro I, Santos AC, Peralta R, Paiva T, Bentes C. 24-Hour Rhythmicity of Seizures in Refractory Focal Epilepsy. Epilepsy & Behavior. 2016 Feb; 55:75–78. doi: 10.1016/j.yebeh.2015.12.005.

Okanari K, Baba S, Otsubo H, Widjaja E, Sakuma S, Go CY, Jones KC, Nishioka K, Oba S, Matsui T, Ueno M, Ukitsu S, Rutka JT, Drake JM, Donner EJ, Weiss SK, Snead OC, Ochi A. Rapid Eye Movement Sleep Reveals Epileptogenic Spikes for Resective Surgery in Children with Generalized Interictal Discharges. Epilepsia. 2015 Sep; 56(9):1445–1453. doi: 10.1111/epi.13081.

Oostenveld R, Fries P, Maris E, Schoffelen JM. FieldTrip: Open Source Software for Advanced Analysis of MEG, EEG, and Invasive Electrophysiological Data. Computational Intelligence and Neuroscience. 2011; 2011:1–9. doi: 10.1155/2011/156869.

Pavlova MK, Shea SA, Scheer FAJL, Bromfield EB. Is There a Circadian Variation of Epileptiform Abnormalities in Idiopathic Generalized Epilepsy? Epilepsy & Behavior. 2009 Nov; 16(3):461–467. doi: 10.1016/j.yebeh.2009.08.022.

Penfield W, Jasper H. Epilepsy and the Functional Anatomy of the Human Brain. Epilepsy and the Functional Anatomy of the Human Brain, Oxford, England: Little, Brown & Co.; 1954.

Pérez-García F, Lehongre K, Bardinet E, Jannin P, Navarro V, Hasboun D, Fernandez-Vidal S. Automatic Segmentation Of Depth Electrodes Implanted In Epileptic Patients: A Modular Tool Adaptable To Multicentric Protocols. Epilepsia. 2015 Sep; 56:227.

Peter-Derex L, Klimes P, Latreille V, Bouhadoun S, Dubeau F, Frauscher B. Sleep Disruption in Epilepsy: Ictal and Interictal Epileptic Activity Matter. Annals of Neurology. 2020 Nov; 88(5):907–920. doi: 10.1002/ana.25884.

Ponce-Alvarez A, Kilavik BE, Riehle A. Relating Firing Rate and Spike Time Irregularity in Motor Cortical Neurons. BMC Neuroscience. 2009 Jul; 10(1):P298. doi: 10.1186/1471-2202-10-S1-P298.

Ponce-Alvarez A, Kilavik BE, Riehle A. Comparison of Local Measures of Spike Time Irregularity and Relating Variability to Firing Rate in Motor Cortical Neurons. Journal of Computational Neuroscience. 2010 Aug; 29(1-2):351–365. doi: 10.1007/s10827-009-0158-2.

Prince DA, Futamachi KJ. Intracellular Recordings from Chronic Epileptogenic Foci in the Monkey. Electroencephalography and Clinical Neurophysiology. 1970 Nov; 29(5):496–510. doi: 10.1016/0013-4694(70)90066-0.

Prince DA. Inhibition in "Epileptic" Neurons. Experimental Neurology. 1968 Jul; 21(3):307–321. doi: 10.1016/0014-4886(68)90043-5.

Prince DA, Wong RKS. Human Epileptic Neurons Studied in Vitro. Brain Research. 1981 Apr; 210(1-2):323–333. doi: 10.1016/0006-8993(81)90905-7.

Quigg M. Circadian Rhythms: Interactions with Seizures and Epilepsy. Epilepsy Research. 2000 Nov; 42(1):43–55. doi: 10.1016/S0920-1211(00)00157-1.

Quigg M, Clayburn H, Straume M, Menaker M, Bertram EH. Effects of Circadian Regulation and Rest-Activity State on Spontaneous Seizures in a Rat Model of Limbic Epilepsy. Epilepsia. 2000 May; 41(5):502–509. doi: 10.1111/j.1528-1157.2000.tb00202.x.

Quon RJ, Meisenhelter S, Camp EJ, Testorf ME, Song Y, Song Q, Culler GW, Moein P, Jobst BC. AiED: Artificial Intelligence for the Detection of Intracranial Interictal Epileptiform Discharges. Clinical Neurophysiology. 2022 Jan; 133:1–8. doi: 10.1016/j.clinph.2021.09.018.

R Core Team. R: A Language and Environment for Statistical Computing. Vienna, Austria: R Foundation for Statistical Computing; 2013.

R Core Team. R: A Language and Environment for Statistical Computing. Vienna, Austria: R Foundation for Statistical Computing; 2015.

Reddy DS, Chuang SH, Hunn D, Crepea AZ, Magant R. Neuroendocrine Aspects of Improving Sleep in Epilepsy. Epilepsy research. 2018 Aug; 147:32–41. doi: 10.1016/j.eplepsyres.2018.08.013.

Reus EEM, Cox FME, van Dijk JG, Visser GH. Automated Spike Detection: Which Software Package? Seizure. 2022 Feb; 95:33–37. doi: 10.1016/j.seizure.2021.12.012.

Rocamora R, Andrzejak RG, Jiménez-Conde J, Elger CE. Sleep Modulation of Epileptic Activity in Mesial and Neocortical Temporal Lobe Epilepsy: A Study with Depth and Subdural Electrodes. Epilepsy & Behavior. 2013 Aug; 28(2):185–190. doi: 10.1016/j.yebeh.2013.04.010.

Rossi GF, Colicchio G, Pola P. Interictal Epileptic Activity during Sleep: A Stereo-EEG Study in Patients with Partial Epilepsy. Electroencephalography and Clinical Neurophysiology. 1984 Aug; 58(2):97–106. doi: 10.1016/0013-4694(84)90022-1.

Sammaritano M, Gigli GL, Gotman J. Interictal Spiking during Wakefulness and Sleep and the Localization of Foci in Temporal Lobe Epilepsy. Neurology. 1991 Feb; 41(2 Part 1):290–290. doi: 10.1212/WNL.41.2_Part_1.290.

Scarlatelli-Lima AV, Sukys-Claudino L, Watanabe N, Guarnieri R, Walz R, Lin K. How Do People with Drug-Resistant Mesial Temporal Lobe Epilepsy Sleep? A Clinical and Video-EEG with EOG and Submental EMG for Sleep Staging Study. eNeurologicalSci. 2016 Sep; 4:34–41. doi: 10.1016/j.ensci.2016.06.002.

Scheuer ML, Bagic A, Wilson SB. Spike Detection: Inter-reader Agreement and a Statistical Turing Test on a Large Data Set. Clinical Neurophysiology. 2017 Jan; 128(1):243–250. doi: 10.1016/j.clinph.2016.11.005.

Shouse MN, Farber PR, Staba RJ. Physiological Basis: How NREM Sleep Components Can Promote and REM Sleep Components Can Suppress Seizure Discharge Propagation. Clinical Neurophysiology. 2000 Sep; 111:S9–S18. doi: 10.1016/S1388-2457(00)00397-7.

Smyk MK, van Luijtelaar G. Circadian Rhythms and Epilepsy: A Suitable Case for Absence Epilepsy. Frontiers in Neurology. 2020; 0. doi: 10.3389/fneur.2020.00245.

Spencer DC, Sun FT, Brown SN, Jobst BC, Fountain NB, Wong VSS, Mirro EA, Quigg M. Circadian and Ultradian Patterns of Epileptiform Discharges Differ by Seizure-Onset Location during Long-Term Ambulatory Intracranial Monitoring. Epilepsia. 2016; 57(9):1495–1502. doi: 10.1111/epi.13455.

Staba RJ, Wilson CL, Bragin A, Fried I, Engel J. Sleep States Differentiate Single Neuron Activity Recorded from Human Epileptic Hippocampus, Entorhinal Cortex, and Subiculum. The Journal of Neuroscience. 2002 Jul; 22(13):5694–5704. doi: 10.1523/JNEUROSCI.22-13-05694.2002.

Staba RJ, Wilson CL, Fried I, Engel J. Single Neuron Burst Firing in the Human Hippocampus during Sleep. Hippocampus. 2002; 12(6):724–734. doi: 10.1002/hipo.10026.

Staley KJ, Dudek FE. Interictal Spikes and Epileptogenesis. Epilepsy Currents. 2006 Nov; 6(6):199–202. doi: 10.1111/j.1535-7511.2006.00145.x.

Steriade M, Contreras D. Relations between Cortical and Thalamic Cellular Events during Transition from Sleep Patterns to Paroxysmal Activity. The Journal of Neuroscience. 1995 Jan; 15(1):623–642. doi: 10.1523/JNEUROSCI.15-01-00623.1995.

Steriade M, Nuñez A, Amzica F. A Novel Slow (< 1 Hz) Oscillation of Neocortical Neurons in Vivo: Depolarizing and Hyperpolarizing Components. The Journal of Neuroscience: The Official Journal of the Society for Neuroscience. 1993 Aug; 13(8):3252–3265.

Steriade M. Sleep, Epilepsy and Thalamic Reticular Inhibitory Neurons. Trends in Neurosciences. 2005 Jun; 28(6):317–324. doi: 10.1016/j.tins.2005.03.007.

Steriade M, Amzica F, Neckelmann D, Timofeev I. Spike-Wave Complexes and Fast Components of Cortically Generated Seizures. II. Extra- and Intracellular Patterns. Journal of Neurophysiology. 1998 Sep; 80(3):1456–1479. doi: 10.1152/jn.1998.80.3.1456.

Tanaka FHKdS, Aranha C. Data Augmentation Using GANs. arXiv:190409135 [cs, stat]. 2019 Apr; .

Temkin O. The Falling Sickness: A History of Epilepsy from the Greeks to the Beginnings of Modern Neurology. 2. ed., rev ed. Baltimore: Johns Hopkins Univ. Pr; 1994.

Timofeev I, Grenier F, Steriade M. Disfacilitation and Active Inhibition in the Neocortex during the Natural Sleep-Wake Cycle: An Intracellular Study. Proceedings of the National Academy of Sciences of the United States of America. 2001 Feb; 98(4):1924–1929.

Tjepkema-Cloostermans MC, de Carvalho RCV, van Putten MJAM. Deep Learning for Detection of Focal Epileptiform Discharges from Scalp EEG Recordings. Clinical Neurophysiology. 2018 Oct; 129(10):2191–2196. doi: 10.1016/j.clinph.2018.06.024.

Traub RD, Miles R, Jefferys JG. Synaptic and Intrinsic Conductances Shape Picrotoxin-Induced Synchronized after-Discharges in the Guinea-Pig Hippocampal Slice. The Journal of Physiology. 1993; 461(1):525–547. doi: 10.1113/jphysiol.1993.sp019527.

Ulbert I, Heit G, Madsen J, Karmos G, Halgren E. Laminar Analysis of Human Neocortical Interictal Spike Generation and Propagation: Current Source Density and Multiunit Analysis In Vivo. Epilepsia. 2004 Jul; 45(s4):48–56. doi: 10.1111/j.0013-9580.2004.04011.x.

Vyazovskiy VV, Olcese U, Lazimy YM, Faraguna U, Esser SK, Williams JC, Cirelli C, Tononi G. Cortical Firing and Sleep Homeostasis. Neuron. 2009 Sep; 63(6):865–878. doi: 10.1016/j.neuron.2009.08.024.

Wang Q, Whitmarsh S, Navarro V, Palpanas T. iEDeaL: A Deep Learning Framework for Detecting Highly Imbalanced Interictal Epileptiform Discharges. Proceedings of the VLDB Endowment. 2023; 16. doi: 10.14778/3570690.3570698.

Wassenaar M, Kasteleijn-Nolst Trenité DGA, de Haan GJ, Carpay JA, Leijten FSS. Seizure Precipitants in a Community-Based Epilepsy Cohort. Journal of Neurology. 2014 Apr; 261(4):717–724. doi: 10.1007/s00415-014-7252-8.

Wickham H. Ggplot2: Elegant Graphics for Data Analysis. Springer-Verlag New York; 2016.

Wilson SB, Emerson R. Spike Detection: A Review and Comparison of Algorithms. Clinical Neurophysiology. 2002 Dec; 113(12):1873–1881. doi: 10.1016/S1388-2457(02)00297-3.